Design of an Interaction Region at C0 in the Tevatron

February 4, 2004

Table of Contents

1 Introduction

The C0 Interaction Region (IR) project provides a solution for creating high luminosity proton-antiproton collisions at the C0 region of the Tevatron for the BTeV experiment. The two largest technical components are modified LHC-style quadrupoles and newly designed corrector magnet packages (spools). This project takes full advantage of the Tevatron luminosity upgrades of the Run II Collider Program to obtain the highest luminosity possible for BTeV. It is designed to allow continued operation of the CDF and D0 experiments concurrently with the BTeV experiment. It makes use of proven existing Tevatron infrastructure to the fullest extent possible without compromising design goals. Modifications to the Tevatron are almost entirely restricted to the region from B43 to C17 (445 meters) and the 3 service buildings above.

The lattice design is robust. It utilizes asymmetric quadrupole triplets on either side of the IR to produce a 35 cm β^* at C0 − the same design β^* as B0 and D0. Additional quadrupoles, some new and some reused from the Tevatron Low Beta Project, match to the Run II lattice at all energies and at all steps of the transition from injection to the low beta lattice. The C0 insertion itself introduces exactly one unit of tune to both horizontal and vertical planes, so that the Tevatron fractional tunes remain unchanged. This design minimizes the impact on Tevatron operation. Corrector magnet packages are designed to give excellent orbit control and coupling correction to provide added insurance against magnet misalignments and imperfections. The power supply configuration is versatile enough to tune out any foreseeable magnet errors. This lattice design is optimized for 36 x 36 bunch operation but does not preclude 132 nsec operation.

The LHC IR quadrupole produced by the Fermilab Technical Division is a well tested and proven magnet. A modification of this design provides a cost-effective and timely solution for the C0 IR project. The modifications are restricted to the cryostat and end enclosures of the magnet − the cold mass remains the same as the original LHC design.

The unique demands of the C0 IR and the antiquity of the original Tevatron spools preclude the use of these spools in this project. New spools will be designed and fabricated. The baseline design uses a standard nested $\cos(n\theta)$ coil package to produce dipole, quadrupole, and sextupole fields. In addition, these spools contain the high current leads for the low beta quadrupoles. Limitations in the helium liquifying capacity of the Tevatron cryogenic system necessitate the use of high temperature superconductor for these leads.

The scope of this project also encompasses the construction and installation of new power supplies, new cryogenic elements in the Tevatron tunnel, modifications to low conductivity water systems, vacuum systems, beam collimation systems, controls infrastructure, software, instrumentation, and operational procedures − all the things necessary to make a high energy accelerator function.

Read on……

2 Accelerator Physics

2.1 Lattice

Every facet of successful Tevatron collider operations is tied intimately to specific details of the optical lattice functions in the ring. As examples, the locations of beam collimators, separators for helix generation, and the feeddown circuits are all determined largely by the distribution of betatron phase advance. So as not to disrupt these nominal Run II operating parameters it is essential that a new C0 Interaction Region (IR) insertion meld seamlessly with this existing Tevatron lattice. This implies the need to create an entirely localized insertion – one which is transparent to the rest of the machine. This constraint has important design implications, the most notable of which are pointed out below:

- An IR design similar to that employed at B0 & D0 is unacceptable as a C0 candidate. The addition of such a (single) low-β region to the machine would raise the tune by a half-integer in each plane, moving them far from the standard operating point and directly onto the 21.0 integer resonance. The nominal (fractional) tunes can be retained by adding 2 low-β's locally in each plane, thereby boosting the machine tunes by a full integer.
- The B0 & D0 IR's are not optically-isolated entities. Progression through the B0/D0 low-β squeeze involves adjusting, not only the main IR quadrupoles, but also the tune quad strings distributed around the ring. The result is that lattice functions at any point in the ring, and the phase advances across any section of the ring, are not fixed quantities, but vary through the squeeze sequence. For the operational mode of B0/D0-only collisions, the C0 insertion must be sufficiently flexible to track these changing matching conditions.
- With collisions only at B0 & D0 the unit of tune added by the C0 insert ensures that the incoming & outgoing helices are automatically matched into the Run II values. To maintain this match with collisions at all 3 IP's, however, would require additional separators in the short B0 – C0 & C0 – D0 arcs. There is no space available for more separators, so high luminosity collisions can only be created at B0 & D0, or just C0, but not all three simultaneously. Furthermore, without new arc separators the 2 IP collision options, B0 & C0 or D0 & C0, are also excluded.

Both the series & independent C0 IR quad circuits are illustrated in Figure 2-1. The specialized IR magnets required fall into 3 gradient ranges. First, there are LHC-like magnets operating at or below 170 T/m. This is substantially less than the >220 T/m LHC design, but the gradients are limited here by the Tevatron 4.5K cryogenics. Second, there are high-field 140 T/m Q1 quadrupoles previously installed for Tevatron collider operation. And third, there are strong (25 T.m/m) quad correction spools for the final optical match into the arcs.

Composition of the quadrupole circuits is described below, with the indicated lengths being magnetic lengths.

- The triplets:

Q1	: 96.5"	170 T/m
Q2	: 173.5"	170 T/m
Q3	: 96.5"	170 T/m

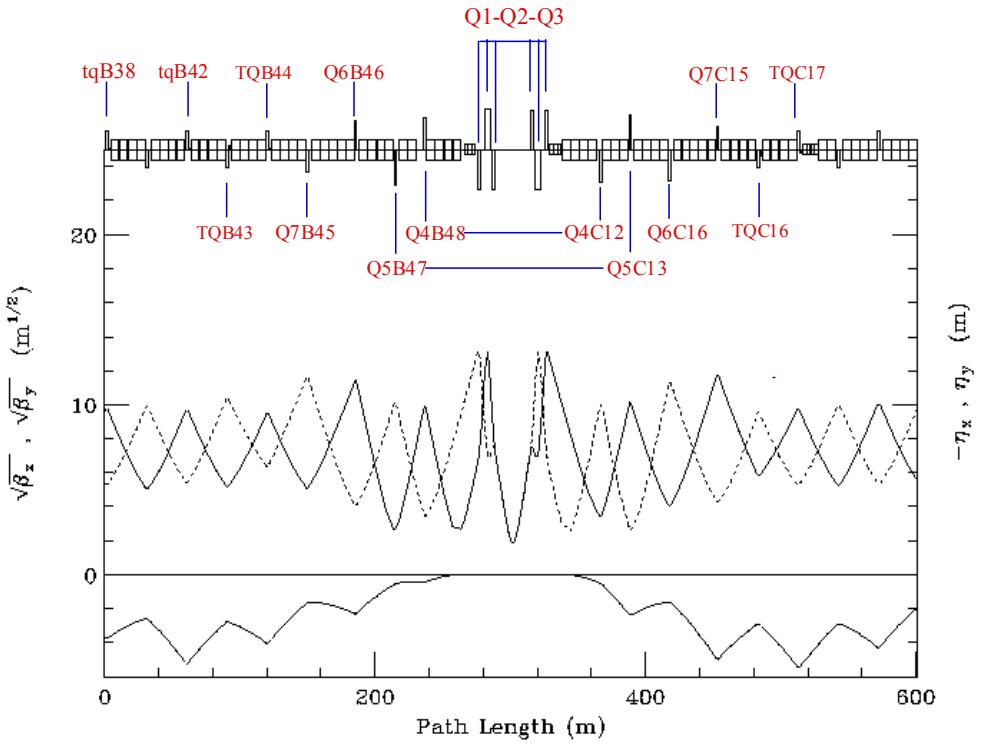

Figure 2-1: Power circuits of the IR quadrupoles.

Schematic layout of an IR triplet is given in Figure 2-2, showing the slot lengths & magnetic lengths of the elements, and spaces allocated for flanges, cryo, coil supports, etc. A special correction package is installed between the Q2 & Q3 magnets. This contains both vertical & horizontal BPM's, dipole correctors in each plane, plus a trim skew quad. The dipole correctors are well situated for beam control at the IP: $\beta_X = \beta_Y > 60\%\ \beta_{max}$, and the betatron phase advance to the IP is almost exactly 90^o in both planes. Because of the almost zero degrees of phase advance across the triplet magnets, the trim skew quad is perfectly located to compensate locally for triplet roll mis-alignments. The final focus triplets are powered in series, with a small additional power source added to Q2 for independent gradient variation to complete the match to the appropriate IP optics.

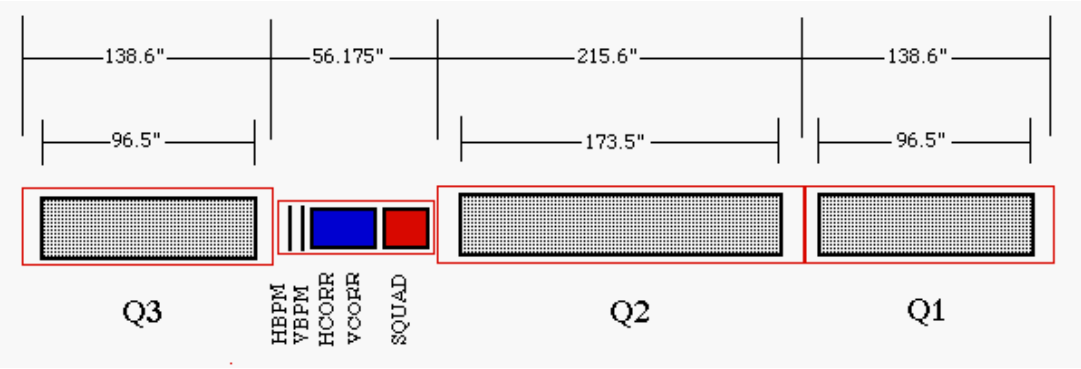

Figure 2-2: Details of the IR triplet

- B48/C12 & B47/C13:

Q4 : 79" 170 T/m

Q5 : 54" 170 T/m

Apart from their magnetic lengths the Q4 & Q5 magnets are the same design as the triplet quadrupoles, having adequate space at each end of the cryostat to accommodate the necessary ancillary hardware (see Figure 2-2). These quadrupoles are accompanied by new, short (56.175") spools, containing BPM's and dipole correctors in each plane. These spools also serve as the magnet power feeds & transport the main bus.

- B46/B45 & C14/C15:

Q6 : 55.19" 140 T/m

Q7 : 55.19" 140 T/m

The four Q6 & Q7 magnets are independently powered. The regular 66" arc quads and their spools at the B46, B45, C14 & C15 locations are replaced with relocated high−field Q1 low-beta quads (defunct in Run II) from CDF & D0, along with their accompanying P spools. The P spools have BPM's and dipole correctors in each plane, plus a skew quad. These spools also serve as the magnet power feeds & transport the main bus.

- B43/B44 & C16/C17:

The normal 72" Tevatron arc spools at these 4 locations are replaced by 72" spools containing high-field (25 T·m/m) trim quads plus standard strength horizontal or vertical dipoles and chromaticity sextupoles.

- B38/B42:

The trim quads (7.5 T·m/m) at B38 & B42 are removed from the main tune quad circuit and powered independently for final optical matching to the arc.

This design uses non-standard separations between some of the insertion's inner arc quadrupoles. Between the B48 & B47 [C12 & C13] quadrupoles space is reduced by 1 dipole, whereas between B46 & B45 [C14 & C15] separation increases by 1 dipole. Extensive simulations have shown that this configuration contributes markedly to the robustness of the IR's tuning range.

Trim quads are allocated in a lopsided configuration, with 2 more installed in the upstream end of the insert. In B-sector it is possible to extend insert elements a good distance back into the arc before interfering with Run II operation. This is not so in C-sector. The 4 vertical separators at C17 are integral components of Run II operation, and therefore define the downstream insert boundary.

There are 15 optical constraints the insertion satisfies. The 6 incoming Twiss parameters are matched at the IP to $\beta_x^* = \beta_y^* = \beta^*$, $\alpha_x^* = \alpha_y^* = 0$, $\eta^* = 0$, $\eta'^* = 0$, and then matched back into the nominal arc values at the downstream end of the insert (at C17). The fractional Run II phase shifts, $\Delta\mu_x$ and $\Delta\mu_y$, are preserved across the insert. The final constraint imposed in the design is that $\beta_{x,max} = \beta_{y,max}$ in the triplets on each side of the IP. While this last restriction isn't really crucial, it is the best choice, minimizing the consumption of aperture in the low-β quads.

Every stage of the C0 low beta squeeze from $\beta^* = 3.50$ to 0.35 m can match exactly to any step in the B0/D0 low beta squeeze. Subsequent sections illustrate these lattice parameters corresponding to the specific operational conditions:

(1) Injection : β^*= 3.50 m @ C0 : (β_x^*, β_y^*) = (1.61,1.74) m @ B0/D0

(2) C0 Collisions : β^*= 0.35 m @ C0 : (β_x^*, β_y^*) = (1.61,1.74) m @ B0/D0

(3) B0/D0 Collisions : β^*= 3.50 m @ C0 : β^* = 0.35 m @ B0 & D0

All gradient entries in the accompanying tables reflect 1 TeV/c operations. Highlighted entries indicate those magnets that must change polarity at some point during the transition between the various operating modes.

2.1.1 Injection

In the injection lattice, shown in Figure 2-3, β^* = 3.50 m results in a β_{max} of 177 m in the triplets. This is appreciably less than the >240 m of the B0 & D0 injection lattices and, so, is not anticipated to pose any aperture problems for Tevatron operations. The corresponding quadrupole gradients are listed in Table 2-1 (at 1 TeV/c).

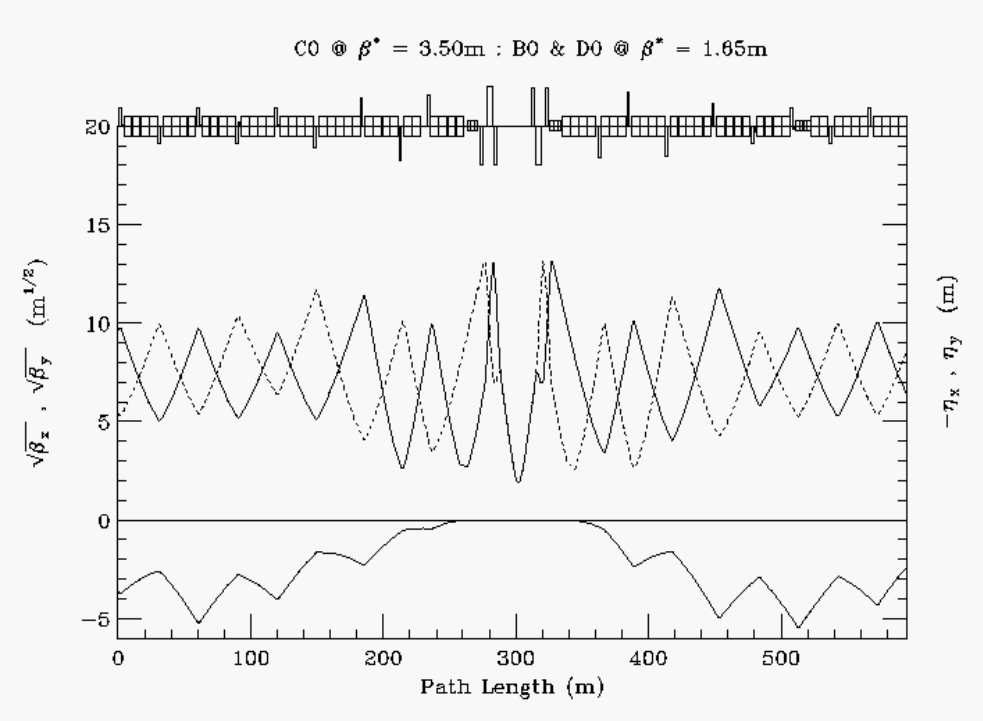

Figure 2-3: C0 injection optics

Table 2-1: C0 IR gradients for 1 TeV/c injection optics.

INJECTION OPTICS : C0 @ β* = 3.50m : B0/D0 @ β* = 1.65m **(1 TeV/c)**					
	Gradient (T/m)	Current (A)		Gradient (T/m)	Current (A)
Q1D	-164.783	9267	Q1F	164.783	9267
Q2F	168.814	9493	Q2D	-168.814	9493
Q3D	-164.783	9267	Q3F	164.783	9267
QB48	133.019	7480	QC12	-133.019	7480
QB47	-145.047	8157	QC13	145.047	8157
QB46	117.055	4045	QC14	-122.786	4248
QB45	-92.551	3198	QC15	92.940	3211
TB44	4.939		TC16	-25.569	
TB43	17.724		TC17	-10.470	
TB42	6.793				
TB39	0				
TB38	3.013				

2.1.2 C0 Collisions

For collisions at C0, the B0 & D0 optics remain in their injection configuration, while at C0 β* is squeezed from 3.50 m at injection to 0.35 m. Current Tevatron Collider understanding and experience suggests that the smallest realistic β* attainable is limited by the adverse impact on the beam by high-order multipoles in the low-β quadrupoles and, therefore, β_{max} in the low beta triplets. In the C0 IR lattice the Q1 magnets at C0 are roughly 15' farther from the IP than the corresponding ones at B0 & D0. As a result, β_{max} is considerably larger at C0 for any given value of β*. With β* = 35 cm, β_{max} has grown to 1660 m (Figure 2-4), which is significantly larger than the β_{max} of ~1130 m for a β* = 35 cm at the other IP's. In addition, the 63 mm physical aperture of the LHC magnets is also less than the 70 mm of the B0/D0 triplets. Nonetheless, dynamic aperture studies indicate that this tighter aperture restriction should not be a limiting factor in determining the minimum β* attainable.

For C0 collisions, β* at the IP is squeezed to 35 cm – the same value as for B0/D0 collisions. The luminosity at C0 will therefore be identical to that of B0/D0 at the end of Run II. Anticipated Collider parameters at the end of Run II are summarized in Table 2-3.

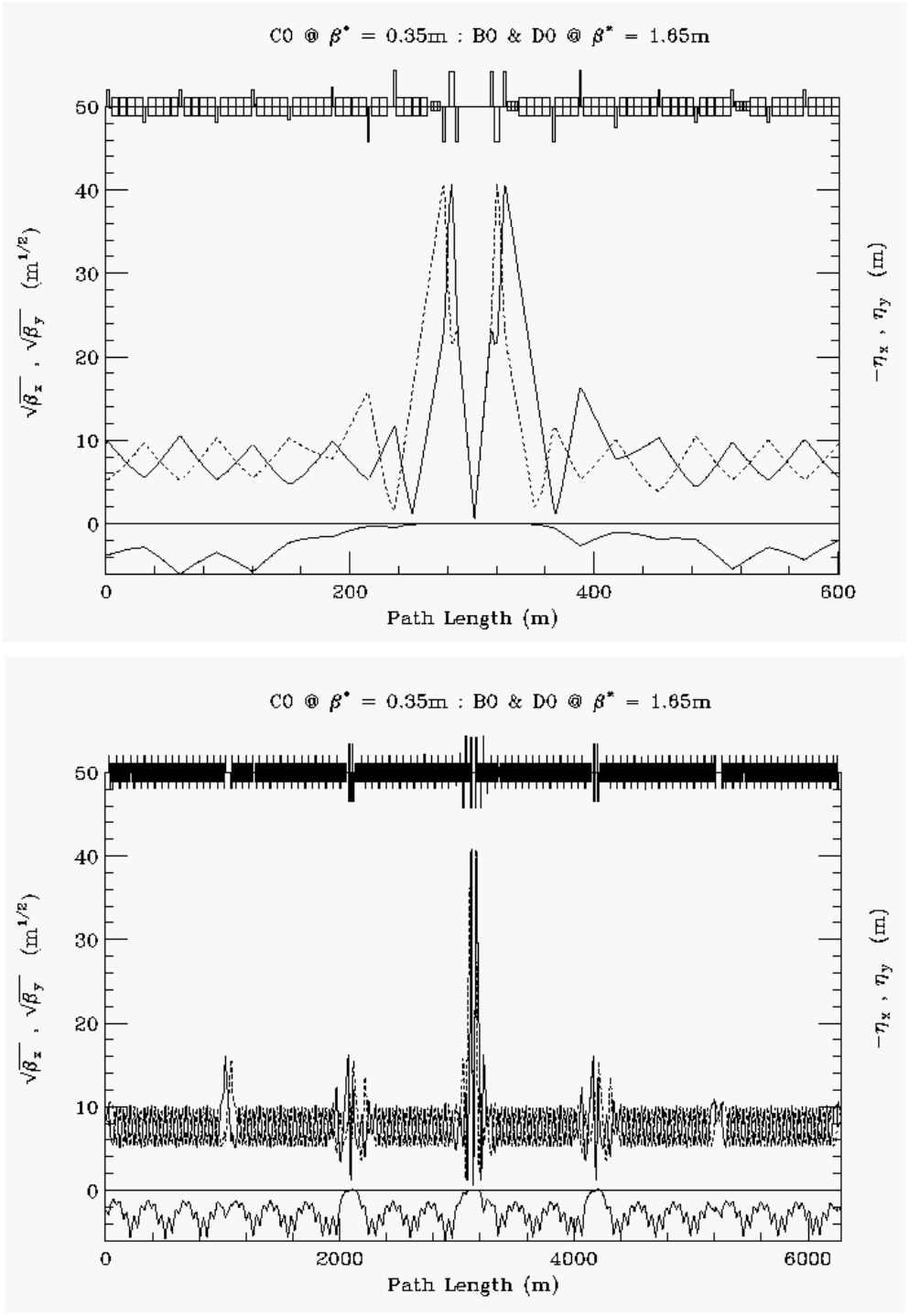

Figure 2-4: C0 collision optics – B38 – C19 (top), and ring-wide (bottom).

Table 2-2: IR gradients for C0 collisions at β* = 35 cm.

C0 COLLISIONS @ β* = 0.35 m : B0/D0 @ β* = 1.65 m **(1 TeV/c)**					
	Gradient (T/m)	Current (A)		Gradient (T/m)	Current (A)
Q1D	-169.228	9517	Q1F	169.228	9517
Q2F	165.397	9301	Q2D	-165.397	9301
Q3D	-169.228	9517	Q3F	169.228	9517
QB48	169.688	9524	QC12	-169.688	9524
QB47	-168.875	9497	QC13	168.875	9497
QB46	91.625	3166	QC14	-101.95	3523
QB45	-66.539	2299	QC15	76.322	2637
TB44	9.528		TC16	-35.373	
TB43	-0.819		TC17	22.589	
TB42	-0.844				
TB39	0				
TB38	-7.424				

Table 2-3: Collider parameters projected for the end of Run II. The 'Base' projection uses conservative performance estimates for Run II upgrade projects. The 'Design' parameters include more ambitious, but realistic, expectations of the upgrades.

C0 COLLISION PARAMETERS			
	BASE PROJECTION	DESIGN PROJECTION	
protons/bunch	250	270	x 10^9
pbars/bunch	76.4	129.6	x 10^9
proton emittance	18	18	π μm
pbar emittance	18	18	π μm
β* at C0 IP	0.35	0.35	m
Bunches	36	36	
Bunch length (rms)	0.45	0.45	m
Hour-Glass Form Factor	0.70	0.70	
Proton tune shift	0.0005	0.0008	
Pbar tune shift	0.0017	0.0018	
Initial Luminosity	160.5	294.0	x 10^{30} $cm^{-2}s^{-1}$

2.1.3 B0/D0 Collisions

For collisions at just B0 & D0, the C0 β* is fixed at its injection value of 3.50 m while at B0 & D0 β* is squeezed from ~1.65 m at injection to 0.35 m (see Figure 2-5). A comparison of C0 IR gradients listed in Table 2-4 with the injection values of Table 2-1 demonstrates the small tuning changes required at C0 to fix β* = 3.50 m while maintaining the ideal optical match to the nominal Run II squeeze lattice.

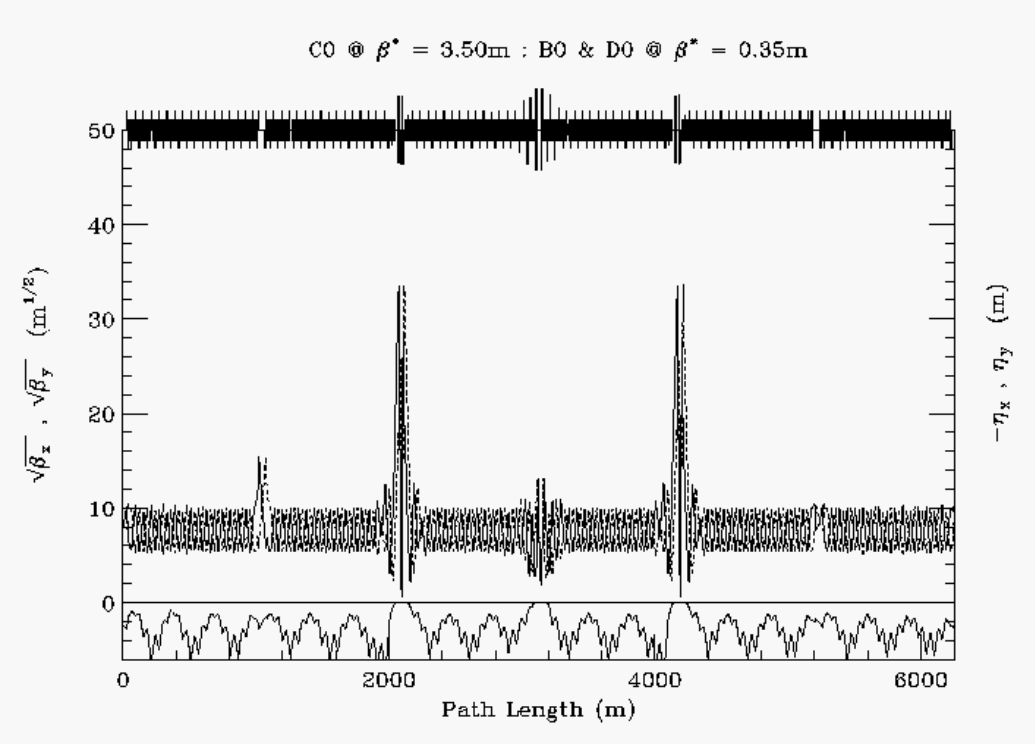

Figure 2-5: B0/D0 collision optics

Table 2-4: C0 IR gradients for B0/D0 collisions and β* fixed at 3.50 m at C0.

B0/D0 COLLISIONS @ β* = 0.35 m : C0 @ β* = 3.50 m (1 TeV/c)					
	Gradient (T/m)	Current (A)		Gradient (T/m)	Current (A)
Q1D	-165.998	9335	Q1F	165.998	9335
Q2F	168.619	9482	Q2D	-168.619	9482
Q3D	-165.998	9335	Q3F	165.998	9335
QB48	131.721	7407	QC12	-131.721	7407
QB47	-144.299	8115	QC13	144.299	8115
QB46	117.055	4045	QC14	-122.786	4248
QB45	-92.551	3302	QC15	92.940	3211
TB44	8.059		TC16	-15.743	
TB43	9.440		TC17	-8.110	
TB42	6.252				
TB39	0				
TB38	3.870				

2.2 Helix

With 36x36 bunch operation in the Tevatron there are 72 potential collision points of the proton and pbar beams. In Run II there are currently 6 sets of electrostatic separator modules available in both horizontal and vertical planes to keep the proton and pbar orbits separated everywhere in the ring except at the B0 & D0 IP's during collisions. One part of the Run II upgrade project is to increase by 6 the number of separator modules in the ring. The optimum sites for these new separators is still being studied. Another part of the Run II plan is to enhance the performance of the existing units. The present separators are run with gradients as high as ~40 kV/cm (~10.3 μrad kick at 1 TeV/c) before sparking becomes a problem. This is believed to be a conservative estimate of the maximum attainable gradient, however, and that with conditioning as much as a 30% increase should be possible. The outcome of these separator upgrades will be a better controlled, smoother helix at injection, where apertures are problematic, and increased beam separation at collision where the helix is limited by the available gradients. In view of the uncertainties still associated with implementing the Run II separator upgrade, however, in the discussions to follow only the currently installed ring separator configuration is considered, and the modules are assumed to have the conservative maximum electric field gradient of 40 kV/cm.

In the BTeV era it is expected that the Tevatron will continue with 36x36 bunch operations. Additional separator modules will then need to be added to create collisions at the C0 IP. Like the other 2 IR's these will be installed immediately outboard of the C0 IR triplets. At B49 there

will be a set of 2 horizontal modules and 1 vertical module, with the reverse configuration installed at C11.

2.2.1 Injection Helix

At the injection energy of 150 GeV, separation of the p-pbar orbits is controlled using a small sub-set of the 12 separators available in the machine. Separator strength is not an issue at 150 GeV, but the large beam sizes lead to aperture problems. The horizontal orbits are largely determined by the B17 separators, and the vertical by the C17 separators. The horizontal B17 gradients in particular are constrained by the aperture restrictions at the F0 injection Lambertson.

One separator solution from Run II is listed in Table 2-5. Here, only 4 sets of separators are used to create the helix, and the new B49/C11 separators are not used at all. The resulting beam separation around the ring is shown in Figure 2-6. Outside of the B38 – C17 C0 insert the helix is unchanged from the Run II value, and through the C0 IR region it can be seen that beam separation is at least as good as throughout the rest of the ring. The average separation is ~8σ.

Table 2-5: Injection Separator gradients at 150 GeV/c.

INJECTION HELIX : C0 @ β* = 3.50m : B0/D0 @ β* = 3.50m **(150 GeV/c)**					
	Horizontal			Vertical	
	#	kV/cm		#	kV/cm
A49	1	0.0	A49	2	0.0
B11	2	-14.800	B11	1	-9.050
B17	4	25.740			
B49	2	0.0	B49	1	0.0
C11	1	0.0	C11	2	0.0
			C17	4	-26.150
C49	1	0.0	C49	2	0.0
D11	2	0.0	D11	1	0.0
D48	1	0.0			
			A17	1	0.0

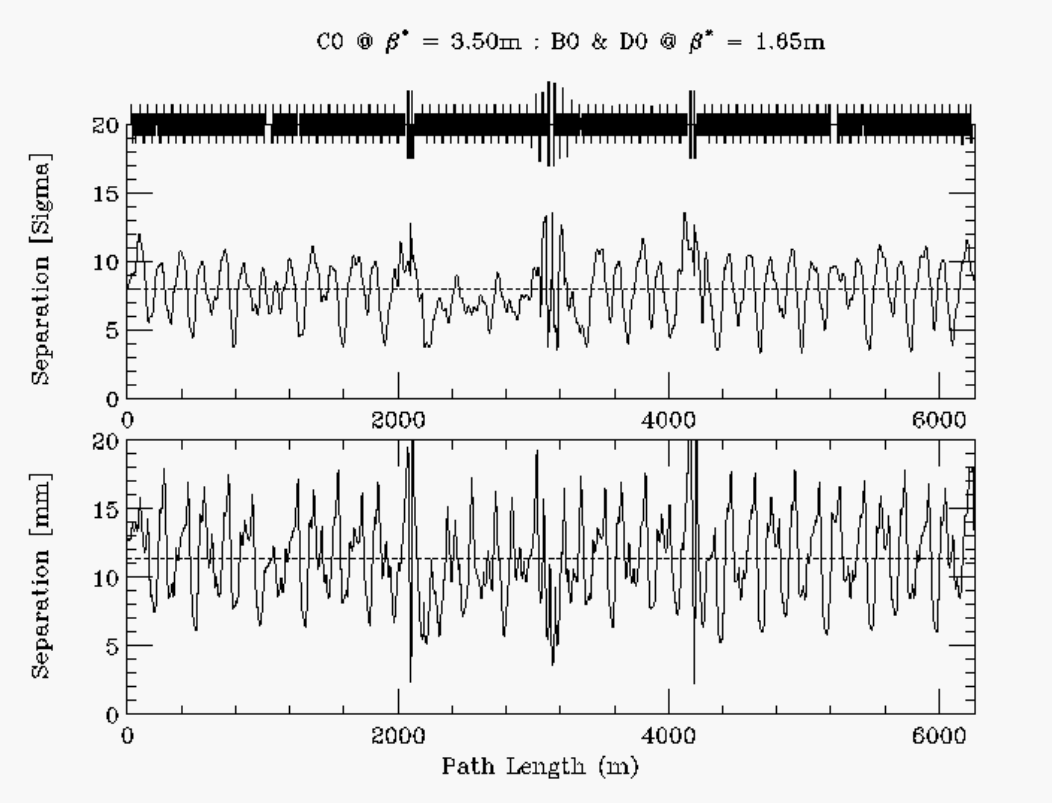

Figure 2-6: Injection helix at 150 GeV/c. $\varepsilon_N = 20\pi$ μm & $\sigma_p/p = 6.E\text{-}4$.

2.2.2 C0 Collision Helix

For collisions at C0 the optics at B0 & D0 remain in their Injection configuration. In this case, all the separators in the ring become available for bringing beams together at the C0 IP, while keeping them separated everywhere else. One possible (minimal) separator solution is given in Table 2-6. The selection of separators has not been optimized particularly, other than to ensure adequate beam separation around the ring. Many more combinations still need to be explored.

Figures 2-7 and 2-8 illustrate the beam separation across the insert from B38 – C21, and also the separation around the ring. With this separator solution the closest approach through the insert is at the 1st parasitic crossing, where separation is about 3.7σ. Although 5σ separation is generally believed to be the minimum acceptable separation in the Run II collision lattice, dynamic aperture studies indicate that these 1st parasitic crossings are relatively benign for C0 collisions. Elsewhere in the ring, separation drops close to 5σ in a few spots, but otherwise the average separation is ~8σ. Oscillations in the helix could probably be smoothed further using a larger subset of separators.

Table 2-6: C0 collision separator gradients at 1 TeV/c.

C0 COLLISIONS @ β* = 0.35 m : B0/D0 @ β* = 1.65 m **(1 TeV/c)**					
Horizontal			Vertical		
	#	kV/cm		#	kV/cm
A49	1	0.0	A49	2	25.744
B11	2	0.0	B11	1	-25.744
B17	4	18.112			
B49	2	-40.000	B49	1	-40.000
C11	1	40.000	C11	2	40.000
			C17	4	-20.355
C49	1	13.486	C49	2	0.0
D11	2	-13.486	D11	1	0.0
D48	1	0.0			
			A17	1	0.0

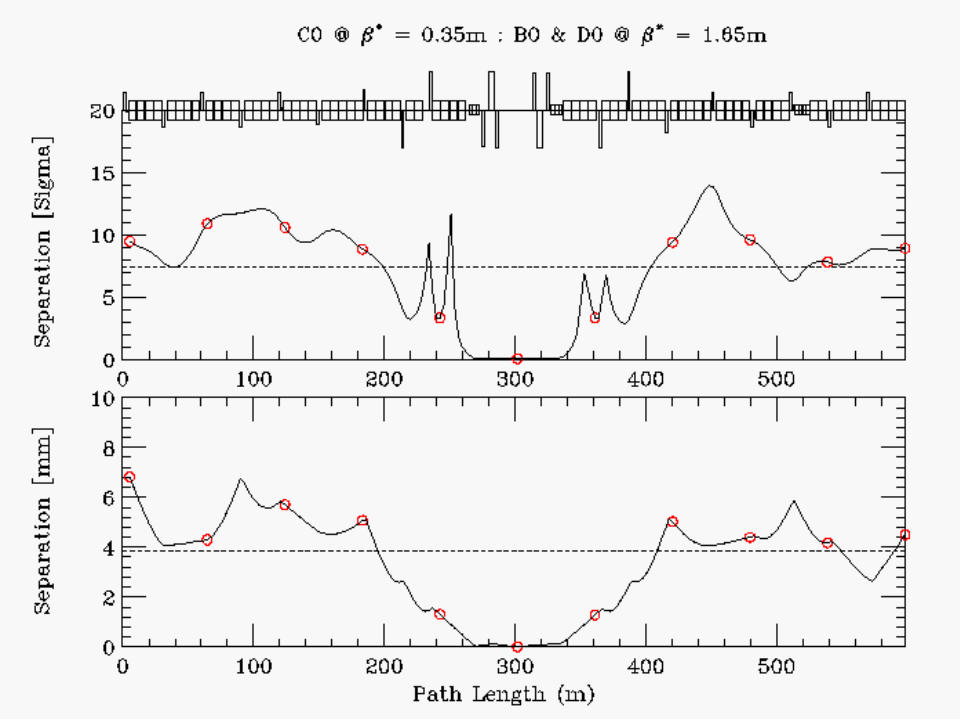

Figure 2-7: Beam separation through the C0 IR during C0 collisions. $\varepsilon_N = 20\pi$ μm & $\sigma_p/p = 1.47E\text{-}4$.

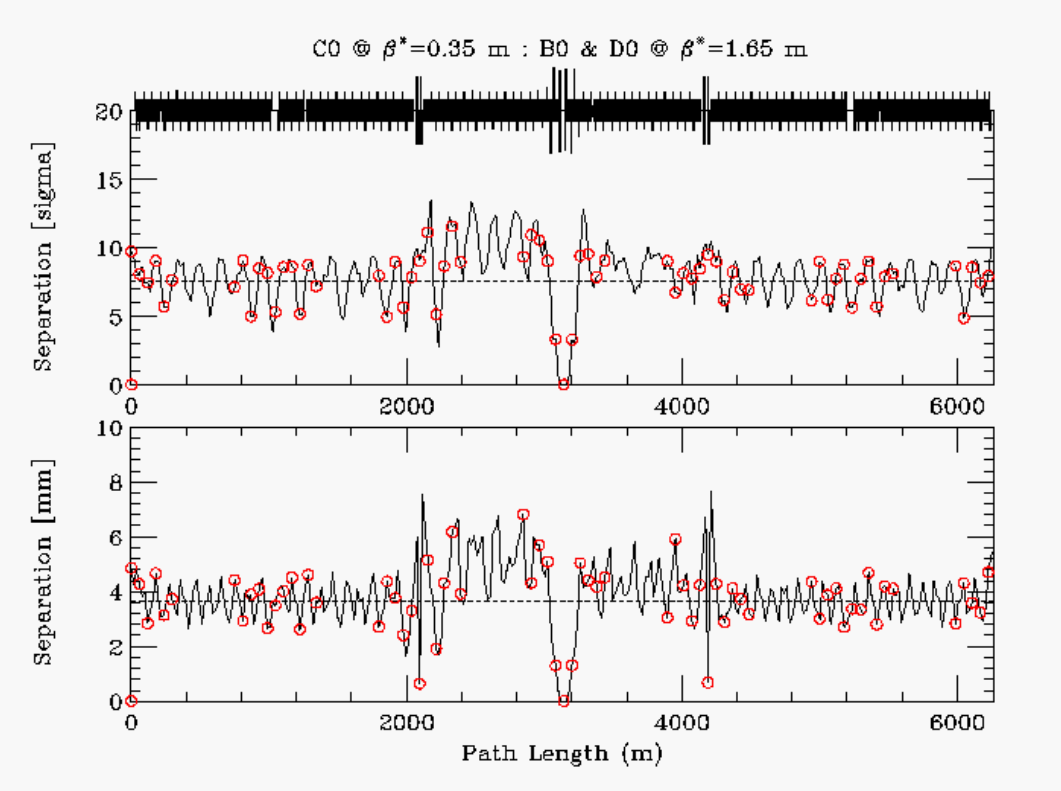

Figure 2-8: Ring-wide beam separation during C0–only collisions. $\varepsilon_N = 20\pi$ μm & σ_p/p = 1.47E-4.

2.2.3 B0/D0 Collision Helix

With collisions at just B0 & D0, the optics at C0 remain at the injection value of β* = 3.50 m, and the B49 & C11 separator voltages are turned up to create horizontal & vertical separation bumps at the C0 IP. Because the phase advance across the C0 separators is nearly 180^o in each plane, to a very good approximation the C0 bumps cancel away from the IR region. The settings of the rest of the ring separators remain essentially unchanged from their nominal Run II B0/D0 collision helix values (see Table 2-7). The resulting beam separation around the machine is shown in Figure 2-9 below. Away from the B0 & D0 IP's beam separation is >5σ everywhere, with an average separation of ~8.5σ.

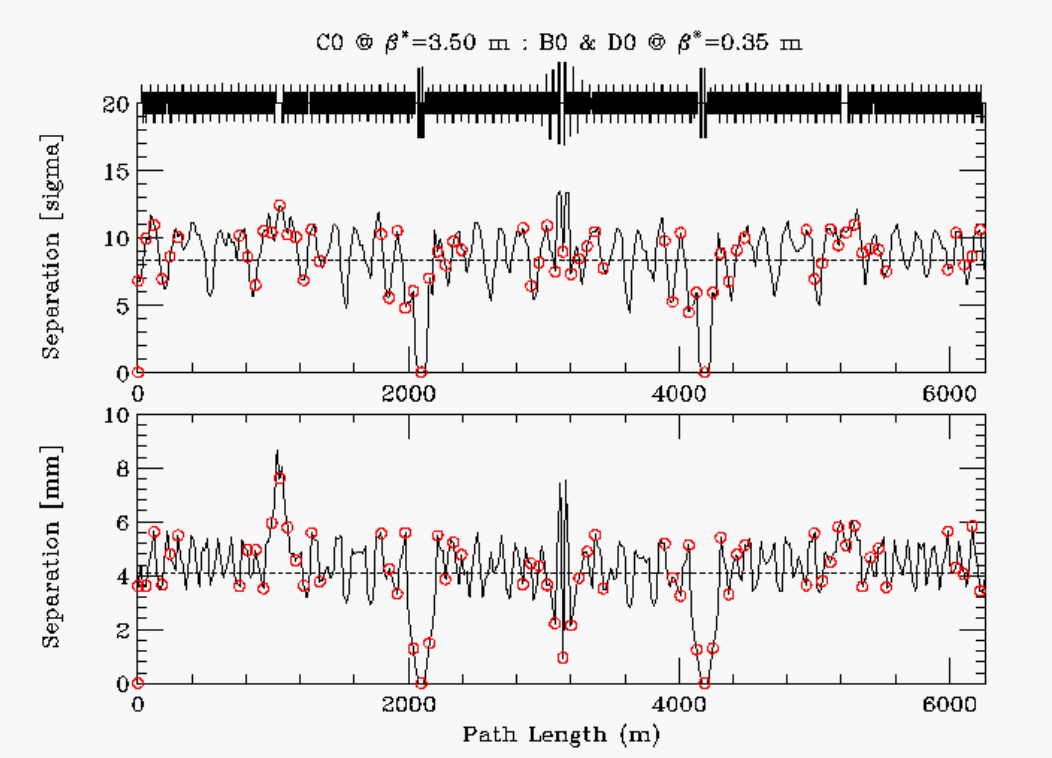

Figure 2-9 Separation during B0 & D0 collisions. $\varepsilon_N = 20\pi$ µm & $\sigma_p/p = 1.47E\text{-}4$.

Table 2-7: Separator gradients for B0/D0 collisions at 1 TeV/c.

B0/D0 COLLISIONS @ β* = 0.35 m : C0 @ β* = 3.50 m **(1 TeV/c)**					
	Horizontal			Vertical	
	#	kV/cm		#	kV/cm
A49	1	40.000	A49	2	-33.287
B11	2	40.000	B11	1	40.000
B17	4	-18.864			
B49	2	40.000	B49	1	40.000
C11	1	40.000	C11	2	40.000
			C17	4	-19.180
C49	1	37.197	C49	2	33.414
D11	2	-34.509	D11	1	40.000
D48	1	-5.162			
			A17	1	1.736

2.3 Orbit Correction and Physical Aperture

From Table 2-8, dipole corrector bumps can be calculated for controlling position and angle at the IP. Tables 2-9 and 2-10 give the correct kick ratios for 2 efficient position bumps and 2 angle bumps in each plane. Other choices of magnet combinations are possible. The dipole correctors have integrated fields of 0.48 T·m. At 1 TeV/c this translates into a maximum kick angle of 144 μrad. Solutions (a) use the triplet spool package correctors, while solutions (b) use only arc correctors.

Table 2-8: C0 IR correctors and lattice functions.

C0 IR CORRECTION SPOOL PACKAGES							
Site	Spool Type	Elements	βx (m)	μx (2π)	ηx (m)	βy (m)	μy (2π)
B38	TSE	HD, QTF, SxF	90.4	0.005	3.66	29.6	0.018
B39	TSB	VD, QTD, SxD	33.2	0.104	3.00	87.2	0.110
B42	TSC	HD, QTF, SxF	103.6	0.182	5.87	30.0	0.217
B43	X1	VD, QT, SxD	29.8	0.278	3.57	100.2	0.301
B44	X1	HD, QT, SxF	84.6	0.371	5.54	32.3	0.395
B45	TSP	H&VD, SQ, H&VBPM	23.1	0.491	2.22	102.7	0.476
B46	TSP	H&VD, SQ, H&VBPM	92.9	0.622	1.48	66.6	0.552
B47	X2	H&VD, H&VBPM	33.4	0.723	0.32	210.6	0.588
B48	X2	H&VD, H&VBPM	123.8	0.767	0.43	1.70	0.777
B49	TSH	H&VD, SQ, VBPM	160.7	1.240	0.00	875.0	1.047
C0 U	X3	H&VD, SQ, H&VBPM	1042.	1.247	0.00	1017.	1.049
C0*			0.35	1.494	0.00	0.35	1.297
C0 D	X3	H&VD, SQ, H&VBPM	1017.	1.742	0.00	1042.	1.545
C12	X2	H&VD, H&VBPM	17.3	1.778	0.43	95.4	2.018
C13	X2	H&VD, H&VBPM	253.4	2.207	2.53	30.6	2.087
C14	TSP	H&VD, SQ, H&VBPM	59.9	2.247	1.03	95.7	2.171
C15	TSP	H&VD, SQ, H&VBPM	99.0	2.320	1.88	17.0	2.356
C16	X1	VD, QT, SxD	20.6	2.447	2.08	104.1	2.474
C17	X1	HD, QT, SxF	90.1	2.558	5.32	29.7	2.571

HBPM & VBPM	- position monitors	
HD & VD	- trim dipoles	0.48 T·m
QTF & QTD	- tune quads	7.5 T·m/m
SxF & SxD	- chromaticity sextupoles	450 T·m/m^2
QT	- strong trim quads	25 T·m/m
SQ	- skew quadrupole	7.5 T·m/m

Table 2-9: Relative dipole kick strengths to vary the beam positions (x*, y*) at the IP while fixing the angles (x'*, y'*) = 0. Positions (x*, y*) are in mm and θ is corrector kick angle in mrad of the strongest corrector.

	X^* POSITION BUMP COEFFICIENTS		Y^* POSITION BUMP COEFFICIENTS	
	(a)	(b)	(a)	(b)
B45			-0.0706	-0.0052
B46	-0.0861	+0.5043		
B47				
B48				
B49		+1.0 θ		-0.3881
C0U	+0.9882		+1.0 θ	
C0	X* = 19.1 θ	7.3 θ	Y* = 18.4 θ	6.8 θ
C0D	+1.0 θ		+0.9043	
C12				+1.0 θ
C13		-0.5461		
C14			-0.0818	+0.2622
C15	-0.0686	-0.4359		

For position control at the IP the solutions (a), using the triplet correctors, are most effective. With β_{corr} > 1000 m for β* = 0.35 m, and with almost exactly 90° of phase between the correctors and the IP, the beam position can be adjusted by as much as ±2.75 mm. This is nearly 3 times the control possible at the B0/D0 IR's. Furthermore, because there is nearly 180° of phase separating the upstream & downstream packages the cancellation between the triplet corrector kicks is excellent, with very little orbit distortion leaking into the arcs for final elimination. The position bumps (b) use only arc spool packages. These would be useful either to supplement the triplet corrector solution, or to provide the IP position control in the event that the triplet dipoles are being used primarily to compensate for triplet quad mis-alignments. In any case, with the much smaller β-functions in the arc, solutions (b) are comparable to the orbit control at B0 & D0. At full corrector field the beam positions at the IP can be shifted by ±1.0 mm with solutions (b).

Table 2-10: Relative dipole kick strengths to vary the angles (x'*, y'*) at the IP while fixing the beam positions (x*, y*) = 0. Angles (x'*, y'*) are in μrad and θ is corrector kick angle in μrad of the strongest corrector.

	X'* ANGLE BUMP COEFFICIENTS		Y'* ANGLE BUMP COEFFICIENTS	
	(c)	(d)	(c)	(d)
B45			+1.0 θ	+1.0 θ
B46	-0.6812	+0.8620		
B47				-0.6505
B48		-0.5443		
B49				
C0U	-0.1467		+0.3003	
C0	X'*= 7.8 θ	11.2 θ	Y'*= 7.6 θ	11.4 θ
C0D	+0.2772		-0.1336	
C12				+0.6029
C13		+0.5708		
C14			+0.6419	-0.8284
C15	+1.0 θ	+1.0 θ		

For angle control at the IP there is no overpowering reason to prefer one of solutions (c) or (d) over the other. In either case the IP angle must be generated out in the arcs and the level of angle control possible at the IP is limited by the aperture in the low beta triplet quadrupoles rather than the available field strengths of the correction dipoles. For a 20π μm beam at 1 TeV, and β_{max} = 1660 m in the triplets, the 1σ beam width is ~2.5 mm. The quadrupole physical aperture has a radius of only 31.5 mm. In an extremely optimistic scenario which imagines the beam orbit can be displaced by as much as 25 mm in the triplet quadrupoles, the corresponding angle control at the IP is ±1.04 mrad.

2.4 Higher Order Correction

2.4.1 Quadrupole Misalignment

The effects of misaligned quadrupoles other than the triplet quadrupoles are straightforward to correct using the arc correction spools between B38 and C17 listed in Table 2-8. The following discussion therefore is limited to the triplets.

Two types of misalignment are particularly harmful – transverse misalignments, which deliver kicks to the beam, and roll of the quadrupoles about the longitudinal axis, leading to coupling of the two transverse planes. The beam optics are not as sensitive to other misalignments, such as displacement of the magnets along their longitudinal axis. Transverse misalignments can be corrected using the position bumps described in the preceding section. With maximum integrated fields of 0.48 T·m, the triplet spool correction dipoles can compensate for systematic transverse displacements of the triplet by ±0.5 mm, and random transverse errors of ±0.25 mm.

Rolls of the triplet quadrupoles introduce coupling that degrades luminosity. Although this coupling can be corrected globally with distributed skew quadrupoles, reduction in luminosity is unavoidable unless there are skew correction elements located physically at the triplets. Table 2-

11 lists the locations of skew quadrupoles, and their contributions to the real & imaginary components of the coupling coefficient. Because there is essentially zero phase advance across the triplets it can be seen that the triplet skew quad elements at C0U & C0D are ideally situated to correct for roll errors of the triplet magnets.

Table 2-11: Skew quadrupole locations and their real & imaginary coupling components. The midpoint optics values of the Q1, Q2, and Q3 IR magnets are also given.

SKEW QUAD CORRECTORS FOR TRIPLET ROLL MIS-ALIGNMENTS					
Spool	βx (m)	βy (m)	2π (μx - μy) (deg)	$\sqrt{\beta x \beta y} \cdot \cos(\Delta\mu)$ (m)	$\sqrt{\beta x \beta y} \cdot \sin(\Delta\mu)$ (m)
PACKB45	23.1	102.7	5.4	48.49	4.58
PACKB46	92.9	66.6	25.2	71.17	33.49
PACKB49	160.7	875.0	69.5	131.32	351.24
Q3D	570.0	1593.	70.9	311.75	900.28
PACKC0U	1042.	1017.	71.3	330.05	975.08
Q2F	1660.	467.9	70.9	288.44	832.96
Q1D	619.5	538.0	70.9	188.90	545.50
Q1F	538.0	619.5	70.6	191.75	544.50
Q2D	467.9	1660.	71.3	282.62	834.95
PACKC0D	1017.	1042.	70.9	336.84	972.75
Q3F	1593.	570.0	71.3	305.46	902.43
PACKC14	59.9	95.7	27.4	67.22	34.84
PACKC15	99.0	17.0	-13.0	39.97	-9.23

To estimate the integrated skew gradient of the triplets, 1000 random cases have been studied with all six quadrupoles rolled independently. With uniformly distributed rolls between ±Φ, the real and imaginary parts of the integrated skew gradients (when multiplied by $\sqrt{\beta_x \beta_y}$) are 980 and 2835Φ T·m, respectively (with Φ in mrad). The maximum integrated field of the C0U & C0D skew quadrupoles is 7.5 T·m/m, so that the triplet correctors are capable of compensating *locally* for random roll angles Φ as large as 2.5 mrad. For larger roll mis-alignments the B49 corrector is useful for global compensation, and the B45, B46, and C14, C15 correctors can be used to fine tune cancellation of the real coupling component.

2.4.2 Feeddown Circuits

The Tevatron sextupole and skew sextupole circuits are used to adjust the tunes and coupling of the protons and pbars independently during collider operation. In particular, these circuits can adjust the difference in horizontal & vertical tunes, and sine and cosine components of the coupling between the proton and pbar helices. The 7 feeddown families and their functionality in Run II are listed in Table 2-12. Four of the families are used for the injection helix and another set of four is used for the B0/D0 collision helix. (The S1 family is shared.) The family elements are given in Table 2-13.

Table 2-12: Feeddown circuits and their functionality: $\Delta\nu_x$, $\Delta\nu_y$ are the differential tunes; ΔC_{sq}, ΔS_{sq} are the cosine and sine components of the differential coupling.

Circuit	Injection Helix	Collision Helix
S1	$\Delta\nu_x$	ΔC_{sq}
S2	$\Delta\nu_y$	
S3	ΔC_{sq}	
S4		$\Delta\nu_x$
S5		$\Delta\nu_y$
S6	ΔS_{sq}	
S7		ΔS_{sq}

Table 2-13: Locations, magnet elements, and polarities of the 7 feeddown family members.

Circuit Name	Polarity	Magnet location	Spool type	Circuit Name	Polarity	Magnet location	Spool type
C:S1B1A	-	B19	E	C:S3A2A	+	A17	C
C:S1B3A	+	B38	E		-	A24	C
C:S1C2A	+	C24	E	C:S3D2A	-	D19	C
	-	C32	G		+	D26	C
C:S1E2A	+	E24	E	C:S3D4A	+	D38	C
	-	E28	E		-	D46	C
C:S1F2A	+	F19	E	C:S3E1A	-	E17	C
	-	F26	G		+	E22	C
C:S1F3A	+	F34	E	C:S3E3A	-	E32	C
	-	F38	E		+	E36	C
C:S2A1A	-	A14	D	C:S4C2A	+	C19	E
C:S2A3A	+	A33	D		-	C26	G
C:S2B4A	-	B43	D	C:S4C2B	+	C22	G
	+	B47	D		-	C28	E
C:S2C3A	+	C27	D	C:S4F2A	+	F24	E
	-	C33	D		-	F28	E
C:S2D2A	-	D23	D	C:S5A2A	+	A18	D
	+	D27	D	C:S5A3A	-	A37	D
C:S2F1A	+	F12	D	C:S5D3A	-	D33	D
	-	F16	D		+	D37	D
C:S2F2A	+	F23	D	C:S5F1A	-	F14	D
C:S2F4A	-	F43	D	C:S5F3A	+	F33	D
				C:S6A4A	+	A46	T:SF
				C:S6C4A	-	C46	T:SF
				C:S7B1A	+	B14	T:SD
				C:S7D1A	+	D14	T:SD

- Spool types TSC & TSD contain skew sextupoles -- all others contain normal sextupoles.

When the beams travel off-axis through the sextupoles, they see feeddown normal and skew quadrupoles, the effects of which depend on the orientation of the helix, and the polarity and tilt angle of the magnet. Installation of the C0 interaction region will eliminate the 2 skew sextupoles at B43 and B47 from the S2 family. The S2 family is used for adjusting the differential vertical tune, and is used only with the injection helix. Two possibilities are currently being explored to compensate for the missing elements: (i) Since there will still be 10 S2 elements distributed in the ring, it might be acceptable simply to increase the S2 circuit current by ~20%; (ii) It should be possible to move these 2 elements to other locations in the ring which have the appropriate helix orientation & lattice functions. Example replacement sites are listed in Table 2-13 below.

Table 2-13: Possible locations in the ring where the B43 & B47 skew sextupole S2 circuit elements could be relocated.

Site	Spool	βx (m)	βy (m)	μx – μy (deg ^{o})	Xo (mm)	Yo (mm)
B43	TSD	32.7	95.4	26.6	-0.50	-5.20
D43	TSD	33.1	94.9	30.8	+0.66	+5.76
E43	TSF	33.2	93.9	29.2	-0.67	-5.86
B47	TSD	30.5	89.8	28.1	+3.62	+4.02
E27	TSFR	30.7	93.2	28.1	+3.73	+6.39
E47	TSFR	30.5	92.8	25.5	-4.08	-6.01

2.5 Dynamic Aperture Calculations

Realistic tune footprint and dynamic aperture calculations require the inclusion of lattice nonlinearities. The studies described below include the B0/D0 IR triplet quadrupole multipoles, chromatic sextupoles, and the multipoles of the C0 LHC triplet magnets. The LHC multipoles are listed in Table 2-14. All calculations correspond to the top energy of 980 GeV for C0 collisions at β* = 35 cm on the collision helix.

Table 2-14: LHC quadrupole magnetic nonlinearities included in dynamic aperture studies.

LHC HARMONICS @ 11922 A					
	Average	Sigma		Average	Sigma
b3	0.31	0.47	a3	-0.57	0.65
b4	0.02	0.48	a4	0.30	0.39
b5	-0.03	0.13	a5	-0.38	0.18
b6	-0.02	0.45	a6	-0.04	0.11
b7	-0.01	0.03	a7	0.01	0.03
b8	0.00	0.02	a8	0.01	0.03
b9	0.03	0.01	a9	-0.02	0.03
b10	0.01	0.02	a10	-0.03	0.02

- LHC harmonics reported in "units" at a reference radius of 17 mm.
- Harmonics are a weighted average over body + end fields for 6 magnets.
- All data taken at 215 T/m.

2.5.1 Single Beam

The single beam tune footprint can be a good measure of the impact of the machine nonlinearities on the beam. Figures 2-10a,b show the tune footprint extending to amplitudes of 6σ in each plane. Without the C0 triplet magnet errors the horizontal tune spread is twice the vertical spread at ($\Delta\nu_X$, $\Delta\nu_Y$) = (8E-5, 4E-5). The inclusion of the C0 IR errors does not greatly affect the tune spreads; ($\Delta\nu_X$, $\Delta\nu_Y$) = (8E-5, 6E-5), but it can be seen that the shape of the distribution is appreciably altered. For comparison, the corresponding tune footprint in the current Run II Tevatron lattice with B0/D0 collisions is shown in Figure 2-11. The Run II B0/D0 lattice tune spread is approximately 6E-4 in both planes – a factor of 10 or more broader than in the C0 collision lattice.

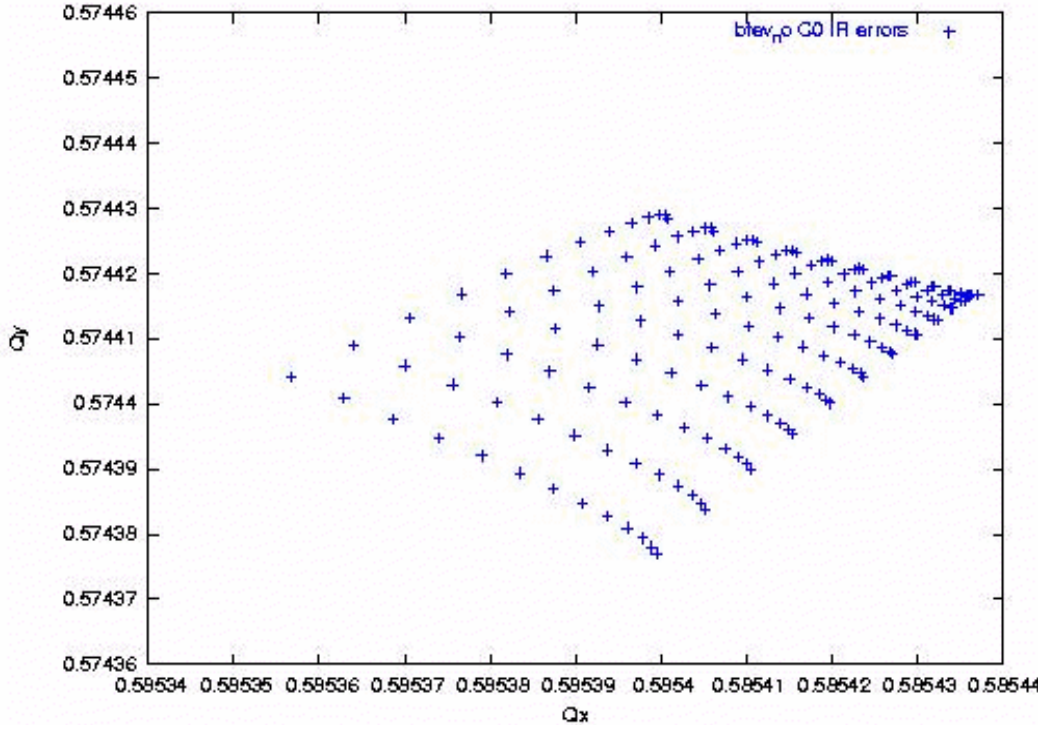

Figure 2-10a: Single beam tune footprint, in the absence of C0 IR quadrupole errors. The base tunes are (.585, .575).

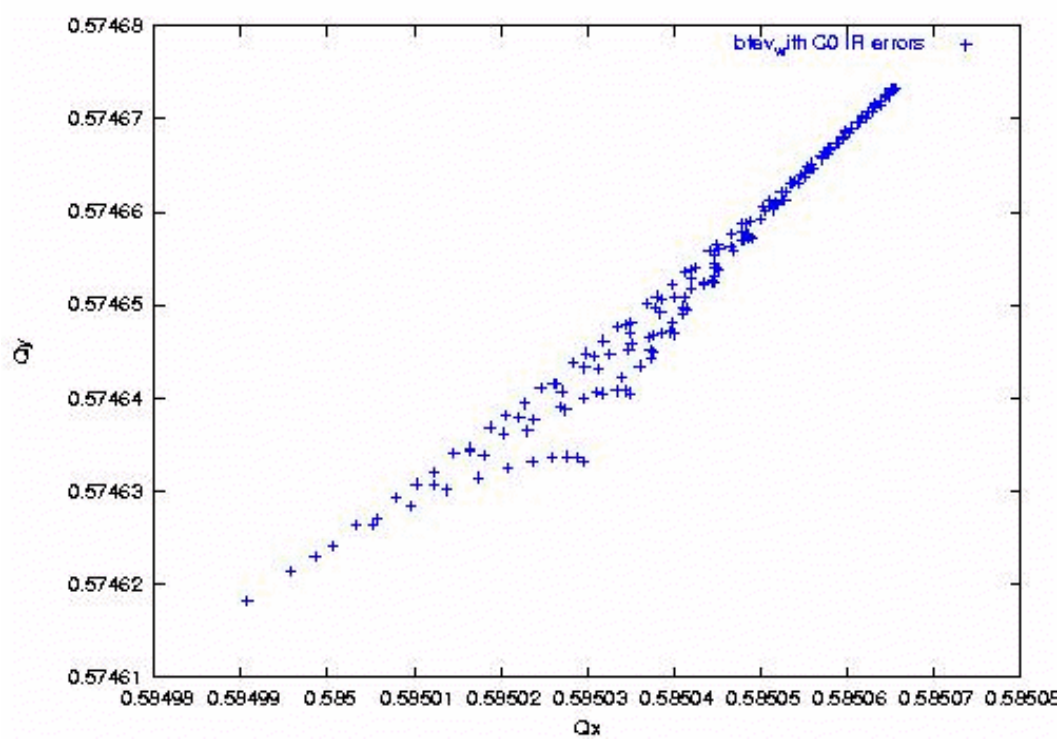

Figure 2-10b: Single beam tune footprint, with the C0 multipole errors of Table 2-14 also included. The base tunes are (.585, .575).

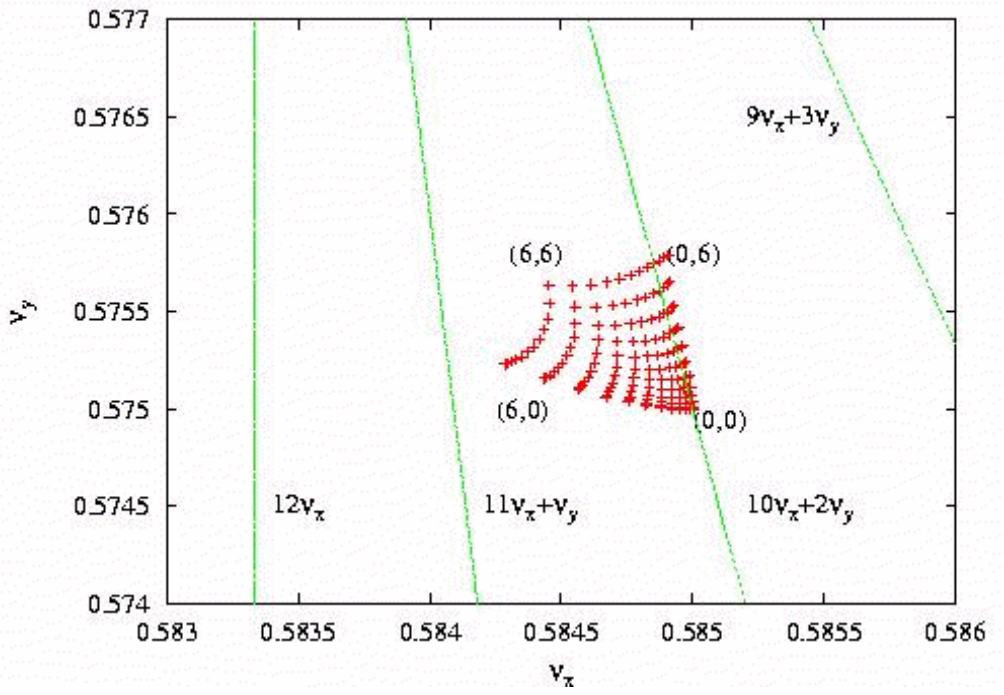

Figure 2-11: Tune footprint of a single beam in the current Run II lattice, with collisions at B0 & D0.

The dynamic aperture is calculated by launching particles at several angles in x – y space. In the following calculations 13 launch points were taken, spaced apart by 7.5^{o} from 0^{o} (horizontal) to 90^{o} (vertical). The radial dynamic aperture at each angle is then calculated to be the largest stable amplitude below which all amplitudes are stable. A comparison of the single beam dynamic aperture with the dynamic aperture including beam-beam forces indicates the relative importance of beam-beam effects.

Figure 2-12 shows the calculated single beam dynamic aperture for C0 collisions averaged over 5 seeds for the magnetic multipoles. The maximum separation launched was 25σ. The average dynamc aperture is 24σ – well beyond the physical aperture of the low–β quads. From Figure 2-13 it can be seen that this C0 collision lattice average dynamic aperture is nearly twice as large as the single beam dynamic aperture calculated for Run II B0/D0 collisions. In that case, also calculated for Δ_p/p = 3E-4, the average dynamic aperture is just 12.3σ

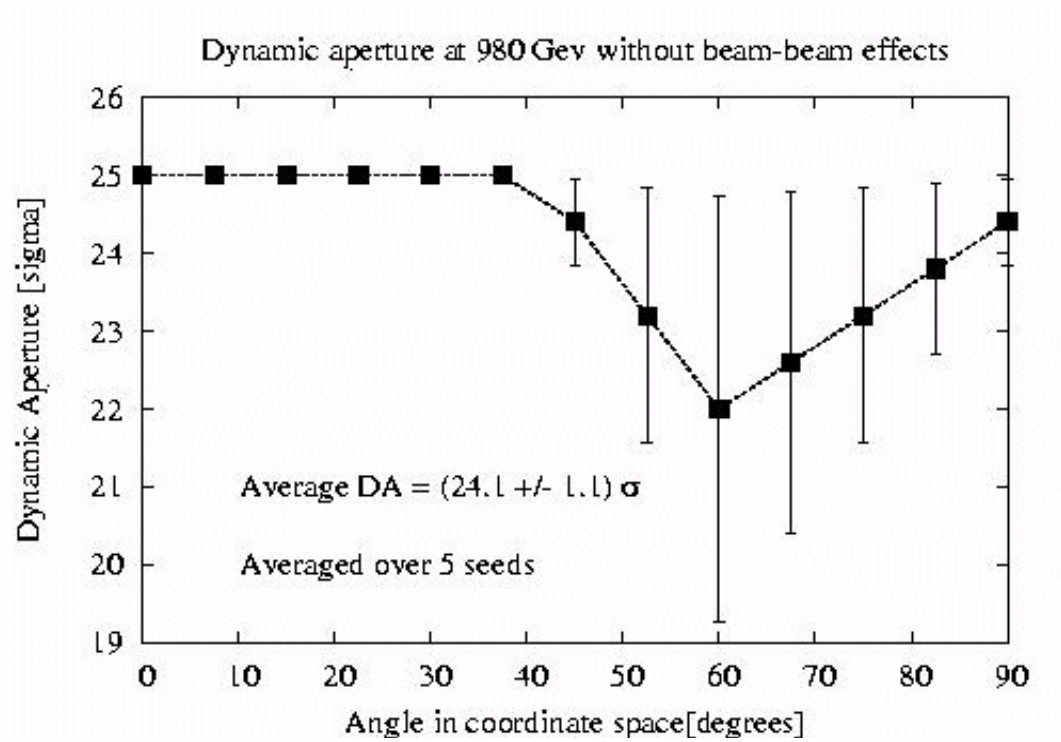

Figure 2-12: Single beam dynamic aperture for C0 collisions with ε_N = 20π μm & Δ_p/p = 3E-4.

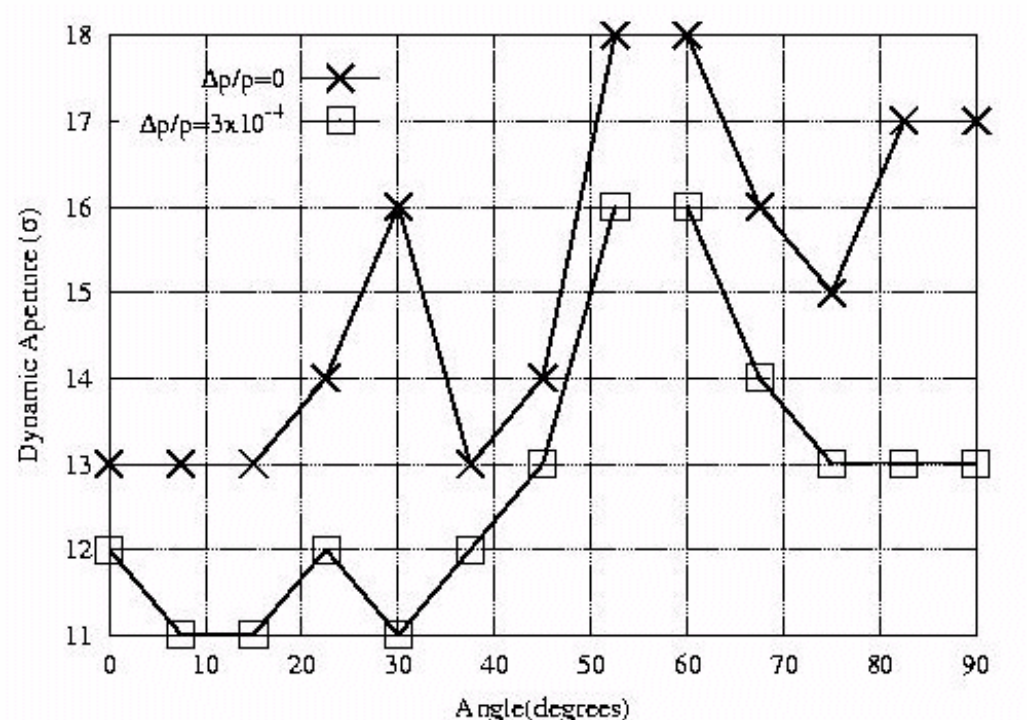

Figure 2-13: Current Run II B0/D0 collision lattice. Single beam dynamic aperture with ε_N = 20π μm & Δ_p/p = 3E-4

2.5.2 Beam-beam

With 36x36 operation there are 71 long-range interactions between the separated proton and pbar bunches in addition to the head-on collision at the C0 IP. The long-range interactions are more complex than the head-on collisions. In addition to changing the tunes, these parasitic interactions also change the orbits, coupling, and chromaticity.

The tune footprint for pbar bunch #6 is shown in Figure 2-14., including the beam-beam forces in addition to the magnetic nonlinearities discussed earlier. The tune spread has grown by about 2 orders of magnitude compared to the single beam analysis, to ($\Delta\nu_x$, $\Delta\nu_y$) = (8E-3, 9E-3). This spread is still a factor of 3 or more less than the corresponding footprint for the Run II B0/D0 collision lattice, as given in Figure 2-15. In the Run II lattice the spread is approximately equal in both planes at $\Delta\nu$ = 2.3E-3. In both of these cases most of the contribution comes, not from the head-on collisions, but from the 1st parasitic crossings on each side of the IP. While the beam separation at the C0 first parasitics is ~3.7σ, or about half the separations at B0 & D0's nearest misses in Run II, this is compensated to a large extent by there being only one IP and two nearest miss points, as compared to the two IP's and four nearest misses of Run II.

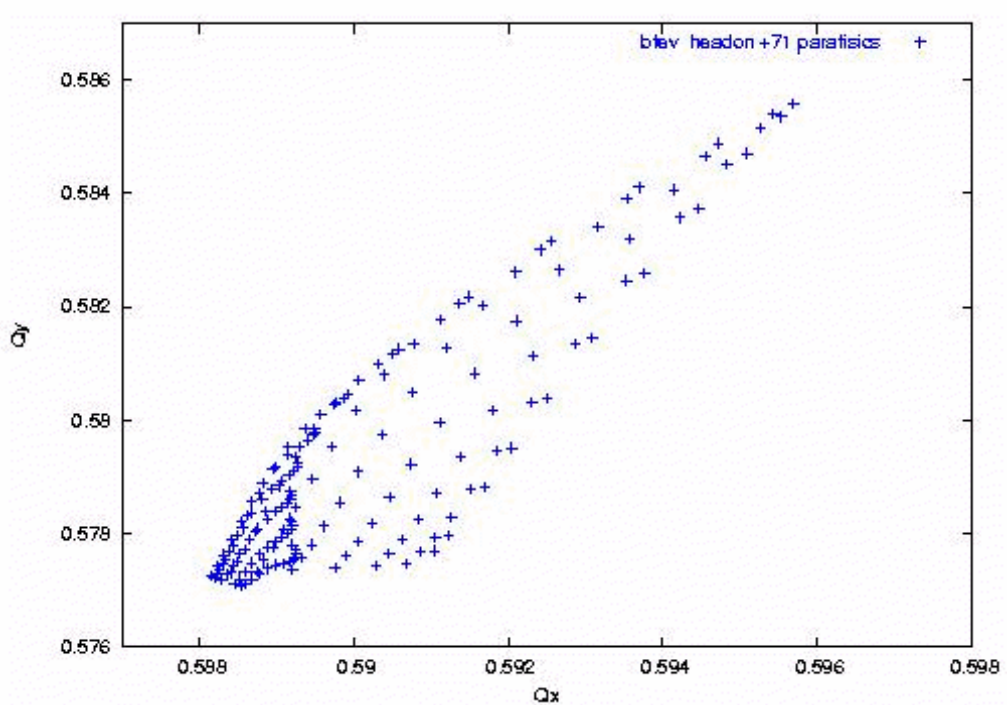

Figure 2-14: Tune footprint of pbar bunch #6 including beam-beam effects for the head-on collision plus the 71 long-range interactions in the C0 collision lattice.

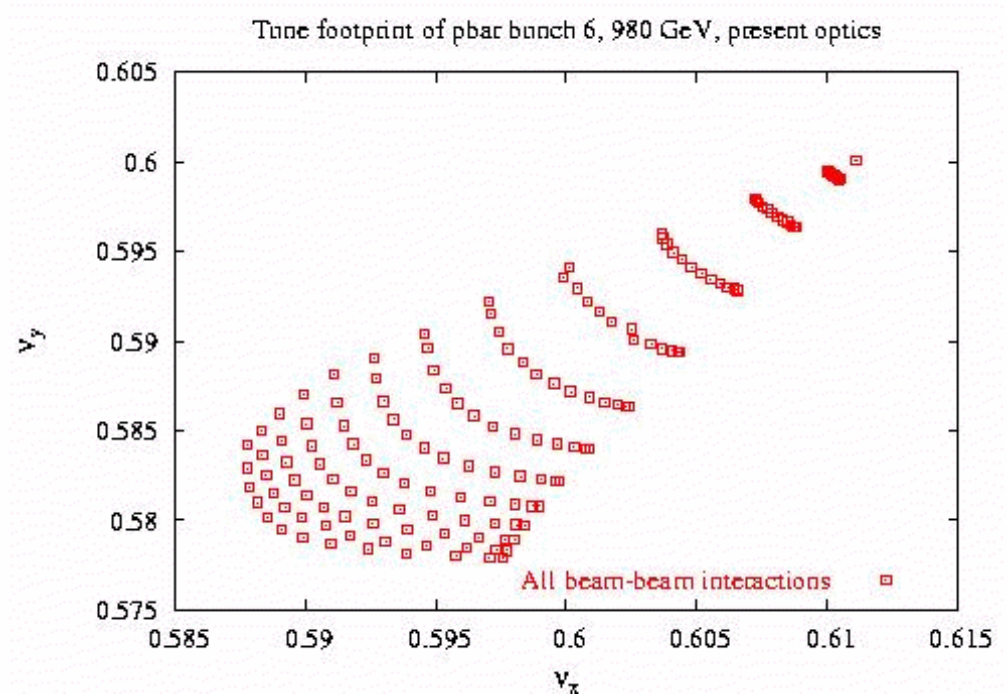

Figure 2-15: Current Run II B0/D0 collision lattice. Beam-beam effects are included for the 2 head-on collisions plus the 70 long-range interactions.

Figure 2-16 shows the dynamic aperture including beam-beam effects for C0 collisions, averaged over the magnetic multipoles generated by 5 seeds. The average dynamic aperture is 14σ, indicating that beam-beam effects reduce the aperture of the machine by a substantial 10σ. However, this analysis also suggests that the minimum dynamic aperture of 12σ should exceed the physical aperture set by the primary collimators, which are typically placed at ~6σ. By comparison with Figure 2-17 it can be seen that the average dynamic aperture in the C0 collision lattice is roughly twice as large as the 8σ average calculated for Run II B0/D0 collisions, and, furthermore, the C0 *minimum* dynamic aperture of 12σ even significantly exceeds the *maximum* 9σ dynamic aperture of the Run II lattice.

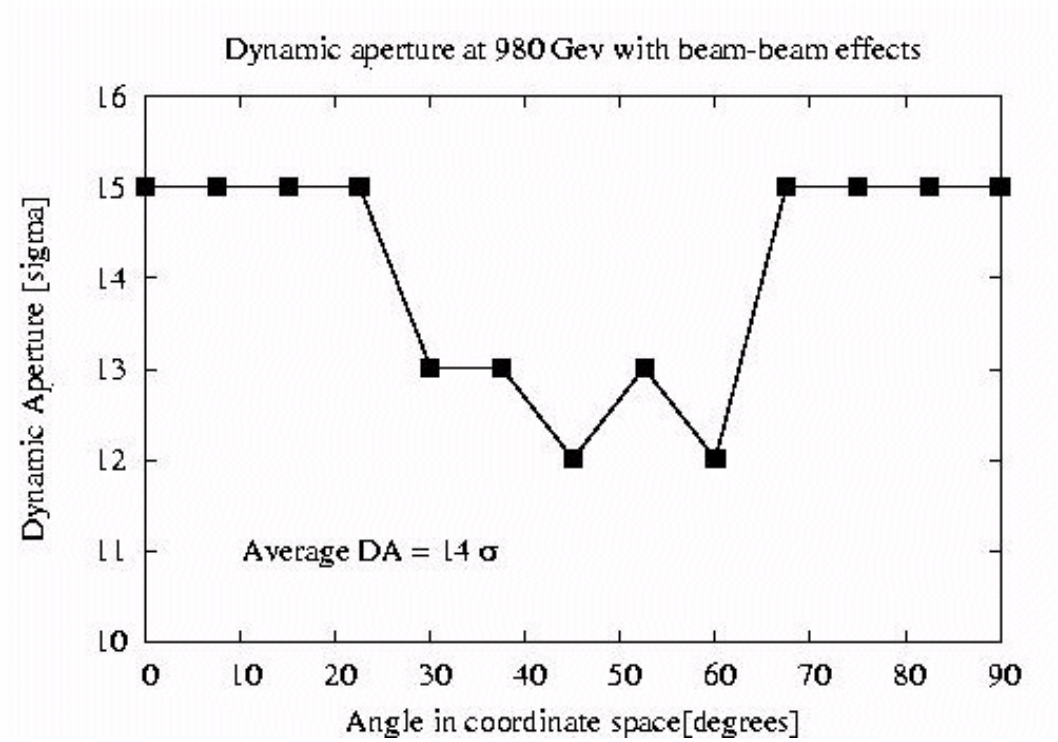

Figure 2-16: Dynamic aperture of pbar bunch #6 with beam-beam effects in the C0 collision lattice.

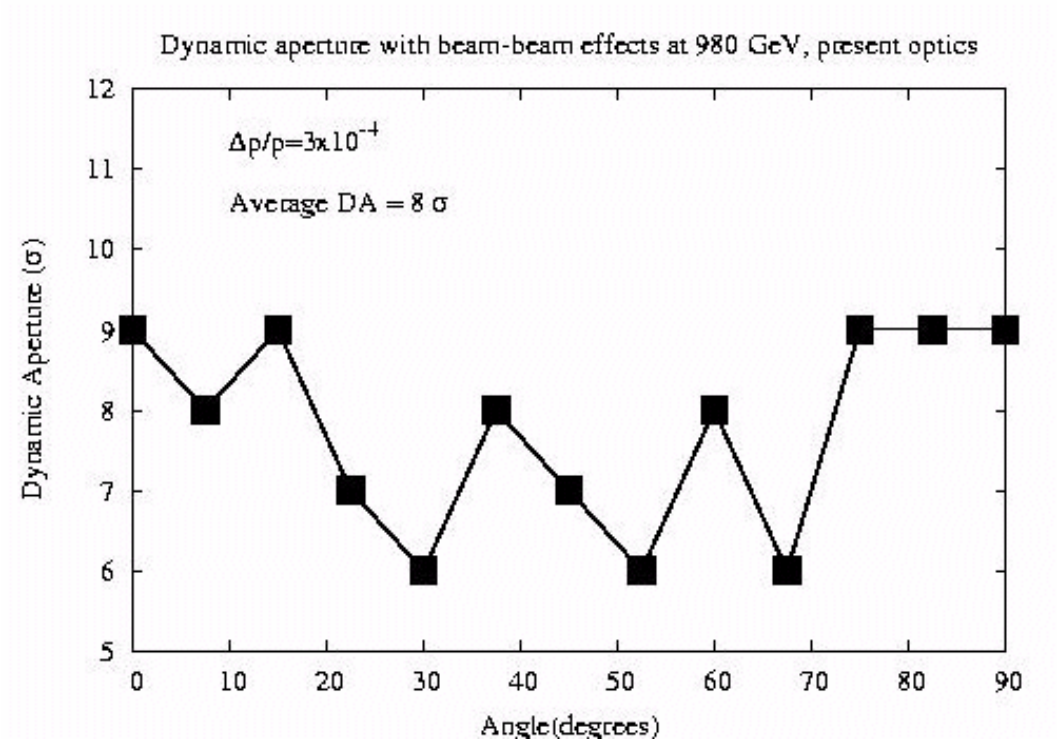

Figure 2-17: Current Run II B0/D0 collision lattice. Dynamic aperture including beam-beam effects.

2.6 Beam Halo Calculations and Collimators

Calculations in progress. NM, SD.

2.7 Emittance Growth Calculations

Calculations to be done.

3 LHC Style Quadrupoles

3.1 Overview and Conceptual Design

The C0 IR described in section 2.0 requires quadrupoles of a new design for the Q1 through Q5 magnets. Table 3-1 shows the locations, gradient, magnetic length and mechanical slot length requirements of these elements. The nominal operating temperature is 4.5K.

Table 3-1: Q1 – Q5 Parameters

Magnet	Nominal Gradient	Magnetic Length	Magnetic Center	Mechanical Slot Length
	(T/m)	(m)	(m from IP)	(m)
Q1	169.2	2.41	14.263	3.520
Q2	165.4	4.43	18.749	5.476
Q3	169.2	2.39	24.661	3.520
Q4	170.0	2.01	65.115	2.974
Q5	170.0	1.37	86.911	2.441

To meet these requirements, we propose a design based on the collared coil assembly of the well proven LHC IR quadrupole currently in production, with the magnet length, iron yoke, cryostat, cryogenic system, and interconnects re-optimized for the C0 IR. Figure 3-1 shows a cross-section of the collared coil of such a magnet.

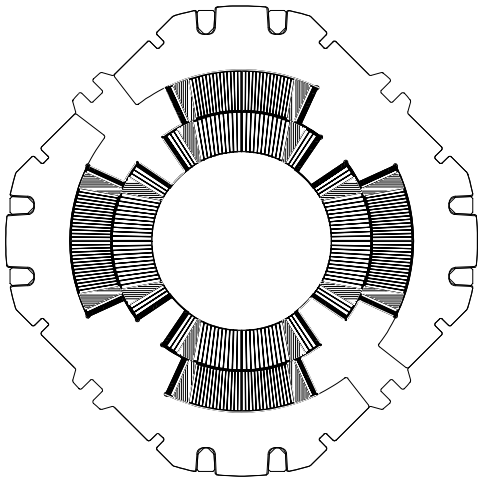

Figure 3-1: LHC Quadrupole Collared Coil.

The coil bore is 70mm, which allows for use of a beam tube with inside diameter 63mm. The reuse of the body design of the LHC quadrupole provides confidence that these magnets can work with minimal redesign, optimized for the Tevatron system. The C0 optics requires a

gradient which is 20% lower than that of the LHC quadrupole. Independent of this, no changes in the coil design or body mechanical support are envisioned. Optimizations will focus on reducing the iron yoke diameter and overall cryostat size such that the height of the beam above the tunnel floor in the Tevatron can be accommodated without any new civil construction in the tunnel.

Changes that have been made include

- Reducing the iron yoke OD
- Reducing the overall magnet OD
- Changing the mechanical support of the ends
- Changing the quadrant splice design
- Changing the expansion loop design
- Changing the pipes included and the interfaces of the cryostat
- Reducing the overall diameter of the cryostat

The redesign of the iron yoke results in a yoke OD of 266.7mm, and an anticipated total OD including stainless steel skin of approximately 280mm. Figure 3-2 illustrates the yoke redesign.

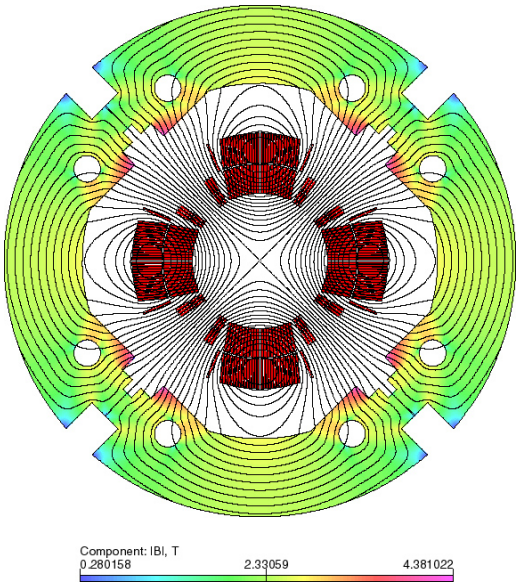

Figure 3-2: C0 IR Magnet Yoke Cross Section

Given the smaller magnet, and the elimination of a superfluid helium heat exchanger required in the cryostats of the LHC Inner Triplet, the C0 quadrupole cryostats are expected to be only 1/2 the diameter of the LHC cryostats, and allow for the beam height to be located 10" above the nominal Tevatron tunnel floor. The cold magnetic length of any of the Q1 to Q5 magnets is expected to be approximately 0.24m shorter than the warm mechanical length of the cold mass, end plate to end plate, as depicted in Figure 3-3. The length of the quadrant splice block, expansion loops, bus connections, instrumentation wires, and other components are included in the cryostat layouts, and at this stage appear consistent with the mechanical slot lengths listed in Table 3-1, as constrained by the lattice design. These lengths are still being optimized.

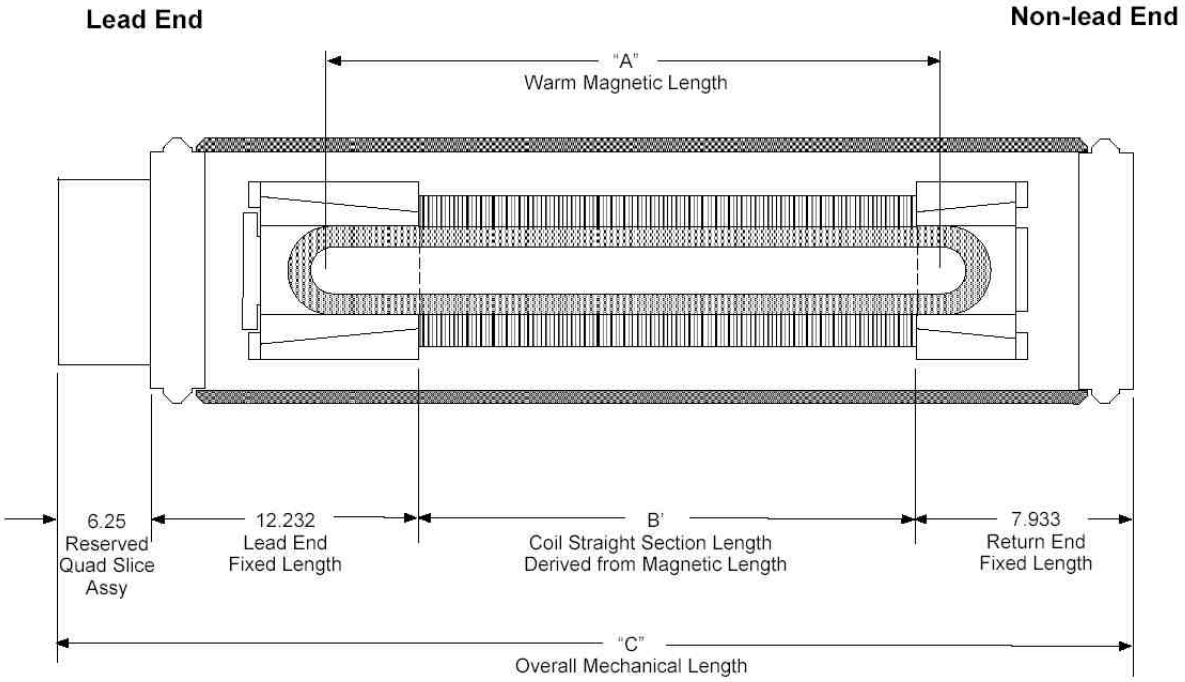

Figure 3-3: Magnetic / Mechanical Length Schematic (dimensions in inches)

The following sub-chapters document the basic quadrupole design, noting the important similarities and differences between the two designs. Necessary R&D and infrastructure is summarized in the last sub-chapter.

3.2 Magnet Coils and Mechanical Description

The collared coil of the assembly shown in Figure 3-1 consists of a two-layer coil of 70mm bore, completely supported by steel collars. The inner coil is formed from 37 strand Rutherford cable, using SSC type wire which is uncoated and unannealed. The outer cable is 46 strand Rutherford cable, again from uncoated and unannealed SSC type wire. Both cables are insulated with two wraps of Kapton insulation, with the outermost wrap including a polyimide adhesive. The end parts are of G11CR.

Table 3-2 details the strand parameters. The conductor for the inner layer has a minimum critical current of 378 A, measured at 7T and 4.22K. The conductor for the outer layer has a minimum critical current of 185 A, also measured at 7T and 4.22K. The values are determined in the standard way, and the specifications are taken directly from SSC and the LHC IR Quadrupole program.

Table 3-2: Strand mechanical and electrical specifications

Parameter	Unit	Inner cable		Outer cable	
		Value	Tolerance	Value	Tolerance
Diameter	mm	0.808	± 0.0025	0.6505	± 0.0025
Cu/SC ratio		1.3 : 1	± 0.1	1.8 : 1	± 0.1
Surface coating		None	-	None	-
Anneal		None	-	None	-
Minimum critical current	A	378	-	185	-
Minimum RRR		70		70	
Twist direction		Left		Right	
Twist pitch	mm	13	± 1.5	13	± 1.5

Fig. 3-4 shows the cable size parameters and Table 3-3 summarizes the cable mechanical and electrical specifications. Again, this specification is identical to that used in the LHC IR Quadrupole program, and there are multiple vendors capable of meeting these requirements.

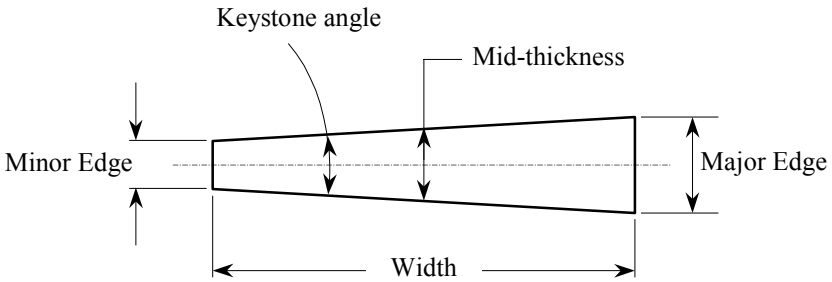

Figure 3-4: Cable size parameters.

Table 3-3: Cable mechanical and electrical specifications

Parameter	Unit	Inner Cable		Outer Cable	
		Value	Tolerance	Value	Tolerance
Number of strands		37	-	46	-
Cable width	mm	15.40	± 0.025	15.40	± 0.025
Minor edge	mm	1.320		1.051	
Cable Mid-thickness	mm	1.465	± 0.006	1.146	± 0.006
Major edge	mm	1.610		1.241	
Keystone angle	degree	1.079	± 0.05	0.707	± 0.05
Transposition length	mm	114	± 5	102	± 5
Lay direction		Right	-	Left	-
Minimum critical current	kA	14.0	-	8.5	-
Minimum unit length	m	200	-	200	-
Residual twist	degree	0 - 90		0 - 90	
Minimum bending radius	mm	7		15	

Figures 3-5 and 3-6 show the inner and outer coils of the LHC quadrupole. For C0 the straight section lengths will be modified but the end parts will remain exactly the same.

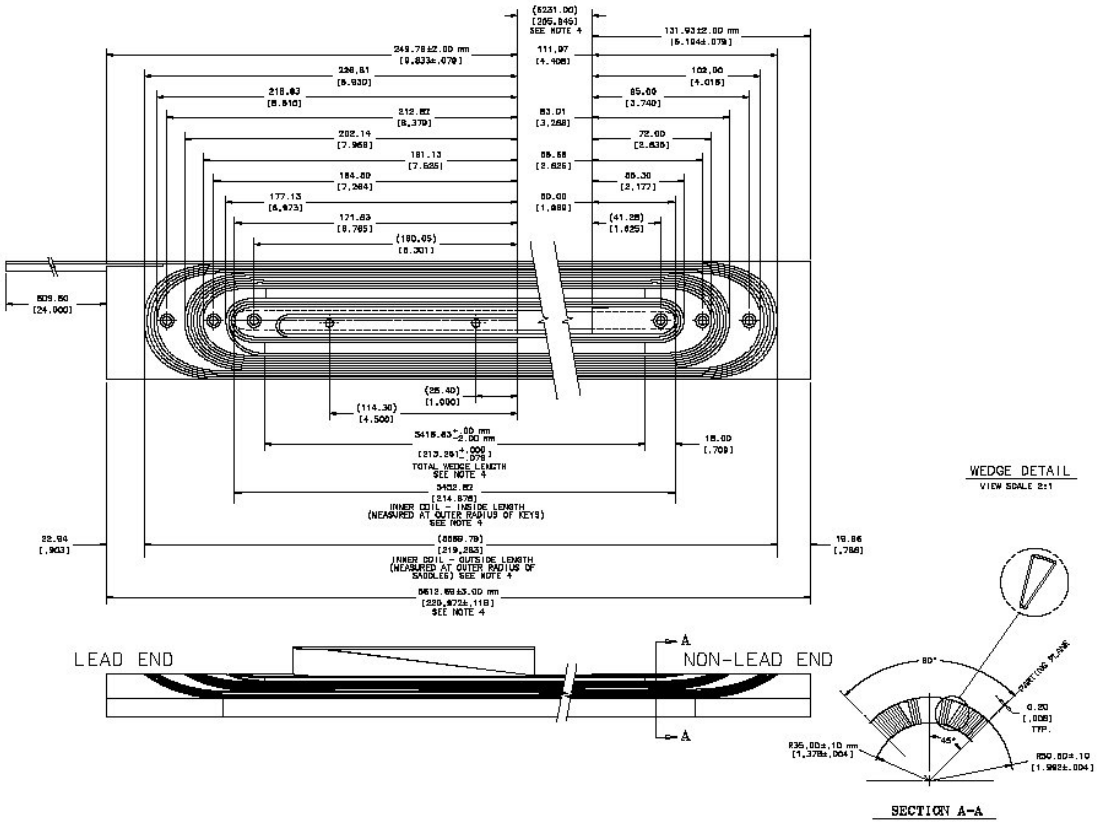

Figure 3-5: LHC Inner Coil. The straight section of the coil will be modified to accommodate the shorter magnet length.

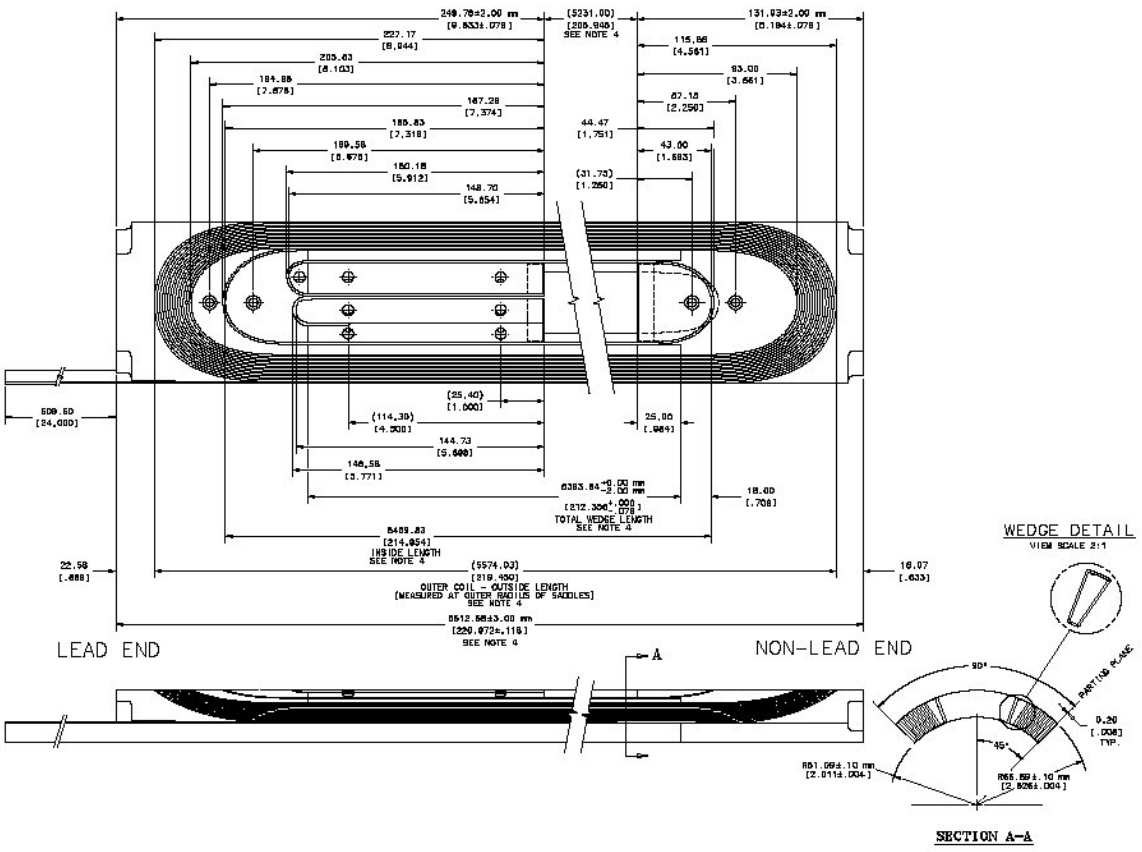

Figure 3-6: LHC Outer Coil. The straight section of the coil will be modified to accommodate the shorter magnet length.

The coils are cured in a two step cure cycle, which sets both the interstrand resistance and the coil size properly. Mechanical support of the coils is provided by Nitronic 40 collars which are stamped, and pre-assembled into 37mm long packs and provide the required rigidity and cooling channels. The collars are keyed with 8 phosphor bronze keys, to a target warm azimuthal prestress of 75MPa in both the inner and outer coils. Prestresses in the range of 55 to 100MPa are known to produce acceptable quench performance. The LHC magnet development and production has included magnets ranging in length from 1.8m to 5.5m having acceptable quench performance. A summary of the 4K quench performance of the LHC model magnets and the LHC prototype magnet is shown in Figure 3-7. The magnets showed no signs of retraining. Since the C0 designs are in between these lengths, we can reasonably expect similarly good quench performance at the maximum C0 operating current of 9560A.

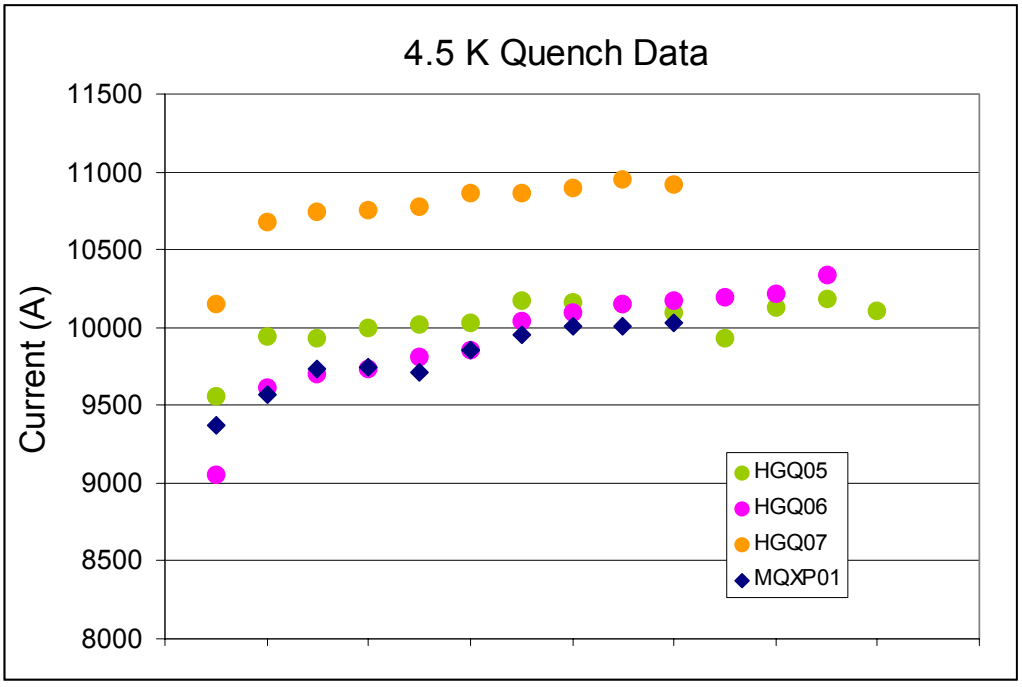

Figure 3-7: LHC Model Magnet and Prototype 4.5K Quench Performance

The iron yoke of the magnet provides flux return, and supports the stainless steel shell that provides helium containment. Since the C0 operating gradient is 20% lower than the LHC requirement, the iron yoke has been re-optimized and the outside diameter reduced to produce a more compact design, with acceptable harmonics. As with the LHC design, we expect to use the ICB welding press to close the skin, after it has been modified for the reduced yoke diameter.

The reduced yoke diameter has an impact on the design of the mechanical support of the ends of the coils. In the LHC magnets, a collet design using tapered blocks and an aluminum end can was used for support of the ends. However, this assembly has an outside diameter of 250 mm, just slightly less than the C0 yoke diameter. Such an assembly would not allow for bus work to pass through the magnet. To accommodate the bus work, full-round collars will be re-introduced to the design, as was used in the early HGQ model magnets and are typically used in other superconducting magnets (LHC arc dipole, for example). Full round collars are identical to the body collars, except that the mechanical pole has been eliminated to allow for the coil end part, as shown in Figure 3-8. Experience has shown that the full round collars can supply the required support, but out-of-plane buckling must be controlled, particularly during assembly. Typically the use of pre-assembled collar packs provides a solution to this problem.

Figure 3-8: Full Round Collar Design, showing coil end parts which must be accommodated

The ends of the cold mass are defined by steel end plates, which are used to anchor the collared coil longitudinally, and provide the geometry for the skin to end plate and end plate to end dome welds to be made. These welds close the cold mass. The thickness of this assembly may be optimized depending on the final weld geometry required for the skin and end dome thicknesses.

The reduced overall diameter of the magnet impacts the quadrant splice block design, which mounts to the lead end of the magnet. The LHC design has the splices in a plane perpendicular to the beam axis, but uses a diameter too large for the C0 design. We have assumed for C0 that the splices will be made parallel to the beam axis, requiring a longer splice block region, as shown in Figure 3-3.

3.3 Field Quality

The C0 IR quadrupole design is based on the LHC quadrupole [1] which was designed to operate at 1.9K in superfluid helium with the critical current and temperature margins necessary to operate in a large radiation induced heat load. The C0 IR quadrupole will utilize this proven design – particularly the collared coil assembly which determines the basic field properties – with modifications as necessary to meet C0 specifications. One such modification is to the iron yoke, originally designed for field gradients up to 230 T/m; it must be reduced in diameter to meet the beam tube height limitations imposed by the Tevatron tunnel.

3.3.1 Iron Yoke Optimization

The cross-section of the HGQ is shown in Figure 3-9. A two-layer collared coil is surrounded by a two-piece iron yoke held together by a welded skin. The iron yoke is penetrated by four large round holes required for longitudinal heat transfer by superfluid helium from the coil to the external HeII heat exchanger and four large rectangular holes reserved for the high-current bus-bars and electrical instrumentation. These holes along with the high nominal field gradient of 215 T/m resulted in the quite large iron yoke outer diameter of 400 mm.

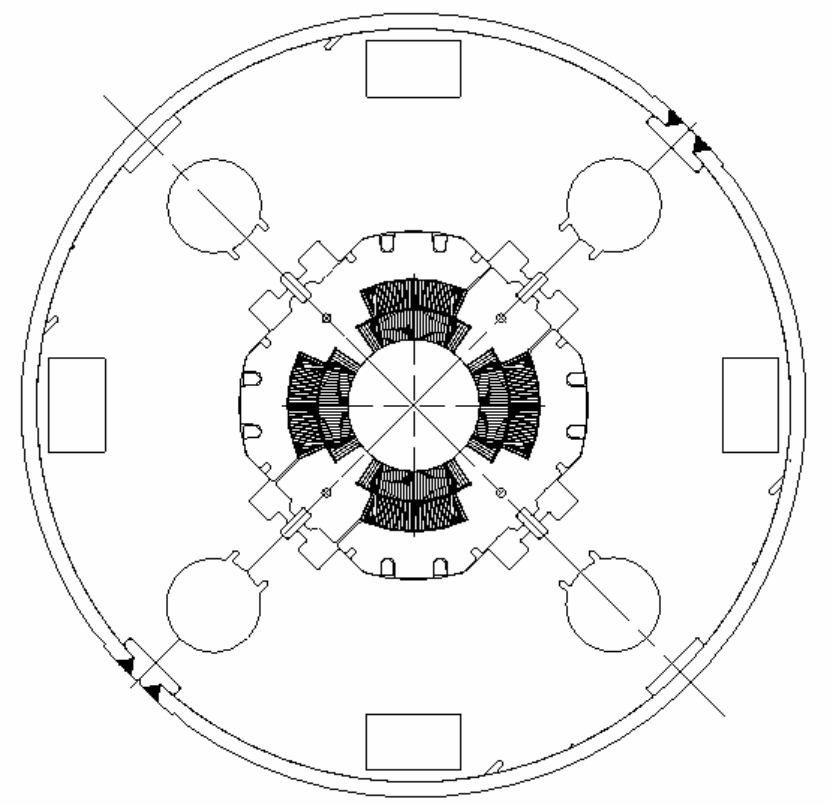

Figure 3-9: Cross-section of HGQ developed for the LHC IRs.

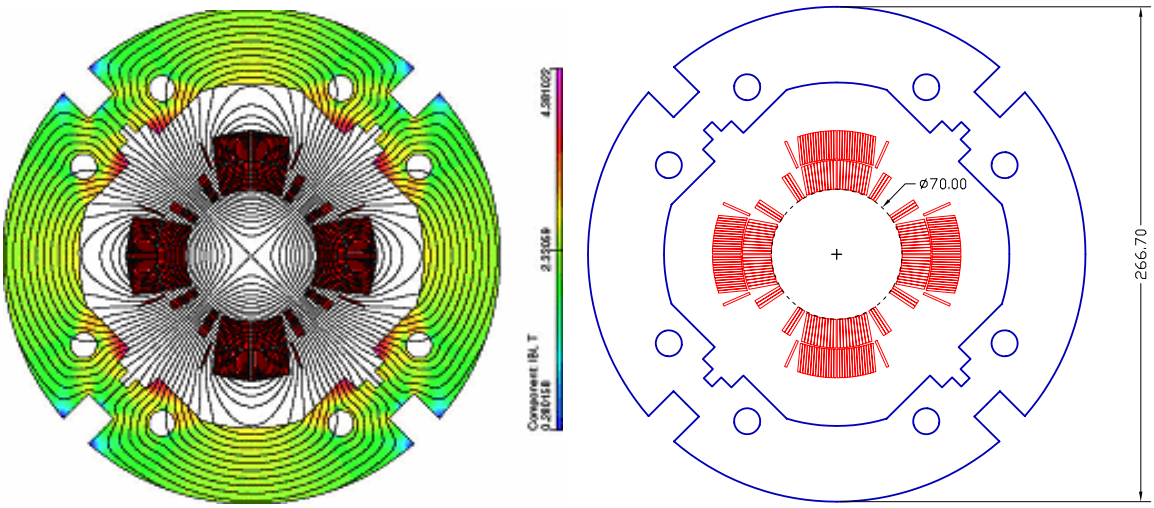

Figures 3-10a, 3-10b: Optimized HGQ magnet cross-section.

The optimization goals for the C0 IR quadrupole were reduction of the iron yoke OD from 400 mm to 267 mm and optimization of the yoke cross-section, minimizing iron saturation effects while providing the channels for power and instrumentation cables as well as for helium flow. The inner shape and the size of the new iron yoke is similar to the shape of the HGQ collared coil. The collared coil is supported and aligned inside the yoke with the help of special alignment keys. As in the HGQ, there is a small gap between the collar and yoke excluding the yoke from the coil mechanical support structure.

The field quality was optimized using the OPERA2D [2] code. Iron saturation effects were kept within tolerable limits through the use of eight round holes: the position and size of the holes were optimized to restrict field quality deviations to the order of 0.15×10^{-4}.

Figures 3-10a, -10b show the optimized iron yoke geometry and the flux distribution in the magnet cross-section. Two 18.5×18.5 mm^2 rectangular holes are sufficient to accommodate 4-6 pairs of 12-15 kA stabilized electrical bus-bars described in [3] and the other two rectangular holes could house the necessary instrumentation wires and cables. If required, the size of these holes could be increased without a dramatical effect on field quality. Eight round holes with a total cross-sectional area of 14 cm^2 and a 1-2 mm annular channel provide sufficient cross-sectional area for helium flow within the magnet cold mass.

3.3.2 Magnet transfer function

Figure 3-11 shows the measured and calculated transfer function for the HGQ short models as a function of current. As can be seen in Figure 3-11, there is good correlation between measured and calculated data at all currents. The reduction of the magnet transfer function at high currents is caused by iron saturation. At an operating current of 10 kA the nominal field gradient is about 180 T/m. We are confident that the transfer function for the modified C0 quadrupole design can be calculated to high accuracy and will provide similar good agreement.

Determination of the field integral ($\int g \bullet dl$) for the C0 quadrupoles will depend on the details of the magnet ends as well as the 'as-built' coil length and thermal contraction when cold. This will be learned from tests of a prototype or model magnet and adjustments to the lengths of the production cold masses.

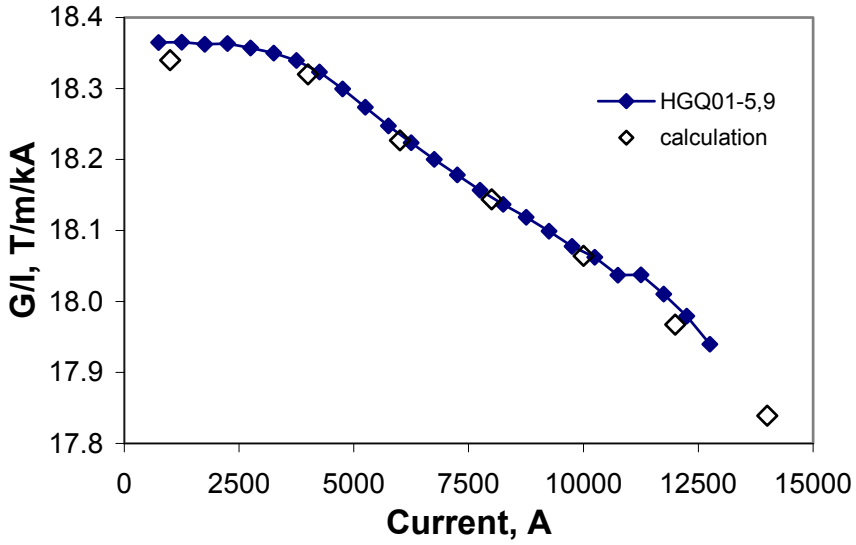

Figure 3-11: Measured and calculated magnet transfer function for HGQ Model Magnets

3.3.3 Field Harmonics

In the magnet body, the field is represented in terms of harmonic coefficients defined by the power series expansion:

$$B_y(x,y) + iB_x(x,y) = 10^{-4} B_2 \sum_{n=1}^{\infty} (b_n + ia_n) \left(\frac{x+iy}{R_{ref}} \right)^{n-1},$$

where $B_x(x,y)$ and $B_y(x,y)$ are the transverse field components, B_2 is the quadrupole field strength, b_n and a_n are the "normal" and "skew" harmonic coefficients (b_2=10^4) at a reference radius R_{ref} of 17 mm.

The field quality expected in the C0 quadrupoles can be estimated from measurements of the roughly 1.5m long model magnets built and tested during the R&D portion of the LHC program and from measurements of the first few full length production magnets. Table 3-4a below shows the mean values and RMS spread at R_{ref}=17 mm of low-order field harmonics over the last five short models HGQ05-09 measured at 6 kA current, while Table 3-4b displays the same harmonics measured at 215 T/m (11922A; the LHC operating current) averaged over the first six full length cold masses.

Differences in average multipole values between the model magnets and production cold masses can be ascribed, in part, to different tooling used in making the coils.

Table 3-4a: Averages and Standard Deviations of field harmonics at 6kA for HGQ05-09.

Harmonic Coefficient	Mean	RMS
b_3	0.49	0.26
a_3	0.12	0.28
b_4	-0.01	0.08
a_4	-0.15	0.37
b_5	-0.02	0.07
a_5	-0.06	0.15
b_6	-0.23	0.17
a_6	-0.03	0.05
b_7	0.01	0.03
a_7	0.02	0.03
b_8	0.00	0.01
a_8	0.00	0.01
b_9	0.00	0.00
a_9	0.00	0.01
b_{10}	0.00	0.01
a_{10}	0.00	0.00

Table 3-4b: Averages and Standard Deviations of field harmonics at 11.9kA for First 6 Full Length Cold Masses

Harmonic Coefficient	Mean	RMS
b_3	0.31	0.47
a_3	-0.57	0.65
b_4	0.02	0.48
a_4	0.30	0.39
b_5	-0.03	0.13
a_5	-0.38	0.18
b_6	-0.02	0.45
a_6	-0.04	0.11
b_7	-0.01	0.03
a_7	0.01	0.03
b_8	0.00	0.02
a_8	0.01	0.03
b_9	0.03	0.01
a_9	-0.02	0.03
b_{10}	0.00	0.02
a_{10}	-0.03	0.02

A detailed comparison of the field quality measurements of HGQ models with the Fermilab Low Beta Quadrupoles [4] is presented in Table 3-5. For direct comparison, the HGQ harmonics are calculated with the Tevatron reference radius of 25.4mm and a weighted end-body average is calculated for a 5.5m cold mass. The field quality of the HGQ is moderately better. The allowed harmonics are smaller, particularly b5, and the variance in normal and skew sextupole is smaller.

Table 3-5: A comparison of the field quality of the FNAL LBQ [5] and LHC IR quad model magnets. Harmonics are given in units (10^{-4} of the main field)

		LBQ						HGQ	
		132"		232"		54"		5.5 m	
	n	average	variance	average	variance	average	variance	<>	s
normal	*b2*	0.61	1.53	-0.55	1.95	0.62	1.03	0.90	0.73
	b3	-0.44	1.01	0.02	0.89	0.21	0.40	-0.04	0.31
	b4	-0.22	0.32	0.28	0.23	0.29	0.50	-0.11	0.61
	b5	-2.42	1.08	-2.01	0.85	-3.10	1.44	0.09	1.08
	b6	0.03	0.36	0.01	0.17	0.05	0.26	0.06	0.31
	b7	-0.04	0.18	-0.06	0.19	0.05	0.11	-0.06	0.09
	b8	-0.03	0.19	0.04	0.12	0.08	0.19	-0.03	0.12
	b9	-0.90	0.20	-0.68	0.11	-0.75	0.17	-0.36	0.28
	b10	-0.04	0.23	0.06	0.10	0.03	0.14		
	b11	0.03	0.25	-0.01	0.06	0.01	0.25		
	b12	0.14	0.25	-0.08	0.16	-0.12	0.51		
	b13	1.30	0.21	1.36	0.24	1.21	0.17	-1.81	0.21
skew	*a2*	0.30	2.59	0.12	3.17	-0.63	2.65	0.32	0.74
	a3	-0.47	0.98	-0.50	0.86	0.13	0.95	-0.43	1.53
	a4	-0.49	0.42	0.35	0.66	-0.31	0.68	-0.28	0.87
	a5	0.08	0.42	0.10	0.24	-0.03	0.59	-0.38	0.36
	a6	0.17	0.26	-0.08	0.39	0.01	0.29	0.24	0.35
	a7	0.06	0.21	-0.07	0.14	0.02	0.15	0.02	0.21
	a8	-0.04	0.20	0.08	0.11	0.05	0.13	0.03	0.14
	a9	0.16	0.20	0.14	0.20	0.17	0.10	-0.02	0.06
	a10	0.06	0.25	-0.04	0.09	-0.07	0.19		
	a11	0.07	0.19	-0.12	0.11	-0.07	0.21		
	a12	-0.04	0.21	-0.11	0.17	-0.19	0.38		
	a13	-0.58	0.26	-0.26	0.20	-0.22	0.87		

Magnetization effects are calculated to decrease b_6 by –(1.2-1.3) units at 4.5K at injection; its decay during the first 900 seconds is less than 0.4 units. The effect of iron saturation on b_6 and b_{10} in HGQ with the optimized iron yoke is shown in Figure 3-12.

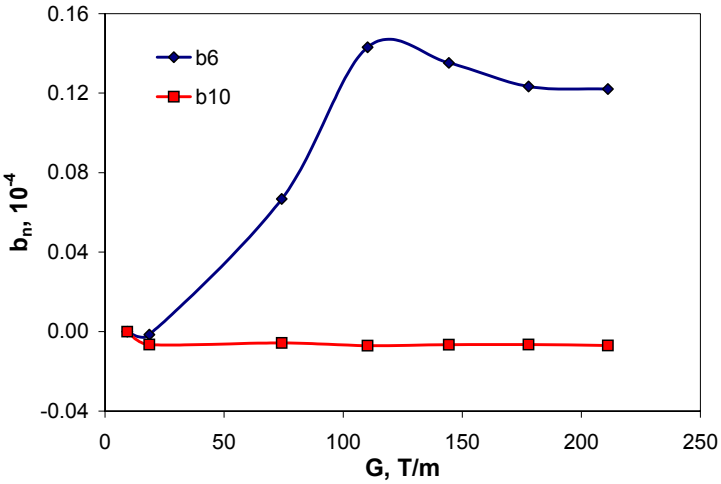

Figure 3-12: The yoke saturation effect.

3.4 Quench Protection, Electrical Specifications, and Bus

Since the design of the new quadrupole magnets for the C0 IR will be very similar to those made for the LHC, their electrical properties will be very similar as well. Quench protection of the C0 high gradient quadrupoles will closely follow the approach used with the LHC quadrupoles. The design of the high current bus will also be based on the LHC design.

3.4.1 Inductance, resistance and stored energy

The new C0 quadrupole coil configuration (number of turns, cable dimensions, end effects, etc.) will be the same as LHC quads, only the length of the coils will be different. Although the inductance depends on the yoke structure (thickness, shape and material properties of the yoke) as well, its contribution to the total inductance is small. For design purposes using LHC magnet inductance values in calculation will be adequate. The LHC magnet inductance is 3.09 mH/m (at 10kA). Based on this inductance, the expected stored energy will be 138 kJ/m (at 9450A, I/Ic=0.875, at 4.5K)

The inductance and Q value measured with an HP4284 LCR meter @ 1kHz for a 5.5 m long LHC quadrupole cold mass assembly is 13.4 mH and 5.2, respectively. The room temperature value of the resistance of a cold mass is 2.3 Ω. The typical RRR value is ~150.

3.4.2 Voltage taps and heaters

The LHC cold mass has voltage taps attached to each quarter coil and each cold mass has two quench heaters (covering all four quadrants) whose room temperature resistance value is 19.5 Ω. The C0 IR cold masses will be instrumented with quarter coil voltage taps. The peak heater surface power must be kept above 55 W/cm^2. This requirement will determine the heater resistance and obviously it will be different for each different length of cold mass.

3.4.3 Quench Detection and Protection

Based on measured values from LHC cold masses, the key quench related properties are estimated as follows:

- Quench velocity: 75m/sec ± 25 m/sec (depends on the quench location; at I/Ic=0.875; 1.9K; at 4.5K one can expect 20 m/sec increase)
- Quench Integral limit: 21 MIITs (over 400K hot spot – estimate only)
- Quench Integral starting from the time the heater is fired: 17 MIITs

  (available 4 MIITs for quench detection or 40 msec at 10kA)
- Quench Detection threshold 0.3 V which is at ~10msec for I/Ic=0.875
- Quench heater operation is expected to be better or equivalent at 4.5K

For the LHC the quench heater firing unit parameters are the following:

- Capacitance: 7mF
- Voltage: 900V

It is important to keep the strip heater peak surface power the same so that we can expect similar heater behavior for the C0 IR design. The quench heater copper to stainless steel strip ratio should be adjusted to the magnet length. Peak voltage plays a bigger role than the total power, so there is no need to change the capacitance value.

3.4.4 Bus

The superconducting bus used for the LHC is suitable for conducting the current to the new magnets. The bus consists of LHC inner cable soldered to a same size cable made from pure copper. This bus was intensively tested at various current values (600A – 12000A) and it was proven that it can be protected adequately if we keep the QI within 150 MIITs (maximum temperature rise will be ~300 K - estimated). We will be well within the QI limit even if the quench detection threshold is set as high as 0.25V.

3.5 Cryostat Requirements

Cryostats provide the magnet closures, proper mechanical and electrical interfaces, mechanical support, thermal insulation, and alignment information needed for a magnet to actually be installed in an accelerator. The fundamental criteria for the new C0 quadrupoles is accommodating the Tevatron beam height off the tunnel floor, without requiring any further civil construction in the tunnel. For economy the Q1 – Q5 cryostat designs will be as similar as possible.

Figure 3-13 shows a preliminary layout of the cryostat for the C0 IR. With the reduced magnet diameter, it appears possible to position the magnet beam line correctly in the tunnel.

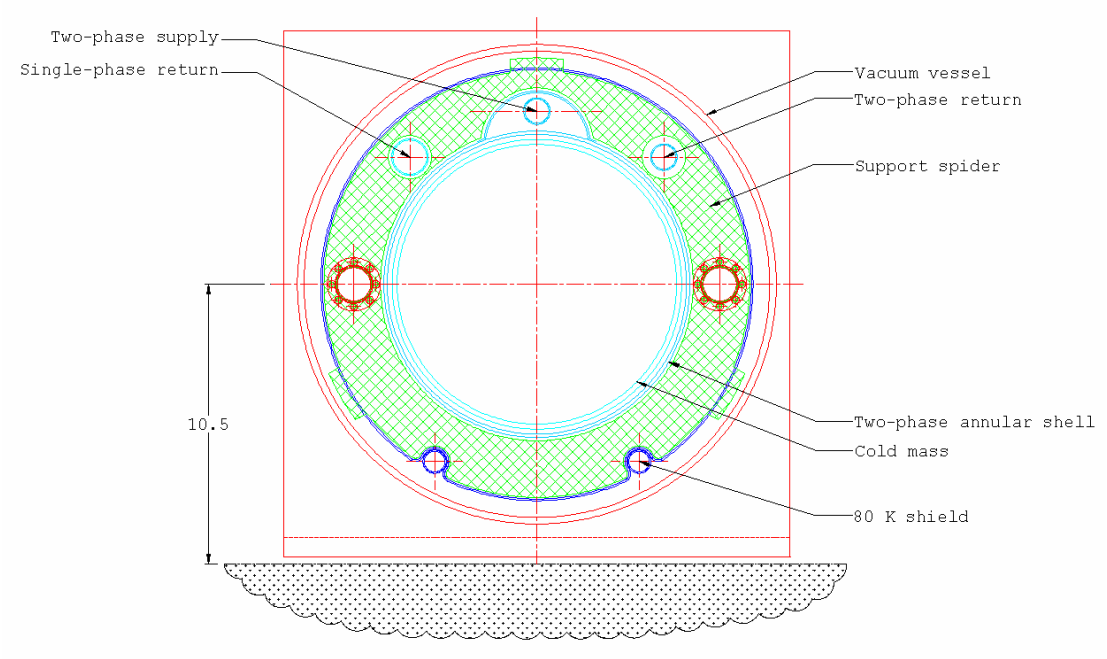

Figure 3-13: Very Preliminary Cross Section of Cryostat

Schematically the Q1 to Q3, Q4, and Q5 cryostats, the main buswork and the associated spools are shown in Figures 3-14, 3-15, and 3-16. The lead end of each magnet is denoted by the elongated end volume and the script $\mathcal{I}$. Details of the spools are discussed in Chapter 4.

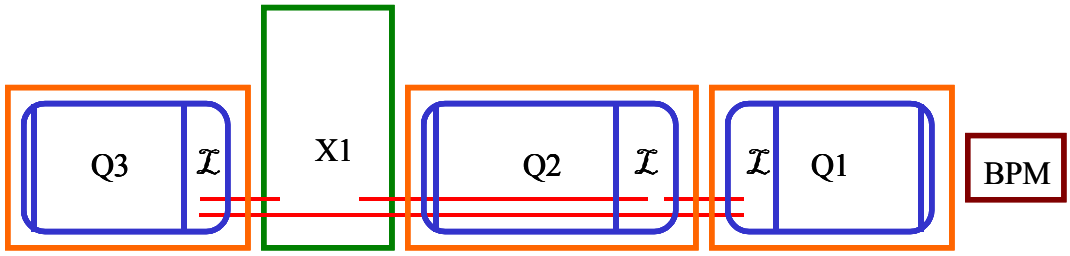

Figure 3-14: Q1 – Q3 Schematic. The IP is to the right, and the triplet mirrors about the vertical axis of the IP when moving from the B sector to the C sector

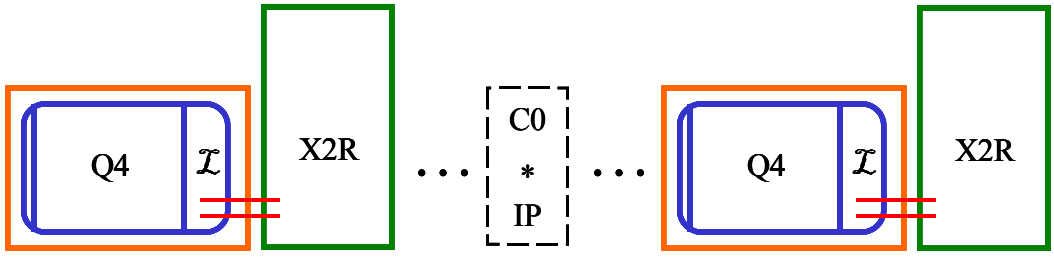

Figure 3-15: Q4 schematic. The Q4 / X2 spool combination translates when moving from the B sector to the C sector

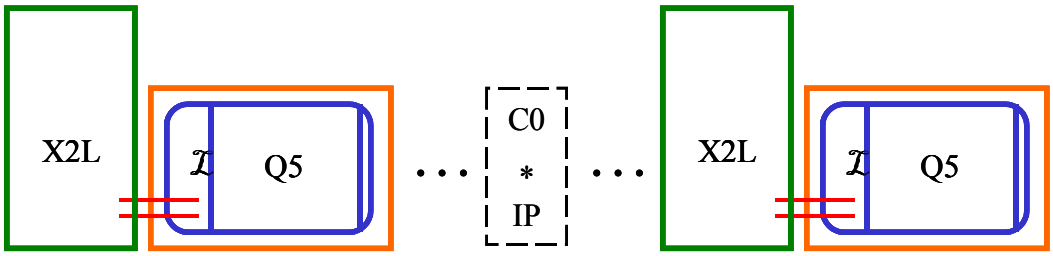

Figure 3-16: Q5 schematic. The Q5 / X2 spool combination translates when moving from the B sector to the C sector

The Q1, Q2 and Q3 quadrupoles will be powered in series, with a trim power supply (not shown) across Q2 allowing for modest variation of it's gradient as needed by machine operations. The orientation of lead and return ends in the triplet allow for minimal bus work to be used, and, if the bus work fix point in the Q2 can be placed at the lead end of the magnet, the expansion loops might be placed in the X1 spool. This also depends on the design of the splice block at the lead ends of the magnets, and the bus expansion loop requirements which are not known at this time.

The BPM shown at the IP end of Q1 may be mounted either internal or external to the cryostat, the choice will depend on details of the design and layout. Details of the vacuum interconnect, gate valve, and other requirements are to be determined.

Preliminary estimates of the end lengths required to close the magnet volumes (including the lead splice block) and accommodate all connection requirements indicate that the cryostatted magnet length will be on the order of 0.464m longer than the mechanical length discussed in section 3.1 (and shown in Figure 3-3). Summing the current estimates of length shows any cryostatted magnet to be on the order of 0.704m longer than the cold magnetic length. Referring to Table 3-1, the minimum difference listed between the slot length and the magnetic length is 0.964m. The current design estimates are less than this, showing no interferences in the design at this conceptual stage.

The Q4 and Q5 magnet arrangements are shown in Figures 3-15 and 3-16, respectively. Given their pairing with a dedicated spool, the bus routing is relatively simple. However, these magnets have the constraint that the end not attached to an X2 spool must be compatible with a standard Tevatron arc interface, and the cryostat must accommodate any through piping, bus, or instrumentation required by the Tevatron string. The asymmetry of the Tevatron interconnect places a more difficult requirement on the X2 spool design, discussed in Chapter 4.

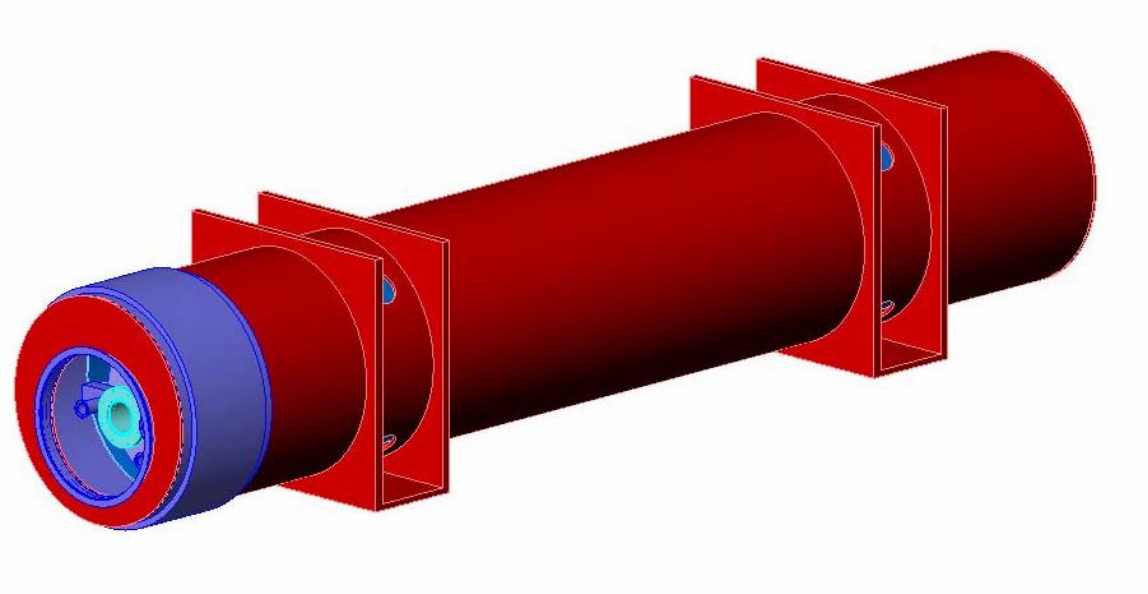

Figure 3-17: Complete Cryostat Assembly Preliminary Concept

Figure 3-17 shows a concept of the completed cryostat assembly. Each magnet will be supported at 2 locations along the length, with the internal and external supports at the same location. Alignment fiducials are located on either side of the external reinforcing sections, and by using the single stretched wire measurement system the average cold magnetic axis can be related to these fiducials to within 200 μm. Lifting of the magnet is accomplished through the use of slings in the region near the reinforcing section.

3.6 Cryogenic Specifications

Each cryostat requires piping as shown in table 3-6. The Q1 through Q3 cryostats are fed in a loop, and thus require return piping. The Q4 and Q5 are located in the arcs of the Tevatron, and require only through pipes. The pipes will need to be sized not only for cryogen flows, but also to accomodate any bus or instrumentation routing required, as is the case for the single phase helium. Similar to the existing Tevatron LBQs installed at B0 and D0, it is envisioned that the magnet will be cooled by a two phase heat exchanging jacket, as shown in Figure 3-18.

Table 3-6: Piping Requirements

Magnet	1θ	2θ	Shield	1θ Return	2θ Return	Shield Return
Q1	X	X	X	X	X	X
Q2	X	X	X	X	X	X
Q3	X	X	X	X	X	X
Q4	X	X	X			
Q5	X	X	X			

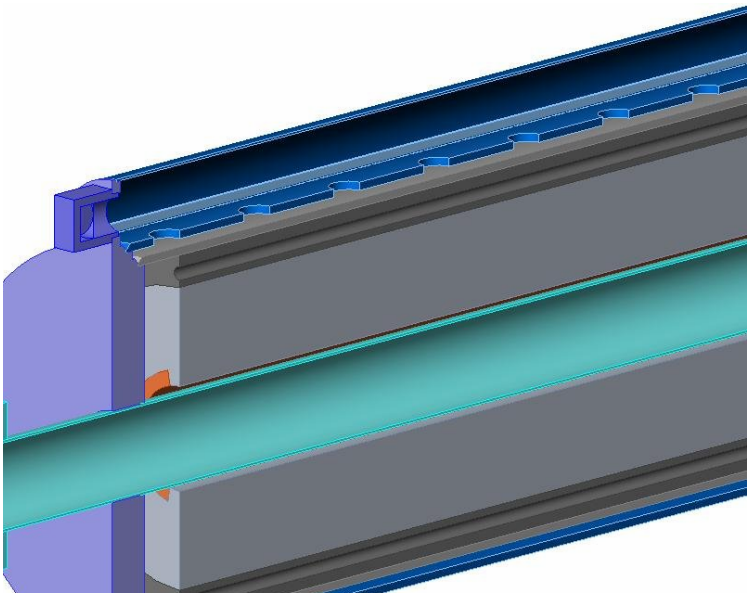

Figure 3-18: Two-phase cooling shell

Analysis of MTF data from previous LBQ tests suggest this re-cooling method is on the order of 65% effective, better than the standard arc dipole helium flow arrangement. Given that the overall size of the C0 IR quadrupole cold mass is very similar to the existing LBQs, we expect the cooling efficiency to be similar.

The heat load to 4K is estimated to be 12W for each Q2 and 7W for each Q1, Q3, Q4, and Q5 assembly

3.7 Design Changes, R&D, and Infrastructure Needs

The LHC IR Quadrupole program provides firm groundwork on which to base the C0 IR Quad design. The body mechanics and harmonics of the LHC design are well understood and repeatable; the cable is readily procured, and the production facility is in large part already completed. Many of the results, particularly at 4.5K, have been quoted in this chapter. However, there are details that are different and must be accounted for in the design of the C0 IR.

First, the reduced yoke diameter changes the harmonics of the magnet, and this must be thoroughly calculated. However, good agreement between electromagnetic calculations and measurements is usually seen. Finalization of the detailed yoke design should verify this.

The yoke diameter also impacts the mechanical support of the ends of the coils. Early LHC model magnets were successfully assembled with full round collars over the return end of the magnet. HGQ01 and HGQ02 had full round collars over the return end only; HGQ03 and HGQ04 have full round collars over both ends (the lead splices in early LHC model magnets were of such a design that full round collars were not possible on the lead end). Test results from these model magnets (only HGQ01 through HGQ03 were tested), suggest there was no difference between the end with the full round collars and the end with the end can / collett

design; however, these magnets were not particularly good performers and this result is not conclusive. Longitudinal restraint of the magnet was explored with a series of experiments done on HGQ05 and HGQ07. No effect on quench performance was seen, though end restraint does give some control over the magnet length change with cooldown.

Next, the reduced diameter changes the splice block, and the magnet to magnet splices. This is an intricate design task, and impacts the cryostat lengths. The single largest input needed is confirmation of the bus design, and the routing and fix points of the bus design.

The bus design is expected to be very similar to the LHC bus, however given the magnet diameter we may need to explore ways to make it more flexible. The use of LHC outer cable as opposed to inner cable is one possibility. Once this is fixed, details of the bus slots in the yoke, the required lengths and space for splices in the interconnects, and the required volumes for expansion loops can be determined.

The major R&D item then is the rebuild of an LHC model magnet, preferably HGQ09, with full round collars over the end to confirm that the mechanical support provided by the collars is acceptable. Detailed design work for the bus and quadrant splice block must also be completed early to allow the overall design to progress.

As far as infrastructure, the LHC production facility in the Industrial Center Building provides the basis for the C0 production. The change in cold mass diameter and length(s) will require new mandrels for winding and curing of coils, and potentially new handling tooling if the current fixtures are simply too long for practical use. The yoke/welding press will need to be reworked to the smaller diameter of the cold mass, and qualification runs made to prove the weld quality.

In the Magnet Test Facility, C0 will require a new test stand, capable of supplying 4K helium and 10kA. The varying designs of the magnet and spool interconnects mean the test stand will require several adapters to accommodate the various interconnects. Most of the measurement equipment from LHC can be used directly for the C0 magnets. The baseline design will include 2 pair of Tevatron (ASC) HTS current leads. We will scale back to one pair if early tests indicate one pair is sufficient.

The BTeV feed box will have standard Tevatron test stand instrumentation (in and out thermometry, pressure taps, voltage taps on current leads, a gauge panel, etc.) We do not propose new features for precise thermal tests except better 80K thermal shielding for lower heat loads. Thus, heat load measurements of the +/-5 Watt variety typical of the Tevatron test stands will be adequate. In addition to the standard instrumentation, we will include nitrogen gas flow instrumentation for the feed box HTS leads and for spool pieces with HTS leads.

The BTeV feed box will operate in typical Tevatron magnet test modes and will have the standard MTF Tevatron test temperature range (from 4.8K down to 3.6K minimum, at the Tevatron pressure of 2.2 bar) and helium flow range (about 15 to 40 grams/sec). Helium subcooling will be provided by the existing stand 6 cold pump and subcooler.

The C0 quadrupoles will require a dedicated turnaround box in addition to the feed box, but it will be as simple as possible with no valves and little instrumentation -- basically a turnaround "cap" similar to what was used for the Tevatron low-beta magnets.

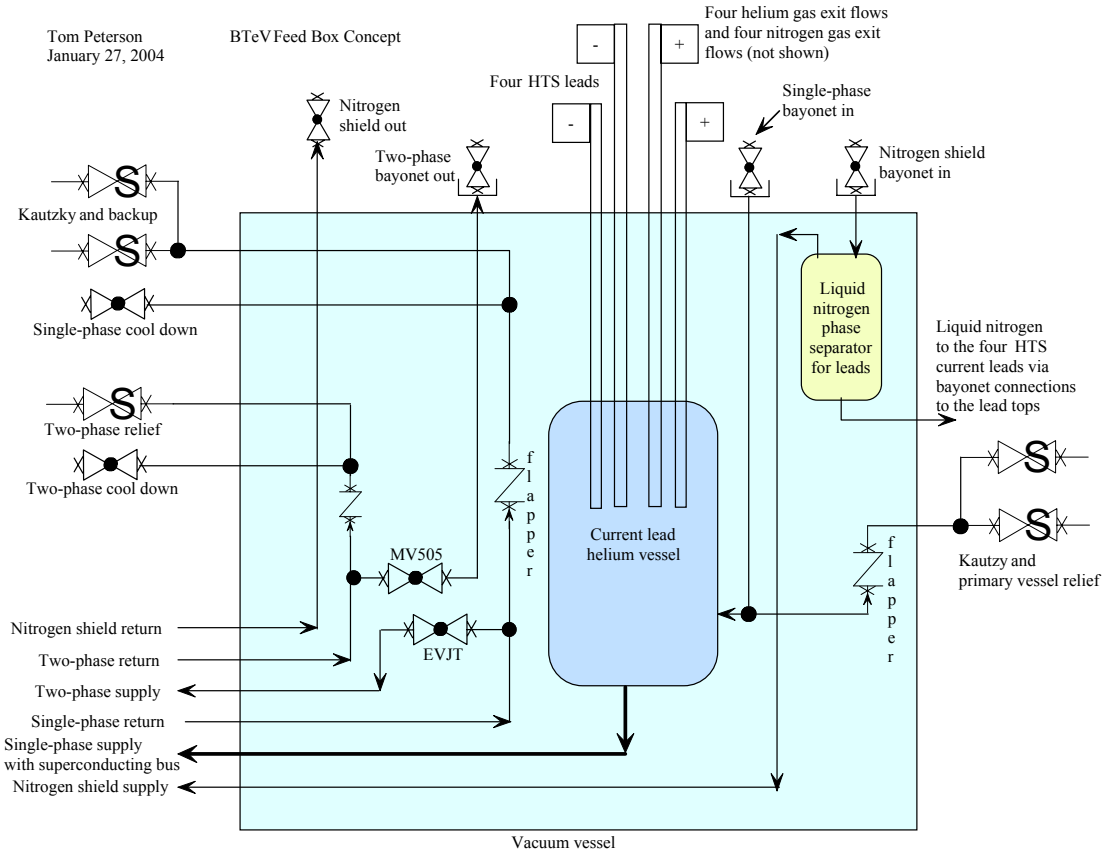

Figure 3-19: Preliminary C0 Feed Can Flow Schematic

References

[1] M Andreev, et al, "Mechanical Design and Analysis of LHC Inner Triplet Quadrupole Magnets at Fermilab", (presented at MT-16 September 1999, Florida) *IEEE Transactions on Applied Superconductivity*, v.10, no.1, p.115 (March 2000)

[2] Vector Fields, Inc., Illinois, 60505, USA

[3] P Bauer, et al, "Busbar Studies for the LHC Interaction Region Quadrupoles" (presented at ASC September 2000, Virgina Beach, VA) *IEEE Transactions on Applied Superconductivity*, v.11, no.1, p.1613 (March 2001)

[4] P Schlabach, private communication

[5] Body harmonics are from model magnets hgq05-09; data for b_{13} only is from model magnets hgq01-03,05; lead end data is from models hgq06-09.

4 New Spools

4.1 Overview and Conceptual Design

Spools typically contain the magnetic correction system, power leads (HTS and/or conventional), beam position monitors (BPM's) and all necessary interfaces. The correction system includes dipole, quadrupole, and sextupole correctors combined in different packages. The different correction schemes at various locations along the interaction region (IR) dictate the total number of spool designs. Based on the current IR layout, we require five different spool designs. Table 4-1 lists the different spool designs with corresponding corrector magnets and required maximum gradients, allotted slot lengths and necessary power leads.

Table 4-1: Elements in different spool designs. Field values listed are the maximum required. "SL" designates safety leads.

Spool	Location	Slot Length, m	VD T. m	HD T. m	SQ T.m/m	Sx T.m/m^2	Q* T.m/m	BPM	HTS Leads	Other Leads
X1V	packb43	1.83	0.48			450	25			3x50A+SL
X1H	packb44	1.83		0.48		450	25			3x50A
X2L	packb47	1.43	0.48	0.48				V&H	2x10kA	2x50A+SL
X2R	packb48	1.43	0.48	0.48				V&H	2x10kA	2 x50A
X3	packc0u	1.43	0.48	0.48	7.5			V&H	2x10kA	3x50A+200A
X3	packc0d	1.43	0.48	0.48	7.5			V&H	2x10kA	3x50A+200A
X2R	packc12	1.43	0.48	0.48				V&H	2x10kA	2x50A
X2L	packc13	1.43	0.48	0.48				V&H	2x10kA	2x50A+SL
X1V	packc16	1.83	0.48			450	25			3x50A
X1H	packc17	1.83		0.48		450	25			3 x 50A+ SL

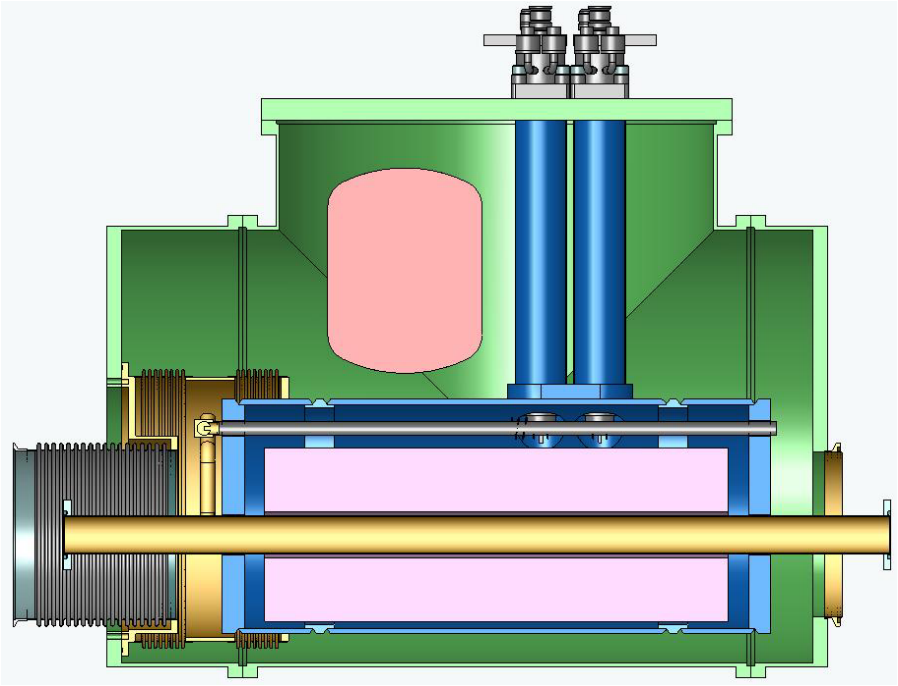

Figure 4-1: Conceptual drawing of an X2 spool layout

The X1 spool has a slot length of 1.83 m with horizontal dipole (HD) or vertical dipole (VD) corrector depending on the location, strong quad (Q*) and sextupole (Sx) correctors. The X2 spool has a slot length of 1.43 m with horizontal and vertical dipole correctors. This spool also contains horizontal and vertical BPM's and a pair of 10 kA HTS power leads. The X3 spool which sits in the triplet region has the same allotted slot length as the X2 spool and has skew quadrupole corrector (SQ) in addition to both horizontal and vertical dipole correctors. It also has both horizontal and vertical BPM's and a pair of 10 kA HTS power leads. There will be a trim supply at this location which requires additional 200 A leads. Safety leads (SL) are also required at B43, B47, C13 and C17 locations. Figure 4-1 shows a conceptual layout of an X2 spool.

4.2 Corrector Design

The most significant change in corrector requirements for the C0 interaction region is the addition of 'strong' quadrupole correctors with an integrated gradient of 25T-m/m. The other corrector strength requirements are comparable to existing Tevatron correctors. In addition, the new correctors do not contain octupole coils or skew sextupole coils, as do some of the original Tevatron correctors. Table 4-2 below summarizes the corrector strengths compared to existing Tevatron coils.

Table 4-2: Corrector maximum strength comparison

Corrector type	Existing Correctors	C0 Requirements	units
dipole	.460	.480	T-m
quadrupole	7.5	7.5	T-m/m
quadrupole	none	25	T-m/m
sextupole (up)	449	450	T-m/m^2
sextupole (down)	346	450	T-m/m^2
octupole	30690	none	T-m/m^3

There are two types of corrector spools necessary for the C0 IR. The shorter spool ("56in"=1420mm) has 800 mm available for correction elements containing both normal and skew dipoles and a skew quadrupole. The longer spool ("72in"=1830mm) has 1200 mm available for correction elements containing either normal or skew dipole, normal quadrupole of 25 T-m/m maximum strength and a normal sextupole of 450 T-m/m^2 maximum strength.

New correctors will be needed to meet C0 requirements. Our baseline approach uses the 'traditional' cos(nθ) design for the magnetic elements, with a separate correction element for each term. The higher order correctors are nested concentrically around the beam pipe, but the strongest lower order corrector is mounted separately. An alternative approach, unique in its flexibility, is a new design in which one unit (a 'flatcoil array') can generate all the required fields and thus reduce the number of different spools and spares required. The two approaches differ in both design and powering schemes. While the baseline design is quite similar to correctors in the Tevatron and those being built for the LHC, the flatcoil array is a new concept which will necessitate some additional R&D. In this section we describe only the baseline version of the correctors. A discussion of the flatcoil array correctors is given in some detail in Appendix 13.2 while the initial R&D required is discussed in Section 4.7.2 below.

4.2.1 56" (1420mm) spool

In order to meet spatial constraints, some of the correction coils must be nested on top of others. The normal and skew dipoles are combined in one magnet assembly since they generate the same field strength and thus have similar magnetic lengths. All coils are based on the same ribbon cable with 10 strands of 0.3 mm diameter, slightly keystoned for maximum efficiency. The conductor critical current density is assumed to be that of the SSC conductor. The coil cross-sections are optimized for the best field quality achievable without wedges using the ROXIE code [1]. At this stage of optimization, the magnetic permeability of the iron yoke is taken to be constant and equal to 1000. The coil inner diameter is fixed at 80 mm.

Figure 4-2 shows cross-section and the field plot in the ND/SD coils at maximum required strength in both coils and Tables 4-3 and 4-4 list the field harmonics. The peak field point is in the outer layer of the (inner) ND coil. The maximum field in the SD coil is 7% lower.

The cross-section and field plot in the skew quadrupole coil is shown in Figure 4-3 and field harmonics in Table 4-5. Peak field point in this case belongs to the pole turn of the inner layer.

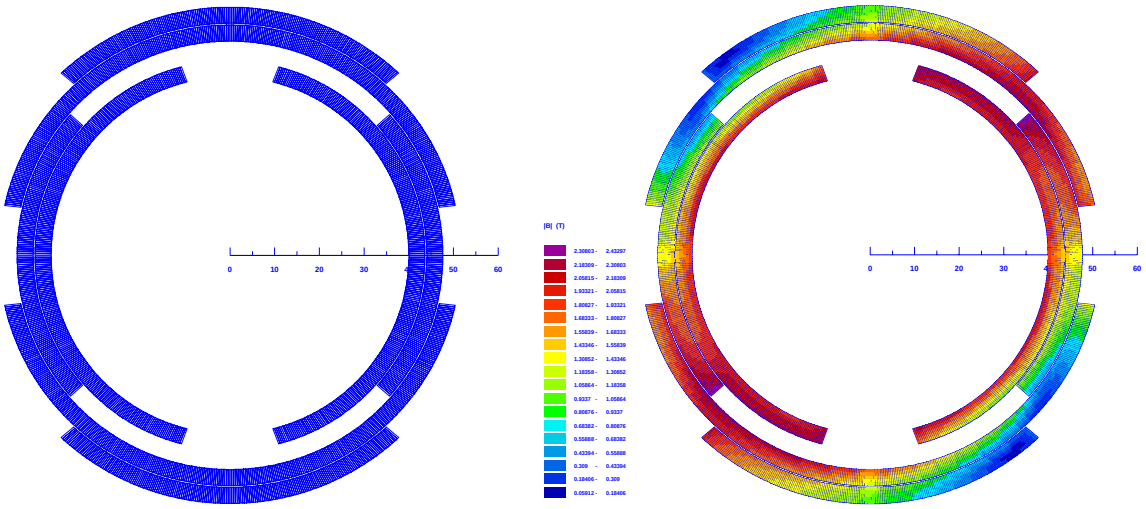

Figure 4-2: ND/SD coil cross-section (left) and field distribution (right).

Table 4-3: ND harmonics at 1” radius (SD=off), nominal current.

MAIN FIELD:	1.36986	NORMAL REL. MULTIPOLES (1.D-4):			
b 1:	10000.00000	b 2:	0.00000	b 3:	-0.63460
b 4:	0.00000	b 5:	-1.32323	b 6:	0.00000
b 7:	-12.19015	b 8:	0.00000	b 9:	-4.21001
b10:	0.00000	b11:	3.30994	b12:	0.00000
b13:	-0.82592	b14:	0.00000	b15:	0.14804
b16:	0.00000	b17:	-0.05274	b18:	0.00000
		SKEW REL. MULTIPOLES (1.D-4):			
a 1:	0.00000	a 2:	0.00000	a 3:	0.00000
a 4:	0.00000	a 5:	0.00000	a 6:	0.00000
a 7:	0.00000	a 8:	0.00000	a 9:	0.00000
a10:	0.00000	a11:	0.00000	a12:	0.00000
a13:	0.00000	a14:	0.00000	a15:	0.00000
a16:	0.00000	a17:	0.00000	a18:	0.00000

Table 4-4: SD harmonics at 1” radius (ND=off), nominal current.

MAIN FIELD:	1.36916	NORMAL REL. MULTIPOLES (1.D-4):			
b 1:	0.00000	b 2:	0.00000	b 3:	0.00000
b 4:	0.00000	b 5:	0.00000	b 6:	0.00000
b 7:	0.00000	b 8:	0.00000	b 9:	0.00000
b10:	0.00000	b11:	0.00000	b12:	0.00000
b13:	0.00000	b14:	0.00000	b15:	0.00000
b16:	0.00000	b17:	0.00000	b18:	0.00000
		SKEW REL. MULTIPOLES (1.D-4):			
a 1:	10000.00000	a 2:	0.00000	a 3:	0.41534
a 4:	0.00000	a 5:	-0.59540	a 6:	0.00000
a 7:	6.09581	a 8:	0.00000	a 9:	-0.35612
a10:	0.00000	a11:	-0.48422	a12:	0.00000
a13:	-0.09084	a14:	0.00000	a15:	-0.01239
a16:	0.00000	a17:	-0.00356	a18:	0.00000

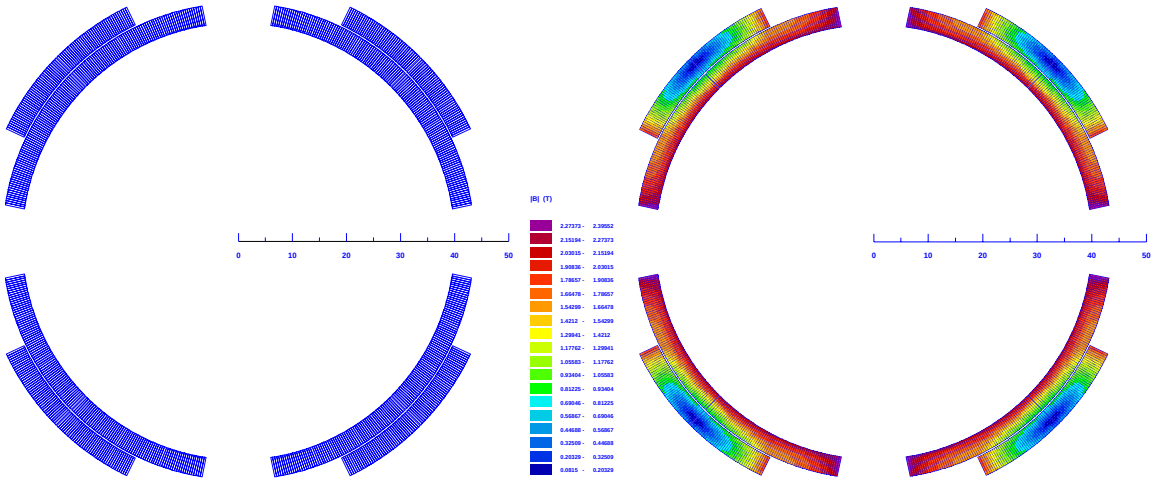

Figure 4-3: SQ coil cross-section (left) and field distribution (right).

Table 4-5: SQ harmonics at 1" radius, nominal current.

```
MAIN FIELD:     1.33057 NORMAL REL. MULTIPOLES (1.D-4):
b 1:      0.00000  b 2:      0.00000  b 3:      0.00000
b 4:      0.00000  b 5:      0.00000  b 6:      0.00000
b 7:      0.00000  b 8:      0.00000  b 9:      0.00000
b10:      0.00000  b11:      0.00000  b12:      0.00000
b13:      0.00000  b14:      0.00000  b15:      0.00000
b16:      0.00000  b17:      0.00000  b18:      0.00000


                              SKEW  REL. MULTIPOLES (1.D-4):
a 1:      0.00000  a 2:  10000.00000  a 3:      0.00000
a 4:      0.00000  a 5:      0.00000  a 6:      0.20147
a 7:      0.00000  a 8:      0.00000  a 9:      0.00000
a10:     -1.23434  a11:      0.00000  a12:      0.00000
a13:      0.00000  a14:     -0.30396  a15:      0.00000
a16:      0.00000  a17:      0.00000  a18:     -0.18879
```

The parameters of the correction elements are summarized in Table 4-6. Since they are more complicated in design, the nested ND/SD coils are provided with 55-59% quench margin while the single SQ coil has 38% margin. To provide the necessary integral field strengths, the ND/SD coils have a magnetic length of 0.35 m and the SQ coil length is 0.14 m. Given reasonable assumptions for the coil end lengths, the physical lengths of ND/SD and SQ magnets are 0.55 m and 0.25 m respectively. These lengths fill all the space available for correction elements.

Table 4-6: 56" spool corrector parameters.

Parameter	Unit	ND	SD	SQ
n		0	0	1
Coil IR	*mm*	40.0	48.0	40.0
Yoke IR	*mm*	60.0		53.0
Strands/cable		10		
Bare strand diameter	*mm*	0.300		
Cu/nonCu ratio		2.0		
J_{nonCu}(5T, 4.2K)	A/mm^2	2750		
Maximum strength required	$T \cdot m/m^n$	0.48	0.48	7.5
Current @ maximum strength	*A*	27.2	23.6	49.0
Quench margin at nominal current in all the coils	*%*	54.7	58.8	38.2
Inductance	*H/m*	15.16	25.03	6.48
Stored energy at I_{nom}	*kJ/m*	5.61	6.97	7.78
Magnetic length	*m*	0.350	0.351	0.143
Physical length	*m*	0.55		0.25

4.2.2 72” (1830mm) spool

Similar to the 56” spool, some of the coils in the 72” spool must be nested. To reduce Lorentz forces, the normal quadrupole and sextupole coils are combined in one magnet assembly. All coils are based on the same ribbon cable used in the 56” spool. Again, the coil cross-sections are optimized for the best field quality achievable without wedges using ROXIE code; the magnetic permeability of the iron yoke is taken to be constant and equal to 1000; the coil inner diameter is fixed at 80 mm.

Figure 4-4 shows the cross-section and field plot in the NQ/NS coils at the nominal current and Tables 4-7 and 4-8 list the field harmonics. The peak field point is in the inner layer of the (inner) NQ coil. The maximum field in the NS coil is 6% lower.

The cross-section and field plots for the normal dipole coil is shown in Figure 4-5 and field harmonics in Table 4-9. Peak field point in this case is in the pole turn of the inner layer.

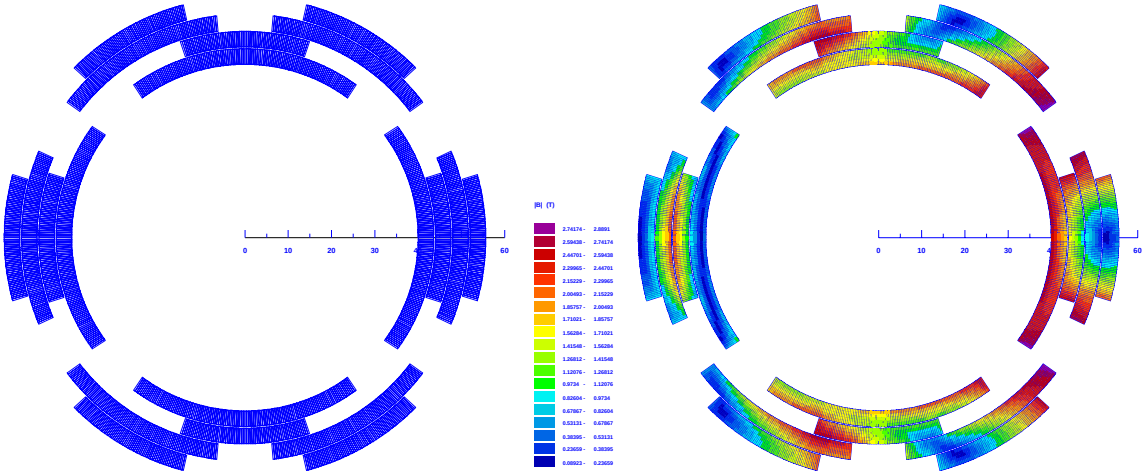

Figure 4-4: NQ/NS coil cross-section (left) and field distribution (right).

Table 4-7: NQ harmonics at 1” radius (NS=off), nominal current.

MAIN FIELD:	0.93930	NORMAL REL. MULTIPOLES (1.D-4):			
b 1:	0.00000	b 2:	10000.00000	b 3:	0.00000
b 4:	0.00000	b 5:	0.00000	b 6:	0.17997
b 7:	0.00000	b 8:	0.00000	b 9:	0.00000
b10:	0.39959	b11:	0.00000	b12:	0.00000
b13:	0.00000	b14:	0.46534	b15:	0.00000
b16:	0.00000	b17:	0.00000	b18:	-0.22728
		SKEW REL. MULTIPOLES (1.D-4):			
a 1:	0.00000	a 2:	0.00000	a 3:	0.00000
a 4:	0.00000	a 5:	0.00000	a 6:	0.00000
a 7:	0.00000	a 8:	0.00000	a 9:	0.00000
a10:	0.00000	a11:	0.00000	a12:	0.00000
a13:	0.00000	a14:	0.00000	a15:	0.00000
a16:	0.00000	a17:	0.00000	a18:	0.00000

Table 4-8: NS harmonics at 1” radius (NQ=off), nominal current.

MAIN FIELD:	0.41682	NORMAL REL. MULTIPOLES (1.D-4):			
b 1:	0.00000	b 2:	0.00000	b 3:	10000.00000
b 4:	0.00000	b 5:	0.00000	b 6:	0.00000
b 7:	0.00000	b 8:	0.00000	b 9:	-0.09100
b10:	0.00000	b11:	0.00000	b12:	0.00000
b13:	0.00000	b14:	0.00000	b15:	-0.17912
b16:	0.00000	b17:	0.00000	b18:	0.00000
		SKEW REL. MULTIPOLES (1.D-4):			
a 1:	0.00000	a 2:	0.00000	a 3:	0.00000
a 4:	0.00000	a 5:	0.00000	a 6:	0.00000
a 7:	0.00000	a 8:	0.00000	a 9:	0.00000
a10:	0.00000	a11:	0.00000	a12:	0.00000
a13:	0.00000	a14:	0.00000	a15:	0.00000
a16:	0.00000	a17:	0.00000	a18:	0.00000

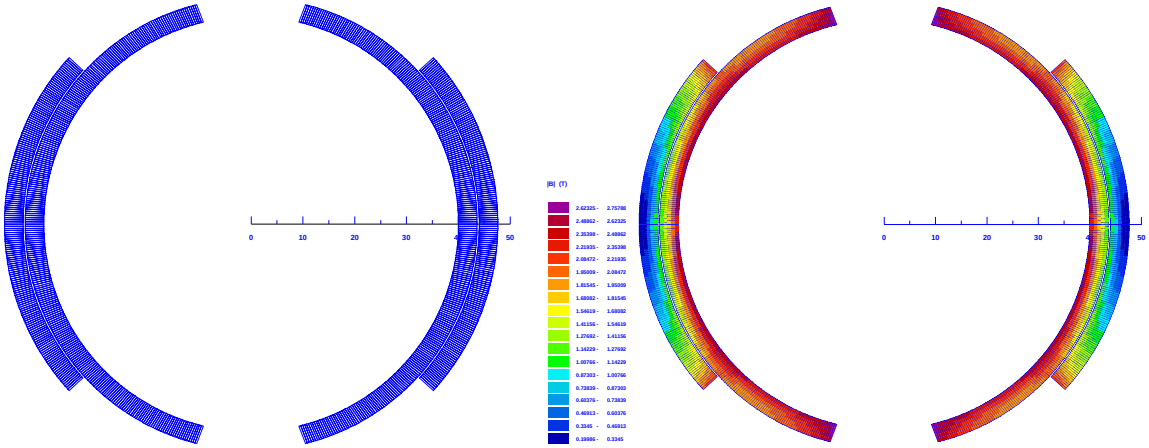

Figure 4-5: ND coil cross-section (left) and field distribution (right).

Table 4-9: ND harmonics at 1” radius, nominal current.

MAIN FIELD:	-2.39854	NORMAL REL. MULTIPOLES (1.D-4):			
b 1:	10000.00000	b 2:	0.00000	b 3:	0.03621
b 4:	0.00000	b 5:	-5.69697	b 6:	0.00000
b 7:	-13.22185	b 8:	0.00000	b 9:	-2.67747
b10:	0.00000	b11:	2.89949	b12:	0.00000
b13:	-0.79648	b14:	0.00000	b15:	0.14924
b16:	0.00000	b17:	-0.05175	b18:	0.00000
		SKEW REL. MULTIPOLES (1.D-4):			
a 1:	0.00000	a 2:	0.00000	a 3:	0.00000
a 4:	0.00000	a 5:	0.00000	a 6:	0.00000
a 7:	0.00000	a 8:	0.00000	a 9:	0.00000
a10:	0.00000	a11:	0.00000	a12:	0.00000
a13:	0.00000	a14:	0.00000	a15:	0.00000
a16:	0.00000	a17:	0.00000	a18:	0.00000

Parameters of the correction elements are summarized in Table 4-10. The nested NQ/NS coils have 41-43% quench margin while the single ND coil has 39% margin. To provide the necessary integral field strengths, the NQ/NS coils will have magnetic lengths of 0.68 to 0.70 m and the ND coil of 0.20 m. Given reasonable assumptions on the coil end lengths, the physical lengths of NQ/NS and ND magnets are 0.8 m and 0.4 m respectively. This utilizes all the space available for correction elements.

Table 4-10: 72" spool corrector parameters

Parameter	Unit	NQ	NS	ND
n		1	2	0
Coil IR	*mm*	40.0	48.0	40.0
Yoke IR	*mm*	60.0		53.0
Strands/cable		10		
Bare strand diameter	*mm*	0.300		
Cu/nonCu ratio		2.0		
J_{nonCu}(5T, 4.2K)	A/mm^2	2750		
Maximum required strength	$T \cdot m/m^n$	25	450	0.48
Current @ maximum strength	*A*	40.0	36.6	43.0
Quench margin at nominal current in all the coils	*%*	40.6	42.9	39.2
Inductance	*H/m*	5.42	6.24	17.01
Stored energy at I_{nom}	*kJ/m*	4.34	4.18	15.73
Magnetic length	*m*	0.676	0.696	0.200
Physical length	*m*	0.8		0.4

4.3 Dimensional Specifications

The length of the corrector packages described in the previous section is designed such that the overall length of the spool matches that of the allotted slot length. Figures 4-6 and 4-7 show the dimensional specifications for the X1 and X2 spools respectively. For the X1 spool, there are no HTS power leads. Hence the outer vacuum vessel houses only the helium vessel that contains corrector package and the necessary interfaces.

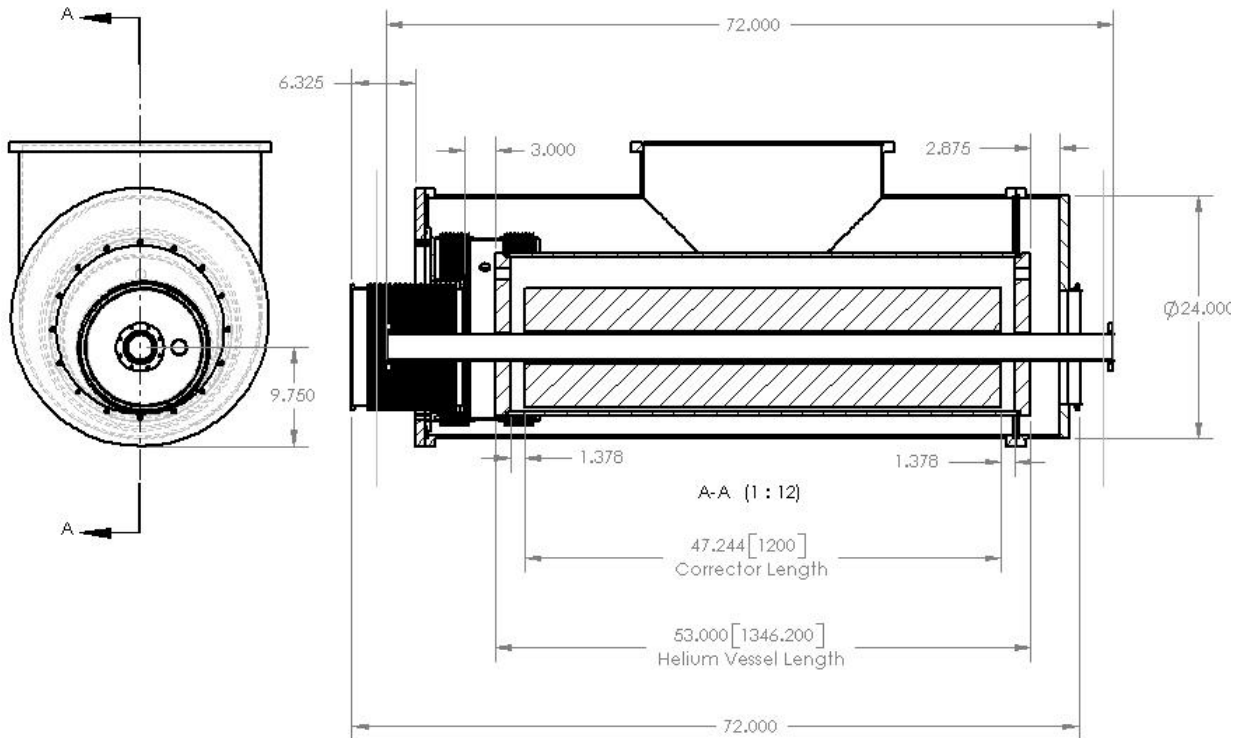

Figure 4-6: Dimensional specifications for X1 spool.

In the X2 spool design, there are two pairs of 5 kA HTS power leads fixed to the top plate. Note that existing HTS power leads are rated for 6 kA and hence we are using a pair of 5 kA leads to reach 10 kA. The nitrogen dewar will also be supported from the top plate. The bottom portion of this support structure will be welded to the helium vessel that houses the corrector package. The two rings that are welded to either side of the helium vessel will be used to align the corrector magnet within the helium vessel. Vacuum breaks and the bellows (for Tevatron interface) will be attached to one side of the helium vessel and flanges to the other side.

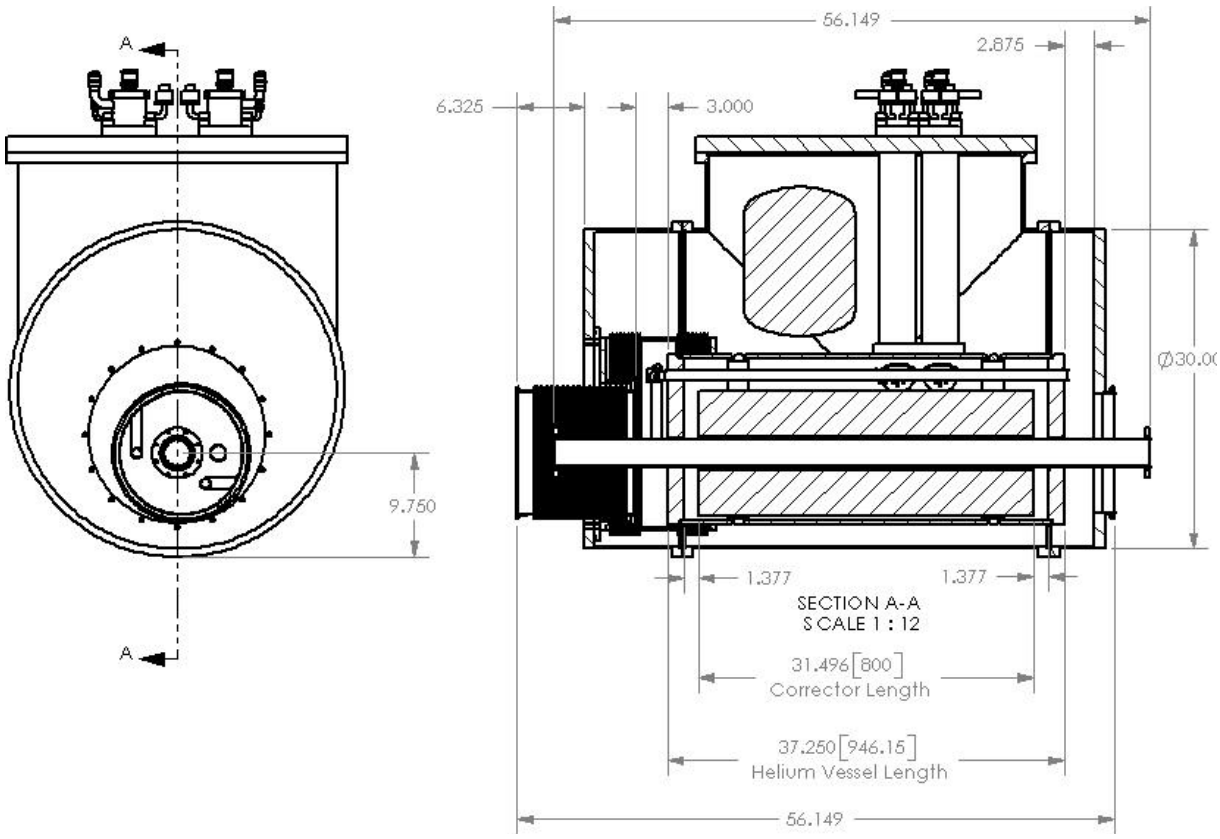

Figure 4-7: Dimensional specifications for X2 spool.

The beam tube has an inner diameter of 63 mm and an outer diameter of 66.7 mm. It will be insulated with Kapton which raises the outer diameter to about 67.1 mm. Note that the bore diameter for corrector magnets is 80 mm and for quadrupole magnets is 70 mm.

BPM's will be embedded in the spool and are located next to the helium vessel inside the vacuum break and the bellows. The allotted slot length for BPM's is 10 inches. The BPM design will be similar to those already installed in the Tevatron.

4.4 Cryogenic Specifications

Table 4-11 gives the expected heat loads for various components in the spool pieces. The design goal for the heat load to 4K in a given spool piece is ≤10W. (This is a conservative number based on measurements of existing spool heat loads and is consistent with allocated refrigeration.)

Table 4-11: Expected heat loads

4.4.1 Item	Heat to 4K (W)	Helium consumption (l/hr)	Nitrogen consumption (l/hr)	Design goal
Each HTS lead		0.7	3.6	
Each AMI lead		12.0		
Each corrector pkg		1.0		
Spool piece	10			5

The 2-phase flow is designed such that it will flow in and out at the top (see Fig 4-1). Liquid drops and fills the 2-phase volume up to the exit port. Each spool will require 3 Kautzky valves: for single-phase, 2-phase, and nitrogen. Furthermore, X1 and X2 spools need to have insulation vacuum breaks. Note that while X1 and X2 spools have piping for only inlet, X3 spools will have both inlet and return feedthroughs.

4.5 Quench Protection

Preliminary calculations indicate that the new corrector magnets (using the skew dipole parameters from Table 4-6 above) can be adequately protected with an external dump resistor of 7.5 Ω. The quench protection threshold should be 1V or less. During a quench, some fraction of the magnet coil becomes resistive which helps to absorb the stored energy. Even if we neglect this extra resistance, the magnet peak temperature will be well under 300K. Also, the peak voltage to ground is estimated to be less than 370V, the maximum voltage across the dump resistor. Although the magnet operating current is roughly 40% of the critical current value, we still expect relatively fast (larger than 1-2 m/s) quench propagation velocity since the coils are epoxy impregnated which reduces the coil cooling drastically. Detailed calculations will be done for the complete set of correctors.

4.6 Connections and Interfacing

Table 4-12 summarizes the interfaces required for each spool. Both X1 and X2 spools at all locations interact with Tevatron interfaces at least on one side. This requires that the cryostat for the quadrupole magnets at these locations also have standard Tevatron interfaces. Figure 4-8 shows the closer view of the X2 spool with all its interfaces.

Table 4-12: Upstream (US) and downstream (DS) interfaces for various spools

Location	*Designation*	*US comp.*	*US interface*	*US bus*	*DS comp.*	*DS interface*	*DS bus*
packb43	X1V	Quad	Tev	Tev	Dipole	Tev	Tev
packb44	X1H	Quad	Tev	Tev	Dipole	Tev	Tev
packb47	X2L	Q5	Modified Tev?	Tev, LHC	Dipole	Tev	Tev
packb48	X2R	Cold bypass	Tev	Tev	Q4	Modified Tev?	Tev, LHC
packc0u	X3	Q3	New	LHC	Q2	New	LHC
packc0d	X3	Q2	New	LHC	Q3	New	LHC
packc12	X2R	Dipole	Tev	Tev	Q4	Modified Tev?	Tev, LHC
packc13	X2L	Q5	Modified Tev?	Tev, LHC	Dipole	Tev	Tev
packc16	X1V	Quad	Tev	Tev	Dipole	Tev	Tev
packc17	X1H	Quad	Tev	Tev	Dipole	Tev	Tev

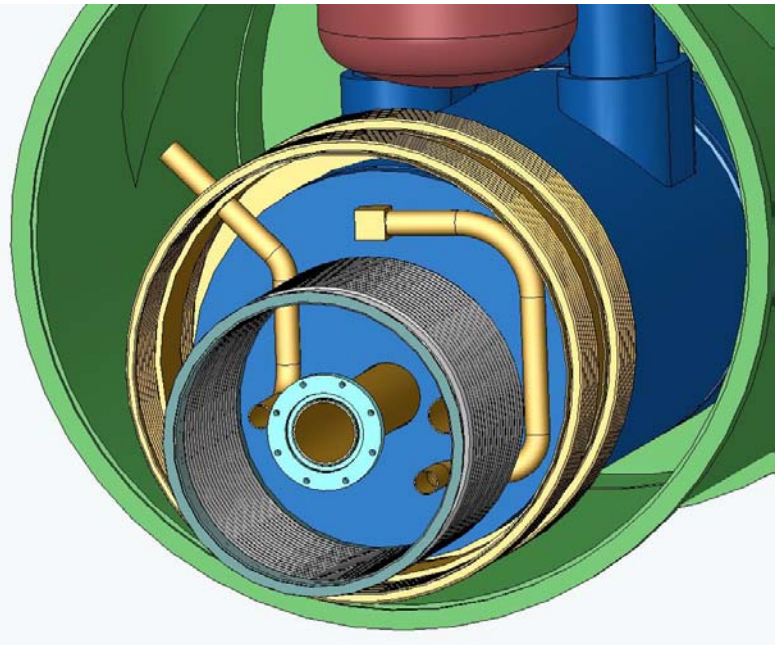

Figure 4-8: Closer view of the TeV interface on X2 spool.

The X3 spool is within the triplet region and is connected to Q2 and Q3 quadrupoles. This allows the X3 spool to have interfaces that are different from standard Tevatron interfaces. These

interfaces are currently being finalized. In addition, the X1 and X2 spools have a Tevatron through bus, whereas the X3 spool has LHC type bus.

Both the X2 and X3 spools will have a pair of 10 kA HTS power leads. The design of these power leads is still under consideration. There are three possible options - test the current 5 kA leads and check if they can carry 10 kA and then use them; double up the current 5 kA leads to reach 10 kA, or develop new 10 kA leads. The first option is currently being investigated and the next section will detail the test results. The second option is being used as the baseline design, and all the spools are designed to accommodate two pairs of 5 kA HTS power leads. At present we have not found a vendor interested in pursuing the third option, and long lead times may make it prohibitive.

Apart from the 10 kA HTS power leads, the spools also have leads for the corrector magnets. For the baseline design, the corrector leads will carry currents less than 50 A. In addition, the X3 spool will have 200 A power lead for a trim supply across the Q2 LHC style quad.

4.7 Measurements and R&D to Date

4.7.1 HTS Leads

The 10kA current leads for the high gradient quadrupoles in the C0 IR will be made from high temperature superconductor (HTS) to avoid additional loading of the 4.5K He system. In the present Tevatron configuration, four spool pieces have been modified to incorporate 5kA HTS leads, and one of these has been installed in the ring for several years. One of these modified spool pieces is shown in Figure 4-9 below. The HTS lead assembly and the LN2 reservoir are clearly visible in the foreground and right side of the picture, respectively. The cost and time scale associated with development of new, optimized 10kA HTS leads does not fit within BTeV constraints, so we have adopted a baseline configuration in which the 10kA power leads are composed of pairs of the existing 5kA design. The drawbacks of this approach are obvious -- it doubles the number of lead assemblies, associated piping, instrumentation, and space allotment.

Figure 4-9: modified H-spool with HTS lead package on the floor at MTF.

Based on R&D tests performed during the 5kA lead program, it appears that it may be possible to operate the leads at higher currents by increasing the coolant flow. We are in the process of developing plans (see Appendix 13.3) to re-test an existing HTS spool to investigate the limits of its electrical and thermal stability. The spool will be mounted on a test stand at the Magnet Test Facility and run at currents up to 10kA, while carefully monitoring the temperatures and voltages across the HTS and conventional lead portions of the assembly. While there is some risk associated with the test, we are reasonably confident that we can detect any runaway condition and protect the leads from damage. The results from this test are expected in the spring of 2004.

4.7.2 Flat Coil Corrector Design

The flat coil array alternative for the corrector design is a departure from conventional approaches. Flat (or 'race track') coils have been used in many applications, but the geometry, construction method, and wide range of operating conditions (and resultant force configurations) of the proposed design are relatively unexplored. A short, focused development effort will be necessary to provide experience in fabrication and assembly of the magnet modules, and data to confirm the basic design.

Pending the availability of resources, we plan to fabricate three flat coils and the yoke and spacer pieces necessary to assemble one quadrant of a corrector (see Figure 4-10 below). Following the successful assembly of the quadrant, mechanical and electrical tests will be performed warm before proceeding with a cold test. A cold test would most likely be performed in a dewar with appropriate current leads, mounting fixtures, and diagnostic instrumentation.

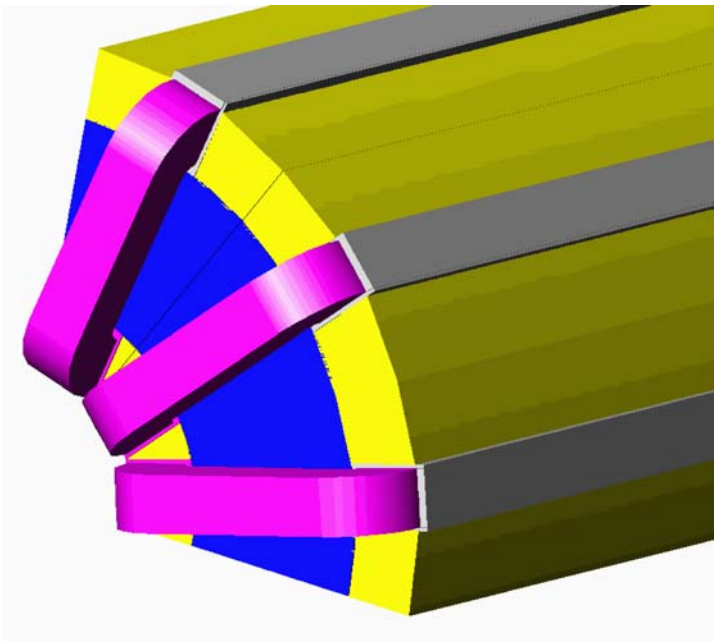

Figure 4-10: Three coil prototype

References

[1] S Russenchuck, "A Computer Program for the Design of Superconducting Accelerator Magnets", CERN AT/95-39, LHC Note 354, Geneva, Switzerland, (September, 1995)

5 Power Supplies

5.1 High Current Power Supply Layout

The low beta quadrupole power supplies for the C0 interaction region will be located in the B4, C0, and C1 service buildings. A listing of these supplies is given in Table 5-1 below.

Table 5-1: High current power supply layout

B4-Service Building

Circuit	Magnet	Power	Volt	Current
C:QB45	B45-"old-Q1"	150 KW	30 V	5,000 A
C:QB46	B46-"old-Q1"	150 KW	30 V	5,000 A

C0-Service Building

Circuit	Magnet	Power	Volt	Current
C:C0Q5	B47-Q5, C13-Q5	300 KW	30 V	10,000 A
C:C0Q4	B48-Q4, C12-Q4	300 KW	30 V	10,000 A
C:C0Q123	B49-Q1, Q2, Q3 C11-Q1, Q2, Q3	300 KW	30 V	10,000 A
C:C0QT2u	B49-Q2		10 V	200 A
C:C0QT2d	C11-Q2		10 V	200 A

C1-Service Building

Circuit	Magnet	Power	Volt	Current
C:QC14	C14-"old-Q1"	150 KW	30 V	5,000 A
C:QC15	C15-"old-Q1"	150 KW	30 V	5,000 A

These high current supplies will be purchased from industry in a similar fashion as the Main Injector P1/P2 Quadrupole supplies. A detailed specification will be written for fabrication of the cabinet and high power conversion equipment (input circuits, bridge and filter). Fermilab will supply the regulation chassis that will be integrated into the supply cabinet and then tested by the vendor.

The main strategy to be used in the purchase will be to specify supplies that are unfiltered at the output voltage of 30 volts and an output current of 5,000 amps. Then for the 10,000 amp

supplies we will use two of these supplies with a filter choke used for isolation and integrated into the required filter. In the case of the 5,000 amp supplies a single converter unit will be used and the choke used in the 10,000 amp units will be used in the required filter to meet specifications. This strategy will allow us to purchase multiple converter units and common filter parts.

5.2 Buswork

Bus work to and from the magnet loads is the main resistive loss in the system and will drive the power supply voltage. The correct amount of copper to use in the bus work is such that the installation cost is equal to the power bill for running the system for a set period of time (like five years). As with the Main Injector, this works out to be on the order of 4 square inches of copper bus per 5,000 A RMS of current. For the 10,000 A runs the plan is to install two 4 square inche runs in parallel for supply and return.

5.3 Electrical Specifications

Table 5-2 lists the main electrical parameters for each high current circuit. In the table, dI/dT is the maximum ramp rate, which occurs during the acceleration cycle in all cases.

Table 5-2: Electrical parameters for high current circuits

B4-Service Building

Circuit	Ind [H]	dI/dT [A/sec]	L*dI/dT [Volts]	Bus L [feet]	R*I [Volts]	PS V [Volts]
C:QB45	0.01075	70	0.8	218	5.0	5.8
C:QB46	0.01075	70	0.8	100	2.3	3.1

C0-Service Building

Circuit	Ind [H]	dI/dT [A/sec]	L*dI/dT [Volts]	Bus L [feet]	R*I [Volts]	PS V [Volts]
C:C0Q5	0.0646	155	10.0	370	8.5	18.5
C:C0Q4	0.0132	155	2.0	642	14.8	16.8
C:C0Q123	0.0096	155	1.5	780	17.9	19.4

C1-Service Building

Circuit	Ind [H]	dI/dT [A/sec]	L*dI/dT [Volts]	Bus L [feet]	R*I [Volts]	PS V [Volts]
C:QC14	0.01075	70	0.8	218	5.0	5.8
C:QC15	0.01075	70	0.8	100	2.3	2.3

5.4 AC Power and LCW Requirements

AC power for the High Current supplies will be derived from the Tevatron Feeder #23. At B4 and C1 a 750 KVA pulsed power transformer (13.8 KV to 480 V) will be installed that will feed a 1200 A panel board to be used for the two high current loads driven from each building. At C0 a 1.5MVA pulsed power transformer (13.8 KV to 480 V) will be installed that will feed a 2,000 A panel board to be used for the three high current loads to be driven from C0.

LCW requirements to be added. JR

5.5 Corrector Power Supply Configuration

The independent corrector power supplies required for the C0 IR are detailed in Table 5-3 and 5-4. For B4 and C1 sectors, the count of independent channels goes from 22 for Run II to 35 for the C0 IR. The B4 and C1 service building corrector power supply installations will be maintained as is and the additional 13 channels will be located in C0 with a new bulk supply and individual switch mode, four-quadrant power supplies providing the regulation off of the bulk supply. The proposed supplies are a very mature design and is a virtual copy of the Main Injector system which is barely 5 years old.

Table 5-3: Correctors in B4 and C1 for Run II

name	type	location	PS	PS @ B4 or C1
packb43	D spool	B43-1a	T:VDB43, T:QDD1, T:SD, C:S1B3A, T:OD	T:VDB43
packb44	C spool	B44-1a	T:HDB44, T:QFA4, (T:SF)	T:HDB44
packb45	B spool	B45-1a	T:VDB45, T:QDD1, T:SD	T:VDB45
packb46	C spool	B46-1a	T:HDB46, T:QFA4, T:SF, T:SQ	T:HDB46
packb47	DR spool	B47-1a	T:VDB47, T:QDD1, T:SD, C:S2B4A	T:VDB47, C:S2B4A
packb48	A spool	B48-1a	T:HDB48	T:HDB48
packb49	H spool	B49-1a	T:HDB49, T:VDB49	T:HDB49, T:VDB49
packc11	H spool	C11-1a	T:HDC11, T:VDC11	T:HDC11, T:VDC11
packc12	F spool	C12-1a	T:VDC12, T:O2	T:VDC12, T:O2
packc13	C spool	C13-1a	T:HDC13, T:QFA4, T:SF, T:SQ	T:HDC13
packc14	F spool	C14-1a	T:VDC14, T:QDD1, T:SD	T:VDC14
packc15	A spool	C15-1a	T:HDC15,T:QFA4, T:SF	T:HDC15
packc16	F spool	C16-1a	T:VDC16,T:QDD1,T:SD	T:VDC16
packc17	C spool	C17-1a	T:HDC17, T:QFA4, T:SQ,T:SF,T:O1	T:HDC17
other PS at B4				T:HB42
other PS at C1				T:VDC18, T:HDC19, T:Q39C
			Total=	**22**

Table 5-4: Correctors in B4 and C1 for the C0 IR

name	type	location	PS	PS @ B4 or C1
packb43	X1 spool	B43-1a	T:VDB43,T:QB43, T:SDB44	T:VDB43,T:QB43, T:SDB44
packb44	X1 spool	B44-1a	T:HDB44, T:QB44, T:SFB44	T:HDB44, T:QB44, T:SFB44
packb45	P spool	B45-1a	T:VDB45, T:SQ	T:VDB45
packb46	P spool	B46-1a	T:HDB46, T:SQ	T:HDB46
packb47	X2 spool	B47-1a	T:VDB47, T:HDB47	T:VDB47, T:HDB47
packb48	X2 spool	B48-1a	T:HDB48, T:VDB48	T:HDB48, T:VDB48
packb49	HTS spool	B49-1a	C:VDB49, T:SQ	C:VDB49
packc0u	X3 spool	B49-3a	T:HDB49,T:VDB49, T:SQB4	T:HDB49,T:VDB49, T:SQB4
packc0d	X3 spool	C10-2a	T:HDC11,T:VDC11, T:SQC1	T:HDC11,T:VDC11, T:SQC1
packc12	X2 spool	C11-5a	T:VDC12, T:HDC12	T:VDC12, T:HDC12
packc13	X2 spool	C13-1a	T:HDC13, T:VDC13	T:HDC13, T:VDC13
packc14	P spool	C14-1a	T:VDC14, T:SQ	T:VDC14
packc15	P spool	C15-1a	T:HDC15, T:SQ	T:HDC15
packc16	X1 spool	C16-1a	T:VDC16, T:QC16, T:SDC17	T:VDC16, T:QC16, T:SDC17
packc17	X1 spool	C17-1a	T:HDC17,T:QC17, T:SFC17	T:HDC17,T:QC17, T:SFC17
other PS at B4				T:HB42, T:QB42
other PS at C1				T:VDC18, T:HDC19
			Total=	**35**

5.6 B4 and C1 QPM Modifications

The only modification necessary to the QPMs at B4 and C1 will be the addition of one HFU at each location and two lead voltages at each house for the high temperature leads in the spool at B48-6 and the feed can at C10-3A.

5.7 Electrostatic Separator Power Supplies

Text to be added. MDC, GK.

6 Cryogenic Systems

The C0 low beta cryogenic components are cooled by a hybrid cryogenic system that consists of the C1 and B4 satellite refrigerators, and the Central Helium Liquefier (CHL). The heat load of the magnets, static and dynamic, is removed by the single-phase, and then is absorbed by the latent heat of vaporization of the two-phase helium. The single-phase helium is also used to cool correction, safety, power and crossover leads. To lower the operating temperature of the magnets, a single stage cold compressor is used in each house. The total load on the cryogenic system is comprised of magnet strings static and dynamic heat load, lead flows, and cold compressor heat of compression.

6.1 Heat Load

Table 6-1 represents the heat load estimate for B4 and C1 cryogenic components. The total heat load is comprised of a refrigeration and liquefaction portion. The refrigeration part of the heat load is used to cover conduction and radiation static heat leak as well as dynamic losses of the cryogenic components. Liquefaction is used to reduce the heat leak associated with leads. The values of existing component heat loads are estimated based on MTF test results, Tevatron operational experience, and engineering calculations. For the C0 quadrupoles, spools, and power lead cans, design parameters for heat leak are used. All of the heat loads are referenced to the 4.5K temperature level. The increase in component heat leak at the normal lower temperature of Tevatron operation is ignored. It should be noted that the additional load associated with the production of the lower temperature refrigeration is not negligible.

Table 6-1: C0 IR Cryogenic Component Heat Load.

Component Type	Heat Load		B4	C1
	Refrigeration	Liquefaction		
	[W @4.5K]	[g/sec]	[each]	[each]
Double Turnaround Box	5	0.017	1	1
Warm Iron Quadrupole	8	0	4	5
Low Beta Quadrupole	8	0	2	2
BTeV Q1,Q3,Q4,Q5	7	0	4	4
BTeV Quadrupole Q2	12	0	1	1
Dipole	8	0	31	34
TSC Spool	7	0.046	1	1
TSD Spool	9	0.060	1	0
TSE Spool	7	0.046	0	1
TSF Spool	9	0.060	0	1
TSP Spool	14	0.877	2	2
TSX1 Spool	10	0.046	2	2
TSHH Spool	14	0.049	1	0
TSX2,X3 10 kA Spool	10	0.098	3	3
Cold Spacer	2	0	2	1
Feed Can	10	0	1	1
Cryogenic Bypass	4	0	2	2
Power Lead Can	12	0	1	1
Valve Box	10	0	1	1
Total Refrigeration Load, [W]			**493**	**516**
Total Liquefaction Load, [g/sec]			**2.310**	**2.307**

6.2 Cryogenic Capacity Limitation

The total cryogenic system refrigeration and liquefaction requirements are provided by the satellite refrigerators and the CHL. The total usable cryogenic system capacity is reduced by the amount necessary to compensate for the heat of compression of the cold compressor for operation below 4.5 K. Heat of compression is determined by the mass flow rate and pressure ratio of the cold compressor.

Mass flow rate depends on the heat leak of the tunnel cryogenic components. Pressure ratio across the cold compressor is determined by the maximum allowable superconductor operating temperature. For a given component, the superconductor temperature depends on the effectiveness of the heat transfer between single-phase and two-phase, as well as dynamic coil losses. Components with ineffective heat transfer are required to be operated at lower temperature and thus lower two-phase pressure and higher cold compressor pressure ratio.

Heat of compression is linear with cold compressor mass flow rate, but is exponential with pressure ratio. Therefore, it is important to not only minimize the heat leak of a component, but also to design the components in such a way as to efficiently transfer the heat to the two-phase in order to minimize the peak single-phase temperature.

The addition of an interaction region to the Tevatron adds both a refrigeration and liquefaction load to the system. Refrigeration loads are jointly satisfied by the satellite refrigerator and CHL. Liquefier loads, such as power lead flows, are satisfied entirely by CHL. The addition of a C0 interaction region to B0 and D0 puts a large burden on CHL to support the liquefier load required by the large number of conventional 2,000 amp and 5,000 amp power lead flows. A design constraint for the C0 IR was to leave the existing B0 and D0 IRs in place and powered. In order to not overload CHL with the C0 IR power lead requirements, high temperature superconductor (HTS) lead designs are being applied in as many circuits as practical. This is particularly important since the design calls for several 10,000 amp circuits.

6.3 Layout

Layout of cryogenic components for the C0 IR are presented in drawings 1650-MC-257471 and 1650-MC-257471 for the upstream (B4) and downstream (C1) systems, respectively. Similar to the existing B0 and D0 IRs, the turnaround box is located before the triplet. This requires both a supply and return circuit for the single-phase, two-phase and nitrogen within the triplet. Quench relieving of the triplet is accomplished on the single-phase supply and return in the turnaround can as well as on each end of the single-phase supply for Q2.

The Tevatron bus power leads are located in an H spool on the B4 side and in the turnaround can on the C1 side. This will require superconductor in the separator bypass on the C1 side. In order to minimize spare requirements, the B4 bypass will also have conductor which will not be connected.

The requirement to mirror the full triplet necessitates the need for a single-phase, two-phase and nitrogen interface transition on the C1 side. This transition is accomplished within the C1 turnaround can. Unlike B0 and D0, this allows the separator bypasses to be identical on the B4 and C1 sides. The B4 and C1 turnaround cans are inherently different due to the transition and different power lead requirements.

6.4 Cryogenic Controls Modifications

Cryogenic controls software modifications are minimal. The ramp permit will be updated to include low beta power leads and spools temperature. Cooldown, Quench Recovery, Kautzky and Lead Controls Finite State Machines will be modified as well.

Additional platinum thermometers and flow control is required for each of the conventional power leads. Each 5kA HTS lead has four platinum resistors and flow controls. Since 10kA HTS leads may consist of two 5kA HTS leads, each 10kA spool will have a total of eight platinum thermometers and flow controls per spool – four for helium and four for nitrogen. Similar to the Tevatron leads, flow control is accomplished with sets of fixed size orifices and solenoid valves. A considerable amount of lead flow tubing and controls cable runs will have to be made to the B4 and C1 refrigerator and C0 compressor buildings.

It is known that there is a long term drift in calibration of Allen-Bradley carbon resistor thermometers. Any new cryogenic components, like spools, that require thermometry should have a pair of the standard 18 Ω calibrated Allen-Bradley carbon resistors and a single calibrated Cernox^{TM} thermometer. Unlike 18 Ω carbon resistors that can be driven by the pulsed current of

the Tevatron thermometry crate, the Cernox^{TM} sensors require a variable current source to maintain the constant voltage signal across the resistor. To drive a Cernox^{TM} thermometer, Lake Shore Cryotronics temperature transmitter model 234 can be used. The transmitter output can be read into ACNET via an ADC channel of the Tevatron satellite I/O crate.

It is desired to try out a new controls scheme to protect Kautzky valves that are located in hard-to-access locations due to the proximity of detector related shielding. The scheme prevents valve chattering which can significantly reduce the valve lifetime. It relies on forcing the relief valve to stay open until the single phase pressure has stabilized below its set point. This scheme is planned to be implemented at B0 and D0 during 2004 Tevatron shutdown.

7 Vacuum Systems

7.1 Layout

Drawing or spreadsheet of all tunnel vacuum devices from B43 to C17 to be included. RR

7.2 Requirements for Cryogenic Vacuum

The Tevatron beam pipe is at 4.5K, therefore cryopumping is very effective in maintaining good vacuum. Keeping the Tevatron at cryogenic temperatures requires an insulating vacuum for thermal isolation. The operational requirement for the insulating vacuum is $1x10^{-4}$ Torr warm and $1x10^{-8}$ Torr cold.

7.3 Requirements for Warm Vacuum

Even though 95% of the Tevatron total length is cryogenic, poor vacuum in warm sections of the Tevatron is currently the major source of beam halo background in the collider detectors at B0 and D0 [1]. Generally the vacuum requirement for the Tevatron warm straight sections is an absolute pressure of $1x10^{-9}$ Torr. This should be used as an operational goal for warm vacuum sections which do not contain electrostatic separators. Individual components should be designed for better than that, perhaps $3\text{-}5x10^{-10}$ Torr, if this can be achieved by reasonable means such as hydrogen degassing, electropolishing and baking. Hydrogen degassing of stainless steel parts is considered particularly important, as this process has historically achieved the most satisfactory results and improvements over the untreated product. The only warm straight section without electrostatic separators and within the scope of this project is the 2.6 meter section near B47-4 which will be used for collimators. Previous experience (14 previous collimator installations in the Tevatron for Run II) has shown that, with proper vacuum techniques, a vacuum of $1x10^{-9}$ Torr can be maintained in these devices.

The vacuum requirement for warm sections which contain electrostatic separators is more stringent. Electrostatic separators run at voltages as high as 125 kV per plate and exceedingly good vacuum is required in order to avoid excessive sparking. A separator spark will generally cause a loss of luminosity and sometimes will even cause the beam to abort. The operational goal is $5x10^{-11}$ Torr. Long term experience with electrostatic separators in the Tevatron has shown that this is achievable. The 8.7 meter B49 and C11 warm sections will each contain 3 electrostatic separators.

The vacuum in the BTeV detector itself may be poorer, with pressures on the order of $1x10^{-8}$ Torr being discussed as an operational goal. Gas load migrating from this region into the Tevatron regions will be mitigated by 50 l/sec ion pumps located at the boundaries of this region.

References

[1] A Drozhdin, et al, "Beam Loss and Backgrounds in the CDF and D0 Detectors due to Nuclear Elastic Beam Gas Scattering", PAC 2003, Portland OR, 2003

8 Controls

8.1 Integration with Current Tevatron Systems

One additional abort input module will be required at B4,C0, and C1 service buildings to accommodate inputs from the low beta power supplies and QPMs. Modifications will be made to the abort application to include these new inputs. No changes are necessary to the Tevatron permit system itself. One additional Camac crate will be installed at the B4 service building which presently has only two Camac crates.

No changes to MDAT itself are required, however, a new Tevatron state will be defined to distinguish between running with collisions at C0 and B0/D0.

The additional separators at C0 will require power supply controls and vacuum monitoring hardware. Additional collimators will require a standard motion control VME crate and motor power supply. Processor boards and controller cards can be moved from other unused collimator locations. All of these will be using standard controls hardware designs, the same as used for existing separators and collimators.

Sufficient Ethernet bandwidth is available in the service buildings for controls requirements.

8.2 Low Beta QPM System

There will be three new quench protection monitor VME crates, one each at B4, C0, and C1 service buildings. These QPMs will be functionally identical to those existing at B0 and D0 but will have fewer circuits in each. The detection algorithms will be the same. There will be no dumps or quench bypass switches, and heaters will be fired to provide quench protection. Each QPM will have uninterruptible power for up to 30 minutes, a 6 second circular memory buffer for quench analysis, and a suite of applications programs for control and data display. The QPMs will communicate via Ethernet to the ACNET control system in the standard fashion. Standard low beta QPM voltage to frequency converters and Tevatron heater firing units will be used.

The crate at C0 will monitor the Q1,2,3 triplet, Q4 and Q5 circuits. The major difference from B0/D0 in these circuits is the maximum current and the allowed number of MIITs. Quench detection thresholds will be adjusted if necessary.

The B4 and C1 QPMs will service the Q6 and Q7 circuits which are single magnet circuits using the 54" low beta quadrupole magnets ("old-Q1's") no longer used at B0 and D0. The major difference for these circuits will be the number of voltage taps available and therefore the number of magnet cells used in the quench detection algorithm. The fewer number of voltage taps effectively increases the quench detection voltage from 0.33 volts to 0.5 volts. The quench limits will be lowered to compensate for the fewer taps to keep the effective quench detection threshold at the same .33 volts.

Connections to the refrigerators at B4 and C1, the abort and Tevatron clock will be done in the same fashion as for B0 and D0. The existing B0/D0 low beta QPMs have no MDAT connections and these are also not required for the C0 IR.

8.3 Controls Modifications

Tables 8-1 through 8-3 list controls software and hardware modifications required to commission the C0 IR. No major new controls software is required, but minor modifications to a large suite of programs, and some duplication of existing software will be necessary. A significant number of database entries will also need to be made for new power supplies, separators, vacuum devices, etc. Software specific to Tevatron instrumentation is discussed in Section 9.3.

If the conventional nested coil correctors are used in the new spools, then the standard corrector power supply controls will be used. The only software modification will be to add the new correctors to the existing applications programs and database entries for the new devices.

If the new flat coil style correctors are used (described in Appendix 13.2), then a microprocessor will be used to generate the required current programs for the twelve individual coils. Database entries for each type of correction (dipole, quadrupole, sextupole) will be used to drive a matrix algorithm in the microprocessor to determine the current in each of the twelve coils. The microprocessor board and up to 12 D/A convertors will be housed in a VME crate. The same microprocessor could be used for quench protection of the corrector coils if necessary. If this type of corrector package is selected, the estimate for modifications to C49 in Table 8-1 should be increased and the microprocessor front end development would require additional effort from what is listed in Table 8-2.

Table 8-1: Application programs and CLIB routines requiring modification for commissioning the C0 IR

Program Name	Index Page	Changes Needed
UL_CBSAUX	CLIB routine	Add c200 modules at B4,C0&C1
Low Beta Quench Protection	java	Add houses for B4,C0 & C1 QPMs
Tevatron LCW	T12	Add new devices; modify graphics
Tevatron Power Supply status	T21	Add PSs for C0 IR
Tevatron Orbit	C50	Add BPMs
Tevatron Vacuum	T18	Add/modify vacuum devices
Tevatron Abort Status	T67	Add c200 at C0,B4 & C1
Ramp Generator for Collider	C49	Add C0 IR PSs & correctors; new squeeze
Tevatron Sequencer	C48	Add C0 IR squeeze
Tevatron Separators	C13, C15	Add new separators
Scraping Program for Collider	C10	Add new collimators
ADC compare	C23	Add new devices
HOPS	I15	Add new power supplies
Tev Magnet Database	T126	Add new magnets
Sequencer	C48	Add new squeeze sequence

Table 8-2: Front-end code modifications required for commissioning the C0 IR

Front-end	Modifications needed
QPM	New QPM code for B4, C0, and C1 QPMs
Vacuum	add CIA crates for new separators
Collimator	New collimator motion control front end at B4
TLLRF	change in Tevatron orbit length
Refrigerator	added instrumentation
TEVCOL (OAC)	addition of new collimator
GLFRIG (OAC)	addition of new calculation of CC control at B4/C1
CBSHOT(OAC)	addition of SDA data for C0
MCRVCR(OAC)	addition of Video recording of C0 data for SDA
VLOGGR (OAC)	addition of new Tevatron State transition

Table 8-3: Controls hardware modifications/additions required for the C0 IR

System	Item	Description	Number
vacuum	CIA crate & PS	Required by separators	1
	Interface board	Arcnet interface to front end	1
Power Supplies	c460	Control cards for correctors	16
	C468	Control cards for power supplies	9
Camac	Crate	One additional crate at B4	1
	C290	Multiplexed Analog to Digital convertor	1
Quench Protection	QPM	VME Crate w PS and I/0 boards	3
	c184 or Enet	For remote rebooting of QPMs	3
Abort	C200	Abort	3
Separators		c185	6
		c465	3
		c052	3
Collimators	VME crate	Five slot crate with power supply	1
	Power supply	Motor power supply for 8 motors	1

9 Beam Instrumentation

9.1 Synchrotron Light Monitor

The synchrotron light monitor [1] is located in a unique warm straight section in the Tevatron at C11. It is located directly between 2 dipoles, one half-length and one full-length, so that it can monitor both proton and antiproton off-axis synchrotron light, generated at the magnetic transition at the far end of the dipoles [2]. This monitor is the only non-destructive technique currently available in the Tevatron for monitoring beam profiles during a collider store. When the C0 area of the Tevatron is converted to a "normal" straight section, this unique warm straight section at C11 will be lost.

We propose replacing this synchrotron light monitor with two separate monitors. One located at the special "mini-bypass"[3] adjacent to the B spool at D47 will measure pbar synchrotron light. A proton synchrotron light monitor will require a minor lattice modification. An appropriate mini-bypass can be made just downstream of the D47-5 dipole by sliding the 32" quad and associated A spool ~50" downstream and shortening the D48 warm straight section. This will be possible after the D48 separator is removed, which is currently planned for the 2004 Summer shutdown. This quad move will generate a ~5% beta wave [4] which can be cancelled by independently powered trim quads in the E19 – E28 region and the "Bartelson" quads in the region D14 – D17.

Need concept description for detector and signal processing. (emphasizes any differences with current detector. moveable mirror with window on tee shared with vacuum port….. abort gap, coherent oscillations, calibration, ……) S Pordes

9.2 Instrumentation between B4 and C1

There are currently 12 Beam Loss Monitors (BLM) located in each of the B4 and C1 houses. This is more than the usual number per house because additional BLMs were required in this area for the C0 abort. This number is adequate for the C0 IR. They will be repositioned in the tunnel for optimum utility.

There are currently 19 Beam Position Monitors (BPM) located in the B4 and C1 houses. For the C0 IR this number will be increased to 29. The in-progress Tevatron BPM upgrade can accomodate this number of BPMs without adding an additional BPM front-end crate. The new BPM pickups will be identical to either of two designs already present in the Tevatron [5]. The Tevatron BPM upgrade will provide a BPM relative position accuracy of <20μm [6].

Tiltmeters similar to what currently exist on the B0 and D0 low beta quadrupoles will be installed on the C0 low beta quadrupoles [7]. This is an essential piece of instrumentation because the Tevatron orbit and coupling are very sensitive to motion of these quadrupoles due to the large β functions. Unlike on the B0 and D0 low beta quads, robust mounting and alignment of these tiltmeters will be designed into the cryostat housing of the C0 low beta quads.

9.3 Instrumentation Software Modifications

Table 9-1 lists the Tevatron instrumentation which will require minor modification to associated software – either application programs, front-end code, or Open Access Clients (OAC). These instruments are generally dependent on the global Tevatron lattice, Tevatron state, and/or synchronizing clock events (TCLK)

Flying Wires
Synchrotron Light Monitor
Mountain Range Display
Ion Profile Monitor (new device)
1.7 GHz Schottky Monitor
Beam Position Monitors

References

[1] A Hahn, P Hurh, "Results from a Prototype Beam Monitor in the Tevatron Using Synchrotron Light", 1991 PAC, p1177, (1991)

[2] R Coisson, "Angular-spectral Distribution and Polarization of Synchrotron Radiation from a "Short" Magnet", *Phs. Rev. A*, 20, #2, p524, (1979)

[3] Two bypasses of this type were initially installed to accommodate "Roman Pot" detectors.

[4] J Johnstone, "Tevatron Optics with Magnet Moves for Roman Pots at CDF", Fermilab-TM-2157 (2001)

[5] Tevatron Low Beta Quadrupoles – Requirements and Specifications, (the "Pink Book"), Fermilab, (1990)

[6] J Steimel, et. al, "Tevatron Beam Position Upgrade Requirements", Fermilab Beams-doc-554, (2003)

[7] Applied Geomechanics model 711. A 2-axis tiltmeter with 100 nanoradian resolution.

10 Commissioning

10.1 Operational Scenarios

The procedure for operating the Tevatron collider is to load all waveforms (power supply ramps, etc) and timer channels into the control cards in the field prior to beginning the collider fill process. The sequencer (control room application program) then coordinates the sequence of events that initiate beam transfers, state changes, and changes in operating conditions. Since the low beta squeeze process will be different for C0 operation and B0/D0 operation, modifications will be necessary in order to switch between the two modes. Beam transfers into the Tevatron and the acceleration to 1 TeV will be identical for the two operating modes.

There are two possible simple methods of integrating C0 operation into collider operation without completely redefining the current control process. One method is to use the identical set of clock events for C0 operation as for B0/D0 operation to control the optics changes for each mode. In this case the waveforms for the power supplies would be reloaded at the beginning of each collider fill, depending on which mode is desired. The second method is to load both sets of waveforms to the power supply controllers, and determine which set plays by triggering different clock events.

Option 1 (using the same events and reloading waveforms):

This method has the advantage that fewer application programs need to be modified. A second operational file will be defined in the power supply waveform generator page (C49), and the proper file will be activated between stores. A file for dipole correction elements will need to be loaded from the orbit correction program after the C49 file is activated. This process currently takes about ½ hour. It is not particularly prone to errors, however the chance for a mistake by the operator will increase with the number of files that need to be loaded.

Option 2 (using separate clock events and having both sets of waveforms loaded):

This method has the advantage that a single file of ramp waveforms can be used for both modes of operation, and file activation will not be required between stores. More changes will need to be made to C49 to recognize the different sequences. The orbit correction program will need to know about the second set of waveforms as well. The waveform generators, and the design of the sequencer in general, was originally set up to handle this type of mode switching. Figures 10-1 and 10-2 show how some of the waveform ramp cards will be set up in this option. In these examples, XX and YY represent the new clock events for low beta squeeze and unsqueeze of C0 operation.

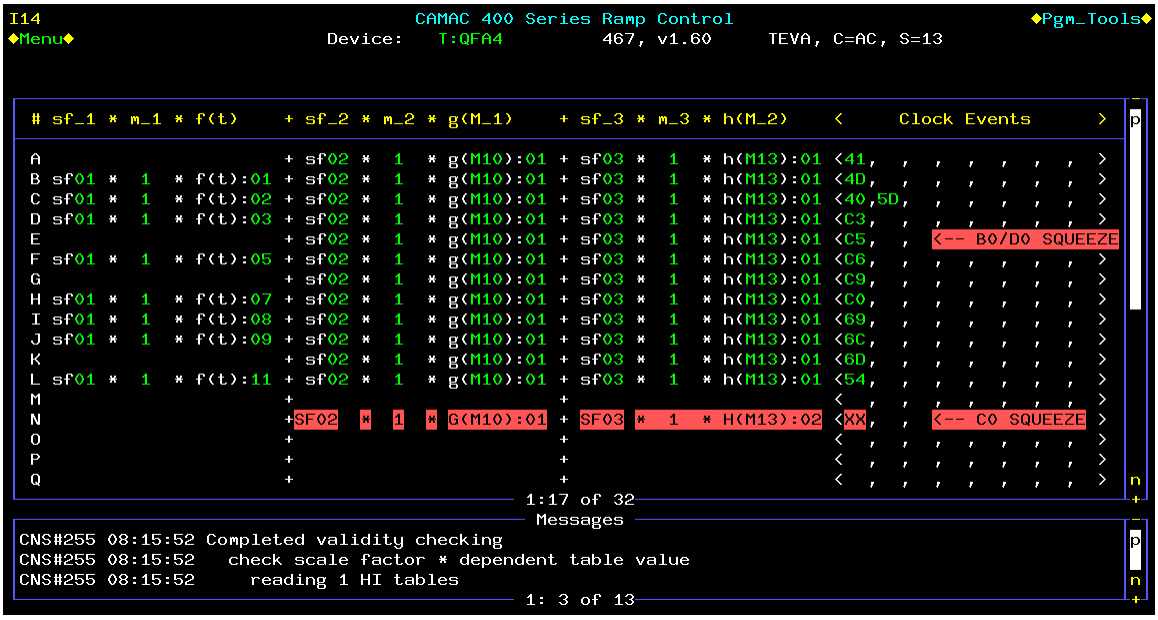

Figure 10-1: Example of the configuration of a tune quad circuit.

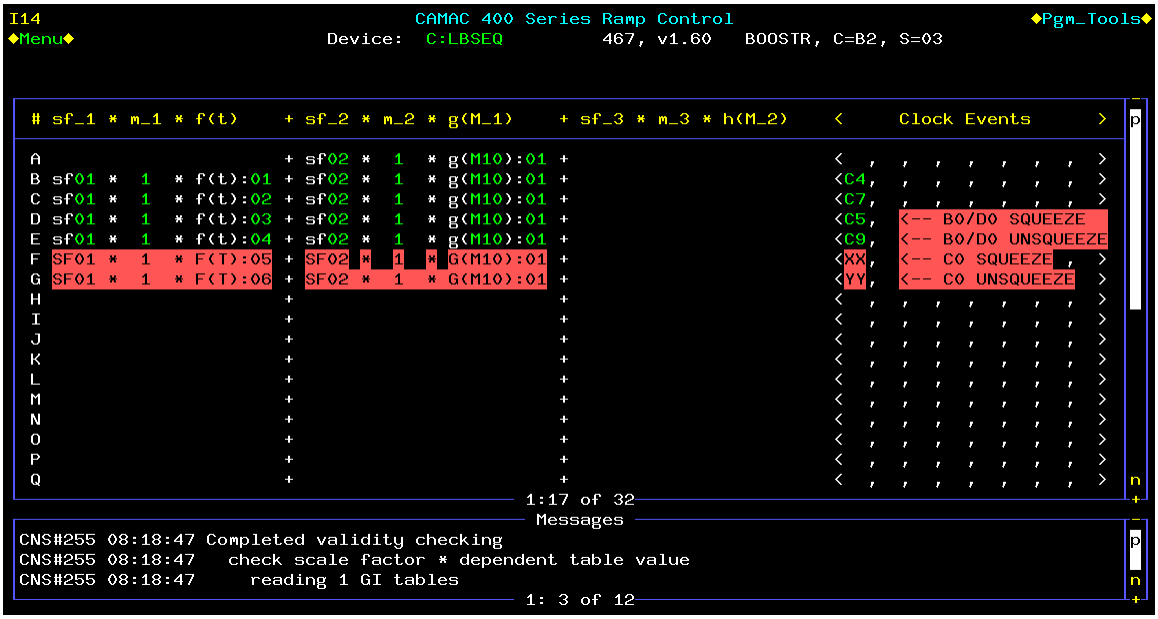

Figure 10-2: Example of the configuration of the low beta controller card.

10.2 Commissioning Plan

Standard commissioning stuff. MDC with review by J Annala.

11 Conversion of C0 to a Normal Straight Section

11.1 Overview

During an early shutdown (currently scheduled for late summer of 2005), the remnants of the Fixed Target abort system at C0 will be removed and replaced with a standard long straight section to allow installation of BTeV experiment components.

11.1.1 Motivation

Currently, the Tevatron straight section at C0 includes the collision hall for BTeV and the remnants of the decommissioned Tevatron abort extraction system for Fixed Target operations. Even before the installation of the low-β* insertion at C0 (currently scheduled for 2009), BTeV plans a phased installation of components into the collision hall during annual accelerator shutdowns for maintenance and upgrades starting in 2006. There are two main reasons for this.

First, there are some prototype components such as the pixel vertex detector that would benefit from early operation in the Tevatron. This operation could be passive -- observing the environment of the circulating proton and antiproton beams and their electromagnetic pulse and the radiation background fields. It could also be active -- inserting a thin transmission target or turning the electrostatic separators off to provide low luminosity collisions at C0 at the end of collider stores. These studies could be used for testing prototype detectors or commissioning the final detector elements and systems. Similarly, the impact of the BTeV components on the Tevatron operations, such as impedances, vacuum, 3-bump dipole spectrometer, and apertures, could be studied early.

Second, the assembly hall at C0, outside of the shielding door, was consciously made too small to stage the entire BTeV experiment before installation. The idea was that each component of the experiment would be fabricated somewhere else, final-assembled and tested in the assembly hall, and, when ready, installed during the next scheduled Tevatron shutdown. The physical size of the SM3 analysis magnet and space needed for assembly requires that it be installed in the collision hall as soon as testing is completed.

In order to make space for the installation of BTeV experiment components, starting with the SM3 analysis magnet, compensating dipoles, and muon toroid in 2006, the remnant components of the Fixed Target abort system must be removed from the C0 collision hall and replaced by a simple beam pipe. This will also require the replacement of two half-length Tevatron dipoles with full-length Tevatron dipoles in the B4 and C1 cryogenic sectors. At this time the ventilation systems of the collision hall and the Tevatron tunnel will be isolated, allowing the collision hall to become ODH Class 0 to facilitate activities by experimenters and contractors.

The BTeV installation, including the low-β insertion, could, in principle, be accomplished without the intermediate step of a standard straight section. However, this more direct approach would preclude much early testing and, subsequently, lengthen the experiment installation and commissioning period, which would then begin only after CDF and D0 are completed.

11.1.2 Scope of Change

The Tevatron C0 straight section had previously been the site of the abort channel for Fixed Target operations with specific abort elements located between the B48 and C12 stations [1]. Since there is no plan for further Tevatron Fixed Target operations, this abort is no longer needed and the C0 area has been assigned to the collider experiment BTeV. The Fixed Target abort consisted of a set of five kicker magnets (at the B48 straight section), two half-length Tevatron dipoles (at B48-3 and C11-3), two C-magnets, and three Lambertson magnets. In January 2003, in order to increase the vertical aperture in the Tevatron collider, the three Lambertson magnets were replaced with four Main Injector dipoles (three 240" long, and one 160" long – slot lengths are 16" longer). The five kicker magnets were also removed and replaced with beam pipe at that time. In the C0 collision hall, the Main Injector dipoles sit on a wall of shielding blocks and the C-magnets sit on a steel I-beam catwalk [2]. Both of these magnet systems interfere with the installation of experimental components for BTeV.

The total bend of the two half-length Tevatron dipoles plus the two C-magnets plus the four Main Injector dipoles (with active trim shunting of the current in the Main Injector dipoles) exactly matches the total bend of two full-length Tevatron dipoles. The basic plan is to remove the two half-length Tevatron dipoles, the four Main Injector dipoles, and the two C-magnets, and replace them with two full-length Tevatron dipoles (to be purchased from inventory, reducing the number of spares available) plus additional vacuum pipe (see Figure 11-1). The full-length dipoles will be placed approximately at the position of the half-length dipoles. Since the effective magnetic bend points will change, all the elements between these half-dipoles must be repositioned transversely inward (toward the center of the Tevatron ring) with the maximum move of 4.2 inches at the 99" quadrupoles near B49 and C11. This will reconstitute a normal long straight section [3] [4].

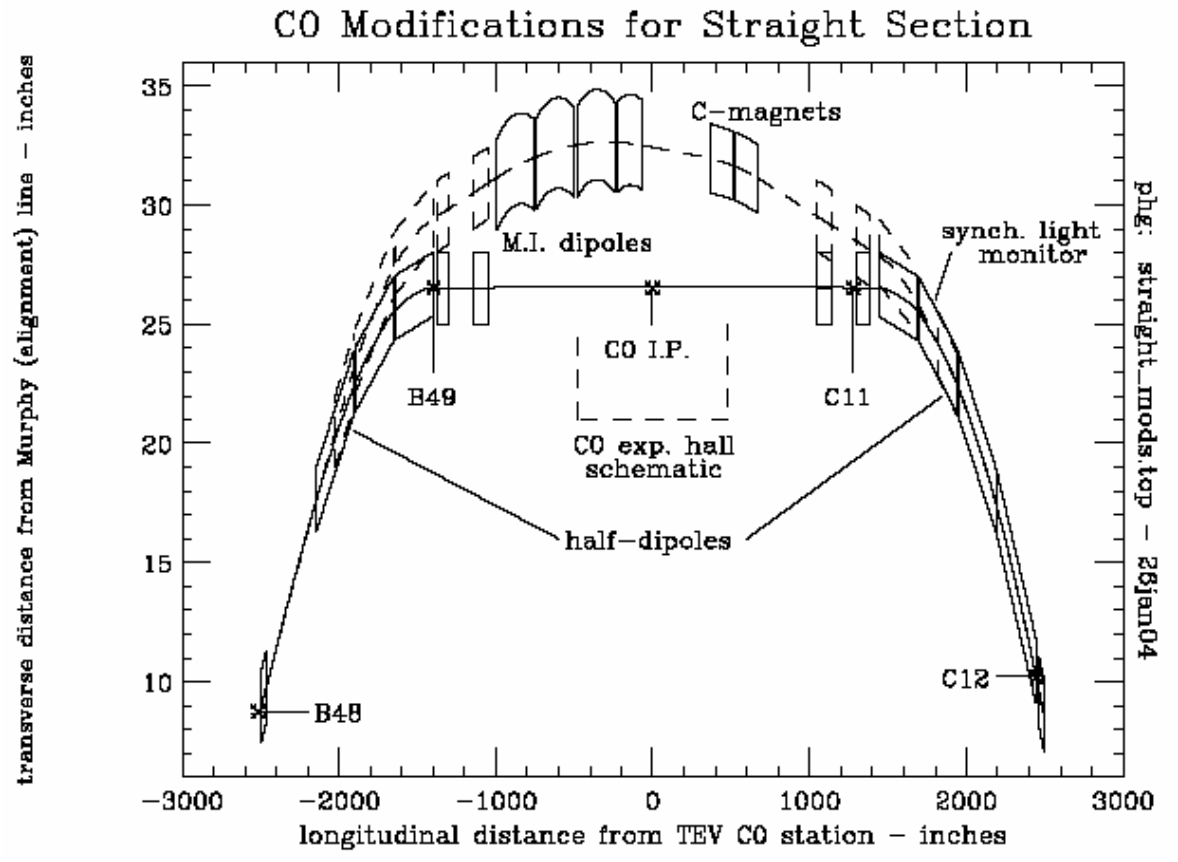

Figure 11-1: The existing C0 abort (dashed) and future straight section (solid) trajectories.

Since the removal of the Main Ring accelerator, there remains an excess capacity in the Low Conductivity Water (LCW) system in the Tevatron tunnel. This system will be slightly reconfigured to cool the BTeV SM3 analysis magnet, the compensating dipoles, toroid, water-cooled power bus, and power supplies (in the C0 collision hall), both for the final installation and for component testing in the assembly hall.

The removed four Main Injector Dipoles and two C-magnets will be replaced with (~107 feet total length) of 4 inch diameter, electro-polished, hydrogen-degassed, stainless steel vacuum pipe which will be baked out. The vacuum goal for this section of beampipe is $1x10^{-9}$ Torr. The existing ion pumps and controls in this region will provide adequate vacuum pumping. A series of simple stands (existing design) will support the vacuum pipe at beam heights of 10.4 inches, 40 inches, and 100 inches above the existing floors.

Two additional horizontal and vertical readout Beam Position Monitors (BPM) will be installed on the C0 side of the last Collins straight section quadrupoles QUADC0U (near B49) and QUADC0D (near C11). These will provide additional diagnostics in understanding the local 3-bump made by the SM3 analysis magnet and compensating dipoles. Signal analysis and readout hardware for these BPMs can be easily accomodated in the existing B4 and C1 BPM controls system.

Although not needed for the configuration change to the straight section, eventually, for the installation of the low-β* insertion, the warm Tevatron power bus must be relocated to the outer wall or ceiling of the flare tunnel and massive amounts of new water cooled bus must be installed for the LHC quadrupoles and relocated Q1 quadrupoles from CDF/D0. In order to minimize time impact during the shutdown for the installation of the low-β* insertion, these bus relocation and additions should be done starting during the early shutdown for straight section reconfiguration and continuing through the shutdowns in between.

11.1.3 Tevatron Beam Optics Considerations

The reconfiguration to a normal straight section changes the longitudinal positions of two bend points, while maintaining the longitudinal positions and strengths of all quadrupole magnets. Therefore, the Tevatron tune is (to very high order) **not** changed, and the lattice functions around the ring are negligibly perturbed. The moving of the bend points does mean that the components in between will move slightly in the transverse horizontal plane, radially inward. The circumference of the Tevatron orbit will thus be decreased by 1.6 mm, in the direction which will reduce the present 39 mm mis-match between the Tevatron and Main Injector rings.

With the B2 compensating dipoles installed in the C0 collision hall, the physical aperture at C0 will be a minimum at the injection energy with beam on the helix. Figures 11.2 and 11.3 show the physical aperture in the C0 straight section in units of transverse beam σ's for 20π-mm-mrad (95% normalized emittance) and $\sigma_p/p = 5x10^{-4}$, which are typical injected proton beam parameters in Run II operation. The size of the beampipe in a B2 magnet is 2.0" horizontally and 4.0" vertically. We have assumed a minimum beampipe ID of 2.0" between the B2's for these plots. Under these conditions the minimum aperture is 10.8σ and is located at the outboard end of the downstream B2 compensating dipole in the horizontal plane. For comparison, in the present Tevatron configuration, the minimum injection energy aperture is at the F0 injection Lambertson and is nominally ~5σ [5]. The nominal injection energy apertures at B0 and D0 low beta quads are ~10σ [6]. The C0 Lambertson magnets mentioned earlier in this section were removed in 2003 because their vertical aperture was ~3σ. The beam trajectories, beam sizes, and apertures must be considered when installing BTeV experiment equipment and beam pipes in the region between the B2's (± 27' from I.P.). The present configuration of horizontal and vertical correctors near C0 allow for independent horizontal and vertical beam position and angle control at C0 in the range of ±9mm and ±0.100mrad at 1 TeV, which is more than adequate steering capability.

The present warm gap next to the half-dipole at C11 is unique in the Tevatron. It provides a location between two cryogenic dipoles for a single synchrotron light monitor to view off-axis synchrotron light from both proton **and** anti-proton beams. With the replacement of the half-dipole with a full dipole, this location will be lost, and alternatives for the synchrotron light monitor must be considered (see section 9.1).

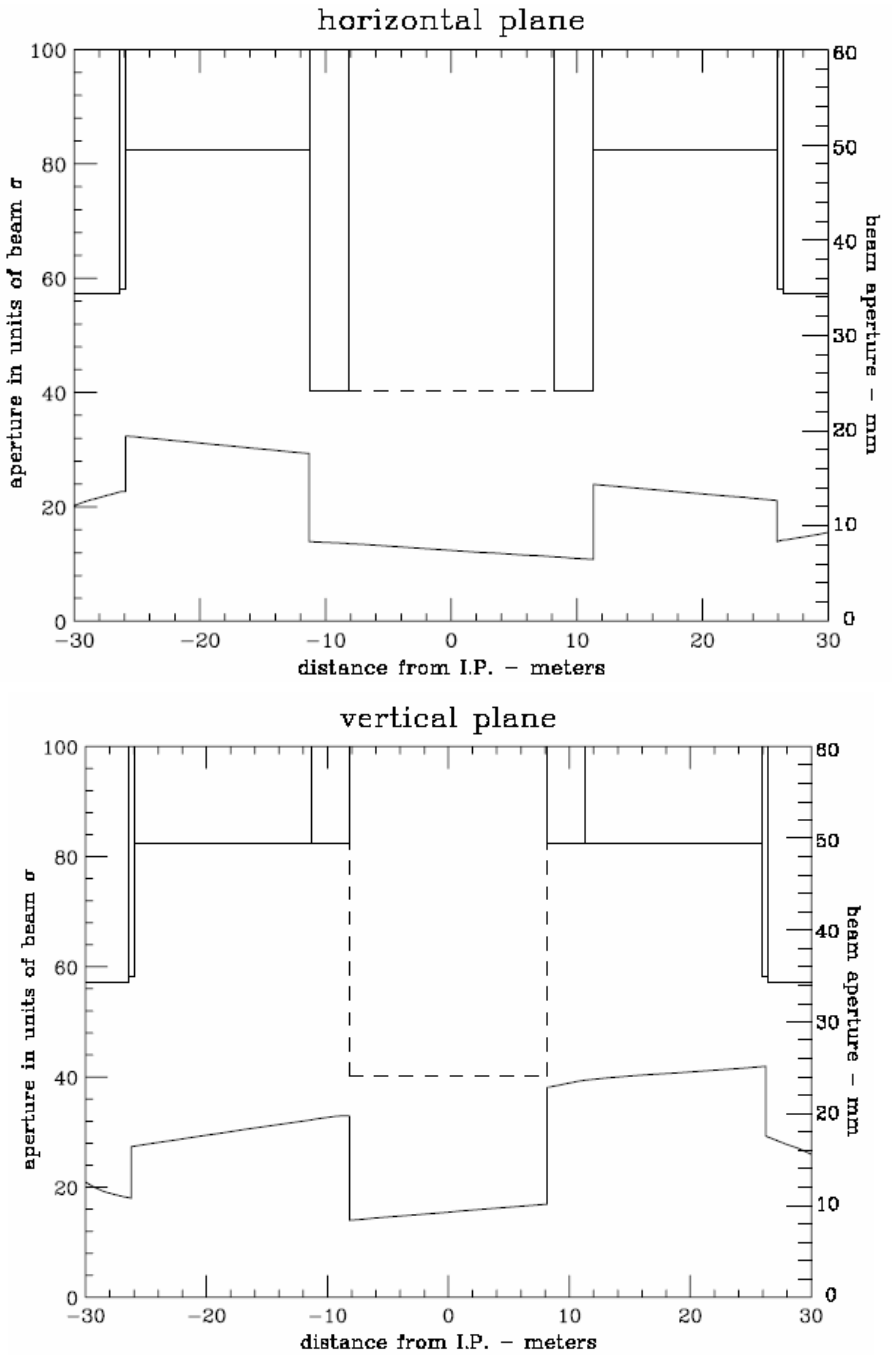

Figures 11-2 and 11-3: Horizontal and vertical aperture and beampipe radius vs. distance from C0. Bottom trace in each plot is the aperture. Beam is @ 150 GeV and on the injection helix.

11.2 Installation Plan

The early shutdown for the installation of the normal straight section is anticipated to be 8 weeks in duration. Not only is the straight section reconfiguration planned for this shutdown, but also considerable utility outfitting in the collision hall (see C0 Outfitting Project CDR). Based on the

effort that was required for the replacement of the C0 Lambertson magnets with MI dipoles in January, 2003, it is anticipated that the rigging work to remove the four Main Injector dipoles and the concrete shielding block base can be accomplished within the first week of the shutdown. In the collision hall, this would leave the middle 5 weeks of the shutdown exclusively for utility outfitting, with the final 2 weeks for vacuum pipe installation, leak checking, and bake-out, along with finishing the utility outfitting work.

Certain activities can be accomplished before the early shutdown begins. These include design and procurement of beam tubes, vacuum components, magnet and beam tube stands, LCW components, simple cryogenic piping extenders, jumpers between power bus and cryo lead boxes, and pre-fabrication of isolation doors between tunnel and collision hall.

The following is a listing of the "work crews" required to complete the conversion to a straight section denoted by the tasks they are to accomplish. This planning is in a preliminary stage. There will likely be some consolidation of crews designation to optimize manpower. The jobs are listed in approximate order of activities.

Once the early shutdown begins, the following tasks must be accomplished in this approximate order for the Tevatron to begin operation again. We are then committed to completion of all items–operation of the Tevatron with any of these items only partially complete is not possible.

1) Warm-up cryogenic houses B4 and C1 (cryo technicians)

2) Unhook water, bus jumpers, vacuum, instrumentation (technicians and electricians):

- Remove water hoses and power cables from 6 warm magnets & 2 cryo lead boxes

- Let up to atmosphere warm vacuum and remove components

- Remove guard rails from shield block wall, isolation gratings, LCW piping, cable trays, and supports in region of FMI dipoles and C-magnets

3) Open shield door (PPD/FESS + riggers or technicians)

4) Remove FMI dipoles & 61 concrete blocks and catwalk for C-magnets (Rigging crew with heavy fork lift)

5) Tunnel magnet moves (technician or rigging crew):

- Remove: 2 half dipoles, 2 C-magnets, two warm bypasses, and remnant (vertical) MR B2 magnet at B48-4 location

- Reposition transversely: 3 full length, 4 quadrupoles, 6 cryo boxes: which include 55.6" bypass, 43" spool, 125.9" spool, 50" spool, and two turn-around boxes

- Install: 2 full dipoles, one warm bypass (existing standard 48-section bypass)

6) As-found, rough component placement, and final alignment of components and vacuum pipe (alignment crews)

7) Cryo device moves: undo 17 cryo interfaces, move remaining components and install new cryo components, make up 16 cryo interfaces (one interface will be eliminated in this reconfiguration), leak check all cryo components (cryo/vacuum technicians)

8) Bus modifications: possibly start on bus modifications for low-β quads (continues thru 2009) (electricians)

9) LCW modifications: extend LCW into collision hall and assembly bldg – interface w/construction (pipefitters)

10) Extensions for cryo relief, suction, and gas piping (cryo/pipefitter)

11) Rehook-up lead boxes to Tevatron power bus (electricians)

12) Install warm beam pipe in place of MI and C-magnets, install beam tube supports, warm vacuum beamline diagnostic components, beam tubes, vacuum pumps, vacuum monitoring components, leak check, and bakeout (vacuum technicians)

13) Install two new BPMs (Instrumentation technicians + electricians)

14) Install two walls at tunnel-collision hall interface (mechanical technicians)

15) Close shield door after completion of collision hall outfitting (PPD/FESS + technicians)

16) Cool-down cryogenic houses B4 and C1 (cryo technicians)

11.2.1 Tunnel modifications

The required modifications to the existing Tevatron tunnel are minimal for this straight section phase. The two junctions of the tunnel with the collision hall will be sealed with solid doors, separating the ventilation systems for the tunnel and the collision hall, providing Oxygen Deficiency Hazard isolation, and maintaining independent search and secure zones for the tunnel and collision hall. The beam pipe and LCW supply and return pipes will penetrate these doors. These doors will have to be able to be opened or removed to allow optical survey and alignment tasks into, and through, the collision hall, as needed.

11.2.2 LCW modifications

The additional BTeV components for the interaction region will need approximately 250 gpm LCW. This LCW at C0 will provide heat dissipation for the SM3 vertex analysis magnet, the two 10 foot-long B2 compensating dipoles, a muon toroid magnet, magnet power supplies (in the C0 assembly building), and copper buswork. The magnets will be power tested in the assembly hall before moving to the collision hall, so provision to bring LCW into the assembly hall is also required. Table 11.1 outlines the LCW requirements for each of the primary components. Later, LCW may also be required to heat the power leads for the superconducting quadrupoles for the low-β^* insertion. The flow requirements are clearly dominated by the vertex magnet. The maximum temperature rise will be approximately 23º F. The flow to the water-cooled bus will be restricted to about 5 gpm per bus pair.

Table 11-1: LCW requirements for 2005 shutdown

System	qty	Current	Power	Min. Flow Rate	Temperature Rise	Diff. Pressure Req'd
		A	*kW*	*GPM* [*L/s*]	*F* [*C*]	*psi*
Vertex Magnet	1	4200	440	151 [9.52]	23 [13]	120
Vertex Power Supply*	2	-	35	11 [.69]	-	100
Vertex Bus	1	4200	<5	5 [.32]	<10 [6]	<100
Toroid Magnet	1	1500	25	25 [1.58]	8 [4]	120
Toroid Power Supplies	1	-	2	5.5 [.35]	-	100
Toroid Bus	1	1500	<5	5 [.32]	<10 [6]	<100
B2 Magnet*	2	2300	76	23.4 [1.48]	23 [13]	110
B2 Power Supply	1	-	6	5.5 [.35]	-	100
B2 Bus*	2	2300	<5	11 [.69]	<10 [6]	<100
		Total	**599**	**242 [15.3]**		

*- power and flow are for both units combined

The LCW will be supplied from the Tevatron LCW system. The existing centrifugal pumps at B4 and C1 will provide the flow needed for BTeV. They are each capable of providing 400 gpm with a pressure head of 140 psi (355 TDH). The Tevatron supply and return header pressures are nominally 160 psig and 20 psig respectively. The typical supply temperature is 90°F. All heat will be rejected to the ponds at B4 and C1 via the heat exchangers located at those service buildings.

The existing 4" Aluminum LCW header will be extended into the collision hall to provide magnet cooling and also into the assembly hall to cool the power supplies. The new header must provide adequate flow to the vertex magnet when it is located in its experimental and assembly (testing) positions. There will not need to be any significant LCW controls or instrumentation upgrades. The current ACNET read backs of temperature, flow, and pressure will suffice. However, local instrumentation will be installed in the assembly hall to aid in troubleshooting the system.

The BTeV/C0 leg of piping will be filled from the Tevatron. This can be accommodated by the Tevatron LCW system since it has a reservoir capacity of well over 3000 gallons and the additional volume of the new BTeV/C0 area will only be on the order of 1000 gallons.

During the conversion of the C0 region to "normal" straight section, LCW hoses feeding the MI dipoles and C-magnets will be removed. Also, existing 2" LCW copper piping on the B4 and C1 side of C0 will be removed to ease magnet removal.

11.2.3 Controls, PS, and QPM modifications

One additional heater firing unit will be required at B4 and C1 service buildings and the inductance value of one quench detection unit at B4 and C1 will increase by one magnet's inductance. Otherwise, no modifications are necessary to the Tevatron QPMs. The shunt circuit on the MI dipoles will be eventually removed from the service building to make room for future PS installations. There will be a need for the installation of two new horizontal and vertical BPMs inboard of the last Collins straight section quadrupole, along with the associated cables and readout electronics. The present set of Beam Loss Monitors (BLM) in the C0 area will be moved to new locations on the beampipe.

11.3 Recommissioning Plan

In the 2/03 shutdown the C0 Lambertson magnets were replaced with MI dipoles, so the Tevatron Department already has experience in recommissioning the C0 straight section after modifications. Since the lattice change is negligible, we expect recommissioning to be straightforward. Aside from the normal recommissioning tasks required after a shutdown, the following steps will be required after C0 has been converted to a normal straight section.

1) Recommission the QPM system: New database constants (inductance and resistance) for the changed magnet strings require verification while ramping magnets. Beam is not required for this step.

2) Train new magnets to 1010 GeV: The newly installed full length Tevatron dipoles need to be ramped to 1010 GeV to verify that there is adequate quench margin for 980 GeV operation. Beam is not required for this step.

3) Change Tevatron injection frequency: This is required because the central orbit length changes. The RF frequency (53.1 MHz) must change by 13.3 Hz. This induces a momentum change of -13.5 MeV. No change is required in MI operation because it phase locks to the Tevatron frequency during beam transfer.

4) Local orbit correction: It is expected that the local orbit will need to be corrected at all energies and at all steps of the low beta squeeze. This step includes local aperture scans to verify that the aperture is adequate. Since the beampipe in C0 will initially be 4"dia, we expect the aperture to be large. This step requires beam.

5) BPM and BLM checkout: The 4 new BPMs and the repositioned BLMs require testing with beam.

6) Synchrotron light monitor: This device will require extensive parasitic studies before it can be considered operational. See section 9.1 for a more detailed discussion.

References

[1] M Harrison, "The Tevatron Abort System", Fermilab UPC-153, 1981

[2] Fermilab Drawing #1780.003-ME-140999 (7 sheets)

[3] S Ohnuma, "Geometry of the Superconducting Ring", Fermilab UPC-163, 1982

[4] CT Murphy, “The Brass Plug Monument System for Doubler Alignment”, Fermilab TM-1067, 1981

[5] P Ivanov, “InjectNote”, Fermilab Beams-doc-990, 2004

[6] M Church, “Summary of B0 and D0 Aperture Scans, Alignment Studies, and Quad Tickling Measurements Done Between 9/01 and 10/01”, Fermilab Beams-doc-900, 2003

12 Installation, Integration, Schedule, and Cost

12.1 Tunnel installation

Tunnel drawings for the shutdown work will be created. For reference, the present magnet and vacuum configuration appears on drawings ME-140999, ME-140070 and ME-140071. A 3 dimensional model, with input from the lattice design program MAD, civil construction drawings, and shell models of tunnel elements, is being developed to help understand interference and integration issues.

Installation work will be assigned as follows:

Warm Vacuum – AD Mech. Support Dept. technicians, with augmentation by other FNAL technicians

Shield door moves, concrete block removal, catwalk removal, shield wall assembly, guard rails and interlock gates removal and installation – subcontracted T&M ironworkers, with FNAL task manager

Cryo beamline components – AD Mech. Support Dept. technicians, with augmentation by AD Cryo. Dept. technicians

Cryo piping – AD Cryo. Dept. technicians and possible subcontracted T&M pipefitters

LCW – subcontracted T&M pipefitters, with FNAL task manager

Water Cooled Bus – subcontracted T&M electricians, with FNAL task manager

Interlock gates wiring and switches – T&M electricians, with FNAL task manager

Alignment – FNAL Alignment and Metrology Group

Cable pulls - T&M electricians, with FNAL task manager

The Alignment and Metrology Group has created a new system of positioning which replaces the Murphy line system. This will be used to align the beamline components of the Tevatron.

12.1.1 Magnetic Element Installation

Tevatron cryogenic sectors B4 and C1 will be warmed to room temperature to perform the installation. All Tevatron dipoles between B45 and C15 (31 magnets) will be moved longitudinally and/or transverselly to accommodate the new lattice arrangement and the shortened Tevatron arc length. All other magnetic elements currently installed between B43 and C17, with the exception of the 4 66” quads at B43, B44, C16, and C17, will be removed (26 magnets). Table 12-1 lists the magnetic elements which will be installed in the Tevatron between B43 and C17.

Table 12-1: Newly installed magnetic elements between B43 and C17

Device	Locations
4 Tevatron Q1's (from A4, B1, and storage)	B45,B46,C14,C15
2 LHC-style 54" Q5's	B47,C13
2 LHC-style 79" Q4's	B48,C12
2 LHC-style 96" Q3's	B49,C11
2 LHC-style 173" Q2's	B49,C11
2 LHC style 96" Q1's	B49,C11
4 new X1 spools	B43,B44,C16,C17
4 Tevatron P spools (from A4,B1, and storage)	B45,B46,C14,C15
4 new X2 spools	B47,B48,C12,C13
2 new X3 spools	B49,C11
1 Tevatron H spool (from storage)	B49
total = 29	

12.1.2 Electrostatic Separators

Six new separators, identical to previously built separators, are required. There will be 2 horizontal and 1 vertical separator at B49 and 2 vertical and 1 horizontal separator at C11. These separators are delicate, and special handling equipment and false floors must be provided to install them. The separators are located above a 2'6" deep channel in the tunnel floor on either side of the collision hall (see Figure 12-1), so that holes do not have to be cored in the tunnel floor to accommodate them. An air spring transporting cart exists for the separators, which is towed behind a golf cart, then pushed into place manually.

Alternatively, these separators could be mounted on girder modules similar to those which were used at D0. Installation equipment exists which was used for the separator girders at D0. The installation of these girders through the D0 drop hatch requires opening up the hatch to its largest configuration and careful handling of the girders, for which a procedure was written at the time of the D0 installation in 1992.

The practical advantage of placing the separators on a common girder is that the separators could be evacuated in the clean shop, backfilled with a nitrogen purge, transported to the tunnel and installed, then evacuated, and never opened to air in the tunnel.

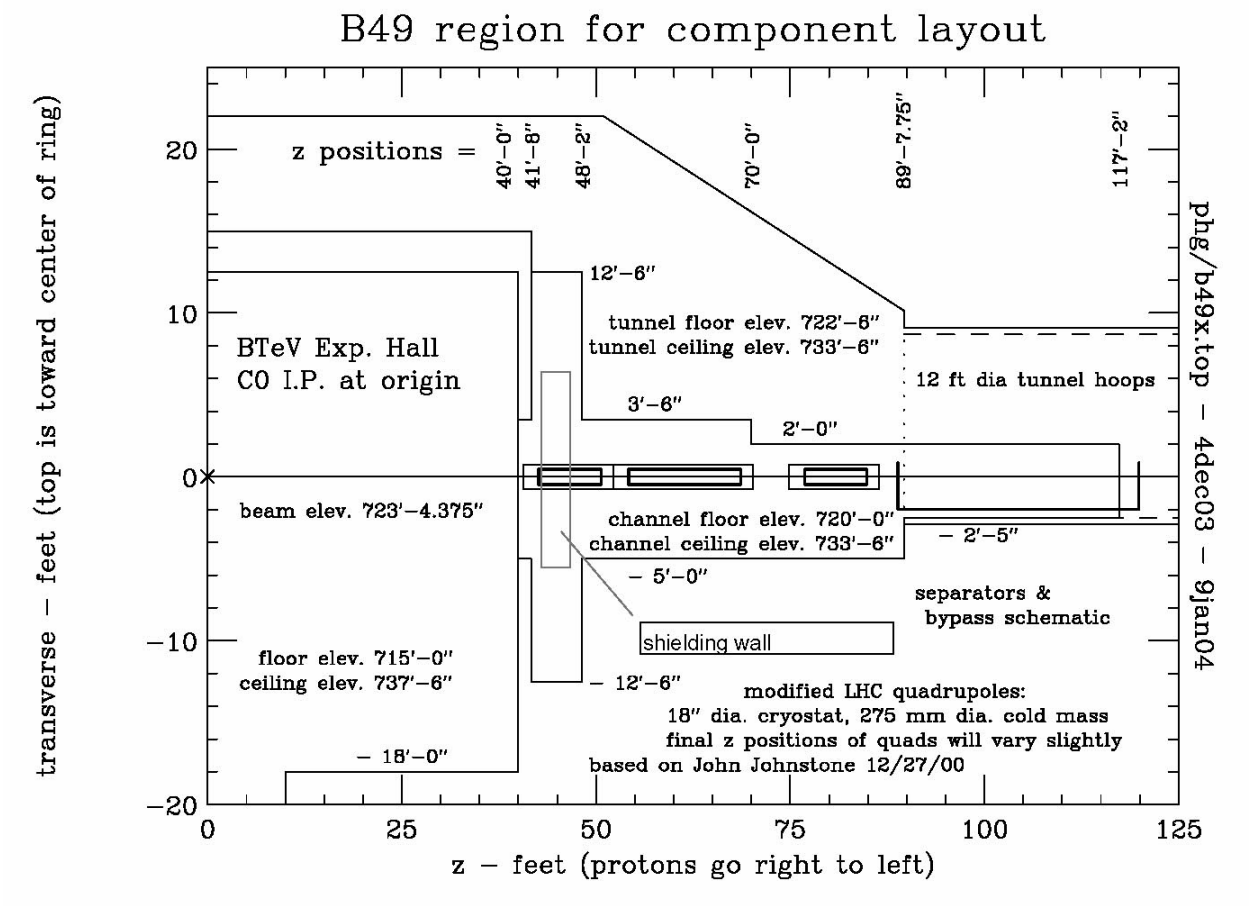

Figure 12-1: Tevatron tunnel plan view on the B side of the collision hall.

12.1.3 Q1 and P Spool Removal from A4/B1

The Tevatron Q1's and the P spools currently installed at A49 and B11 will be removed from those locations and reinstalled at B45 and C15. In the current Tevatron configuration the Q1's are not powered (they have been removed from C49 and D11 to provide space for the D0 Forward Proton Detector), however the present functionality of these 2 devices at A49 and B11 must be replaced.

At A49 the Q1 and P spool are adjacent and the P spool is inboard of the Q1. A dipole is just upstream of the Q1, and the start of the bypass for the separators is just downstream of the P spool. There is main Tev bus through these devices, but it is not connected in these 2 devices. The circuits used in the P spool are HDA49, VDA49, and SQA4 which are all essential for Tevatron Run II operation. HBPMA49 and VBPMA49 are also in the P spool and are essential for Run II operation. The Q1 slot length is 72.827" and the P spool slot length is 56.149".

A plan to replace the present functionality of these devices at A49 is as follows. Replace the Q1 and P spool with two devices: a (new) cold spool containing a horizontal BPM and an H spool. The H spool has VD, HD, and SQ coils and a VBPM. The slot length of an H spool is 49.910" The slot length of the new HBPM spool will need to be 79.066". The H spool should be inboard

of the cold BPM spool in order to maximize the effectiveness of VDA49 in making IR position bumps.

At the B11 location the Q1 and P spool are adjacent and the P spool is inboard of the Q1. The end of the separator bypass is just upstream of the P spool, and an R spool is just downstream of the Q1. A dipole is downstream of the R spool. There is main Tev bus through these devices, but it is not connected in the Q1 or P spool. The circuits used in the P spool are HDB11, VDB11, and SQB1 which are all essential for Run II operation. HBPMB11 and VBPMB11 are also in the P spool and are essential for operation. The R spool has no internal coils and is used only to provide an (external) turnaround for the main Tev bus. It has reversed cryogen pipes. It has a slot length of 40.729".

A plan to replace the present functionality of these devices at B11 is as follows. Replace the Q1, P spool, and R spool with two devices: a (new) cold spool containing a horizontal BPM and an H spool. The H spool has VD, HD, and SQ coils, a VBPM, and will provide an external turnaround for the main Tev bus. The slot length of the new HBPM spool will need to be 119.795". The H spool should be inboard of the cold BPM spool so that the cryogen pipes can be reversed in the BPM spool. This will require Tev through bus in the BPM spool.

12.1.4 Beam Collimators and Shielding

Concrete shielding walls at the upstream and downstream ends of the C0 collision hall will be of a clamshell design and on rollers, so they can be easily moved when changing a magnet in the area. Figure 12.1 shows the approximate location of the shielding wall on the B side of the collision hall. They will surround the Q1 low beta quad cryostat and could have dimensions up to 6' thick, 12' high, and 12' wide. Gaps around the quadrupole cryostat and cryostat stand will be filled with easily removable sandbags. The gaps will be large enough to provide for sighting for alignment needs.

Two new collimators, of standard design, will be installed in a a 2.6 meter warm straight section near B47-4.

12.2 Interfacing with civil construction project

All work performed by any building trades will be the responsibility of FESS, with the exception of ironworkers and electricians removing or installing accelerator components and their related supports, which will be the responsibility of the Accelerator Division. The civil construction subproject of the BTeV project (WBS3.0) will provide AC power distribution to the B4, C1, and C0 service buildings. They will also provide the housing and environmental protection for the external buswork between the C0 service building and the penetration entering the Tevatron tunnel.

12.3 Interfacing with Detector Installation

After C0 is converted to a normal straight section in 2005, the warm vacuum beampipe in the collision hall is not included within the scope of this project. The C0 IR project will provide vacuum gate valves on the inboard ends of the Q1 quads and (possibly) the 50 l/sec ion pumps mounted just inside these gate valves. All work between these gate valves (or ion pumps) is the responsibility of the Detector Group. However, the B2 compensating dipole inside the toroid

must have a provision for changing it in the event of a failure, and we envision this to involve some sort of handling mechanism and equipment in the accelerator tunnel. A cooperative design effort for this magnet changing process between the Accelerator Division and the Detector Group must be carried through.

12.4 Schedule and Cost

To be written. Summary of Open Plan output. MC

13 Appendices

13.1 Table of beamline elements between B43 and C17

device	location	start z coordinate	slot length (m)	high power leads	internal BPM	PS
66" quad	B43-1	0.00	2.3114		vbpmb43	
X1 spool	B43-1a	2.31	1.8288			T:VDB43,T:QB43, T:SDB43
TB	B43-2	4.14	6.4008			
TB	B43-3	10.54	6.4008			
TC	B43-4	16.94	6.4008			
TC	B43-5	23.34	6.4008			
66" quad	B44-1	29.74	2.3114		hbpmb44	
X1 spool	B44-1a	32.05	1.8288			T:HDB44, T:QB44, T:SFB44
TC	B44-2	33.88	6.4008			
TC	B44-3	40.28	6.4008			
TB	B44-4	46.69	6.4008			
TB	B44-5	53.09	6.4008			
cold spool	B-44-6	59.49	0.1276			
old-Q1	B45-1	59.61	1.8498			C:QB45=5KA max
P spool	B45-1a	61.46	1.4262	5KA	hbpmb45, vbpmb45	T:VDB45, T:SQ
feedcan	B-45-1B	62.89	0.7366			
TB	B45-2	63.63	6.4008			
TB	B45-3	70.03	6.4008			
TC	B45-4	76.43	6.4008			
TC	B45-5	82.83	6.4008			
TC	B45-6	89.23	6.4008			
old-Q1	B46-1	95.63	1.8498			C:QB46=5KA max
P spool	B46-1a	97.48	1.4262	5KA	hbpmb46, vbpmb46	T:HDB46, T:SQ
TC	B46-2	98.91	6.4008			
TC	B46-3	105.31	6.4008			
TB	B46-4	111.71	6.4008			
TB	B46-5	118.11	6.4008			
54" LHC quad (Q5)	B47-1	124.51	2.4409			C:C0Q5=10KA max
X2 spool	B47-1a	126.95	1.4268	10 KA	hbpmb47, vbpmb47	T:VDB47, T:HDB47

device	location	start z coordinate	slot length (m)	high power leads	internal BPM	PS
TB	B47-2	128.38	6.4008			
TB	B47-3	134.78	6.4008			
cold bypass		141.18	0.3016			
warm straight		141.48	2.5885			
cold bypass	B-47-4	144.07	0.4286			
X2 spool	B48-1a	144.50	1.4268	10KA	hbpmb48, vbpmb48	T:HDB48, T:VDB48
79" LHC quad (Q4)	B48-1	145.93	2.9743			C:C0Q4=10KA max
TC	B48-2	148.90	6.4008			
TC	B48-3	155.30	6.4008			
TB	B48-4	161.70	6.4008			
TB	B48-5	168.10	6.4008			
HTS spool	B49-1a	174.50	1.2677	5KA for main bus	vbpmb48	C:VDB49, T:SQ
cold spool	B49-1b	175.77	0.2741			
cold bypass	B49-2	176.04	0.4286			
separator		176.47	2.9105			
separator		179.38	2.9105			
separator		182.29	2.9105			
cold bypass		185.20	0.3016			
cryo turnaround	B49-2a	185.51	0.7366			
96" LHC quad (Q3)	B49-3	186.24	3.5204			C:C0Q123, 10KA max
X3 spool	B49-3a	189.76	1.4268	10kA, 200A	hbpmb49, vbpmv49	T:HDB49,T:VDB49, T:SQB4
173" LHC quad (Q2)	B49-4	191.19	5.4762			C:C0Q123, 10KA max; C:C0QT2U, 200A max
96" LHC quad (Q1)	B49-5	196.67	3.5204			C:C0Q123, 10KA max
warm bpms	C-0	200.19	0.2604		hbpmc0u, vbpmcou	
warm straight	C-0	200.45	12.1378			
warm straight	C-0	212.58	12.1378			
warm bpms	C-0	224.72	0.2604		hbpmc0d, vbpmc0d	

device	location	start z coordinate	slot length (m)	high power leads	internal BPM	PS
96" LHC quad (Q1)	C10-1	224.98	3.5204			C:C0Q123, 10KA max
173" LHC quad (Q2)	C10-2	228.50	5.4762			C:C0Q123, 10KA max; C:C0QT2D, 200A max
X3 spool	C10-2a	233.98	1.4268	10kA, 200A	hbpmc11, vbpmc11	T:HDC11,T:VDC11, T:SQC1
96" LHC quad (Q3)	C10-3	235.41	3.5204			C:C0Q123, 10KA max
cryo turnaround	C10-3a	238.93	0.7366	5KA for main bus		
cold bypass	C-10-4	239.66	0.3016			
separator		239.96	2.9105			
separator		242.88	2.9105			
separator		245.79	2.9105			
cold bypass		248.70	0.4286			
TC	C11-2	249.13	6.4008			
TC	C11-3	255.53	6.4008			
TB	C11-4	261.93	6.4008			
TB	C11-5	268.33	6.4008			
X2 spool	C11-5a	274.73	1.4268	10KA	hbpmc12, vbpmc12	T:VDC12, T:HDC12
79" LHC quad (Q4)	C12-1	276.16	2.9743			C:C0Q4=10KA max
TB	C12-2	279.13	6.4008			
TB	C12-3	285.53	6.4008			
TC	C12-4	291.93	6.4008			
54" LHC quad (Q5)	C13-1	298.33	2.4409			C:C0Q5=10KA max
X2 spool	C13-1a	300.77	1.4268	10KA	hbpmc13, vbpmc13	T:HDC13, T:VDC13
TC	C13-2	302.20	6.4008			
TC	C13-3	308.60	6.4008			
TB	C13-4	315.00	6.4008			
TB	C13-5	321.40	6.4008			
old-Q1	C14-1	327.80	1.8498			
P spool	C14-1a	329.65	1.4262	5KA for old-Q1	hbpmc14, vbpmc14	T:VDC14, T:SQ
TB	C14-2	331.08	6.4008			
TB	C14-3	337.48	6.4008			
TC	C14-4	343.88	6.4008			
TC	C14-5	350.28	6.4008			

device	location	start z coordinate	slot length (m)	high power leads	internal BPM	PS
TC	C14-6	356.68	6.4008			
cold spool	C14-6a	363.08	0.1276			
old-Q1	C15-1	363.21	1.8498			C:QC15=5KA max
P spool	C15-1a	365.06	1.4262	5KA for old-Q1	hbpmc15, vbpmc15	T:HDC15, T:SQ
feedcan	C15-1b	366.49	0.7366			
TC	C15-2	367.22	6.4008			
TC	C15-3	373.62	6.4008			
TB	C15-4	380.02	6.4008			
TB	C15-5	386.43	6.4008			
66" quad	C16-1	392.83	2.3114		vbpmc16	
X1 spool	C16-1a	395.14	1.8288			T:VDC16, T:QC16, T:SDC16
TB	C16-2	396.97	6.4008			
TB	C16-3	403.37	6.4008			
TC	C16-4	409.77	6.4008			
TC	C16-5	416.17	6.4008			
66" quad	C17-1	422.57	2.3114		hbpmc17	
X1 spool	C17-1a	424.88	1.8288			T:HDC17,T:QC17, T:SFC17
cold bypass	C-17-2	426.71	0.3016			
open space		427.01	0.0052			
separator		427.02	2.9105			
separator		429.93	2.9105			
separator		432.84	2.9105			
separator		435.75	2.9105			
open space		438.66	0.0052			
cold bypass		438.66	0.4286			
TB	C17-3	439.09	6.4008			
TB	C17-4	445.49	6.4008			

13.2 Alternative Corrector Approach – "Flat Coil Array" Design

An alternative approach to corrector design based on an array of 'flat coils' which provides a combined function magnet has been proposed. In this design, one corrector assembly can be configured to provide any of the required multipole combinations. Having only one design results in several tangible benefits: lower manufacturing costs, reduction in the total number of spares, and higher reliability.

Figure 13.2-1 is a conceptual drawing of the new corrector. Table 13.2-1 lists the corrector properties, where the corrector types – 'A,' 'B', and 'C' – correspond to the different C0 IR spool requirements. This corrector is assembled from 12 identical flat coils of a 'race-track' geometry. The coils are powered from separate power supplies and are capable of generating all of the required dipole, quadrupole and sextupole field combinations. For example, in the case of the normal dipole, quadrupole and sextupole (Type C) configuration, the total field is symmetric relative to the median plane and there are only 5 separately powered windings. The racetrack coil can be made in a very simple manufacturing process. There are no problems to wind the coils under tension and provide pre-stress through the differential shrinkage of the aluminum shell with respect to the low carbon steel core. The coil ends are very short and the corrector is very effective in the longitudinal direction. The magnet can be assembled from 12 identical coil blocks and each of them can be separately tested in a small test cryostat. The magnet cold mass is easily repaired by replacing just the bad coil segment. There are no internal splices, only joints to the current leads which should increase the magnet reliability. While this corrector will require a larger volume of superconductor than the shell type design, the total magnet cost is not dominated by the supercondutor.

Table 13.2-1: Corrector Main Parameters

Corrector type	A	B	C
Integrated dipole field, T*m	0.48		
Integrated quadrupole gradient, T	25		
Integrated sextupole strength , T/m	450		
Effective length, m	0.8	0.8	1.2
Inner coil radius, mm	40		
Inner core radius, mm	63		
Outer core radius, mm	120		
Operational current, A	35 - 77		
Coil number of turns	760 - 1700		
Bare strand diam., mm	0.3 - 0.5		
Max strand diam. with insulation, mm	0.43 - 0.63		
Coil area, mm^2	368		
Cold mass outer diam., mm	300		

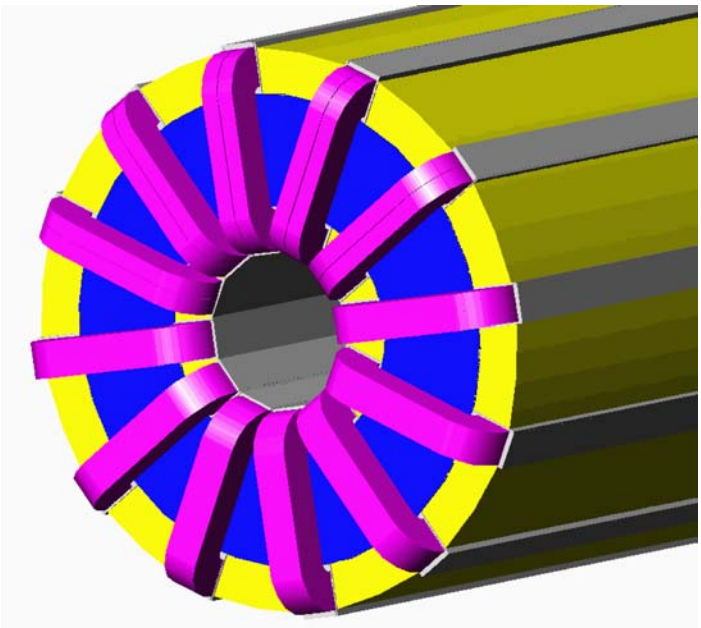

Figure 13.2-1: General view of corrector magnet

13.2.1 Corrector Magnetic Design

The magnetic design is simple: a combined function magnetic field is formed by 12 identical race-track coils distributed equally with an angular separation of 30^o. The number of coils is the minimum necessary to provide the required dipole, quadrupole and sextupole fields. A rectangular coil cross-section was chosen to simplify the winding process. In the most general case, each coil would be powered separately. Field errors are somewhat larger than in the $\cos(n\theta)$ cross section design, but should be tolerable since corrector field errors can produce only second order effects. Adjustment of the corrector currents can compensate for field deviations caused by manufacturing tolerances, iron saturation effects, etc. The outer coil sections produce a fringe field, which can be eliminated by 10mm thick magnetic shield.

13.2.2 Corrector Type-A

This corrector generates horizontal and vertical 0.48 T*m dipole fields and a 7.5 T skew quadrupole field. The corrector parameters are shown in Table 13.2-2 and in Figures 13.2-2 through 13.2-6.

Table 13.2-2: Corrector type A parameters

Dipole field, T	0.6
Effective length, m	0.8
Dipole component ampere-turns, A	Iw_{d1} = 15200, Iw_{d2} = 13300, Iw_{d3} = 7600
Skew quadrupole gradient, T/m	9.375
Quadrupole component ampere-turns, A	Iw_q= 12100
Total coil ampere-turns at max field, A	33000
Maximum flux density in the yoke at max field, T	2.3

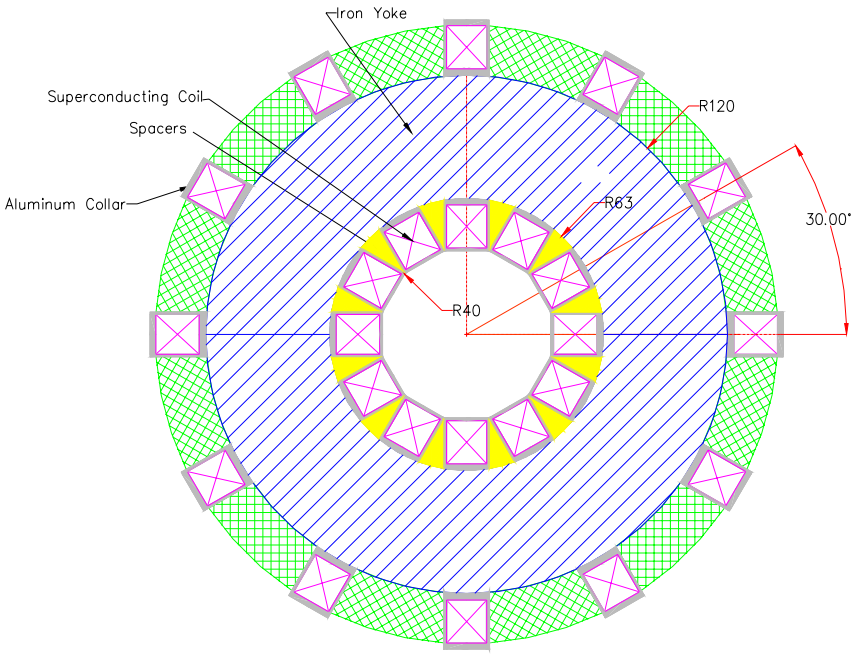

Figure 13.2-2: Corrector A and B cross-section

No	Ncon	Radius/X	Phi/Y	Alpha/Inc	Current	CondName	N1	N2
1	1	40	0	0	7600	BTEVCOR1	20	20
2	1	39.241	12.0325	30	13300	BTEVCOR	20	20
3	1	27.967	30.041	60	7600	BTEVCOR	20	20

```
ERROR OF HARMONIC ANALYSIS OF Br AT RADIUS      25.40 mm
SUM (Br(p) - SUM (An cos(np) + Bn sin(np)))   0.1186E-04


MAXIMUM ABSOLUTE FIELD ERROR (T)
MAX (BrN - SUM (An cos(np) + Bn sin(np)))     0.5036E-03

MAIN FIELD:     -0.59781 NORMAL REL. MULTIPOLES (1.D-4):
b 1:  10000.00000  b 2:       0.00000  b 3:      -0.07739
b 4:       0.00000  b 5:      -2.36804  b 6:       0.00000
b 7:      -0.57585  b 8:       0.00000  b 9:      -0.00717
b10:       0.00000  b11:       5.45918  b12:       0.00000
b13:       0.97742  b14:       0.00000  b15:       0.00011
b16:       0.00000  b17:       0.00027  b18:       0.00000
b19:       0.00019  b20:       0.00000  b

NI/B :    -0.953E+05
```

Figure 13.2-3: Dipole geometry and field harmonics (Dip1rot.data)

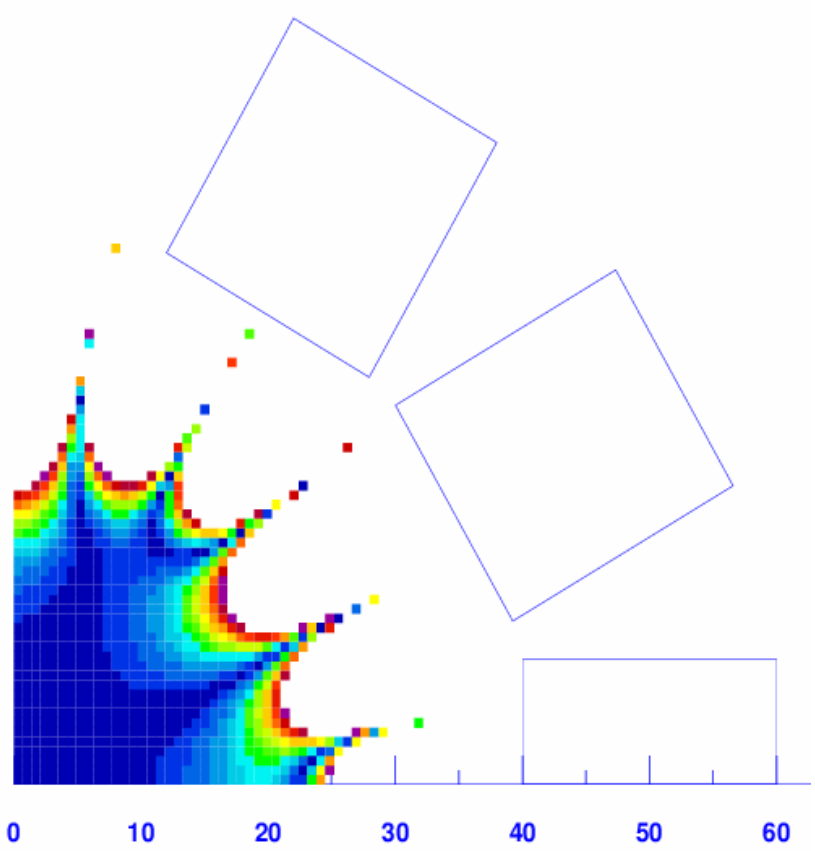

Figure 13.2-4: Dipole field homogeneity

No	Ncon	Radius/X	Phi/Y	Alpha/Inc	Current	CondName	N1	N2
1	1	40	-9.2	0	15200	CORR1	10	10
2	1	39.241	12.0325	30	33000	CORR1	10	10
3	1	27.967	30.041	60	33000	CORR1	10	10
4	1	9.2	40	90	15200	CORR1	10	10
5	1	-12.0325	39.241	120	-6400	CORR1	10	10
6	1	-30.041	27.967	150	-17800	CORR1	10	10
7	1	-40	9.2	180	-15200	CORR1	10	10
8	1	-39.241	-12.0325	210	-8800	CORR1	10	10
9	1	-27.967	-30.041	240	-8800	CORR1	10	10
10	1	-9.2	-40	270	-15200	CORR1	10	10
11	1	12.0325	-39.241	300	-17800	CORR1	10	10
12	1	30.041	-27.967	330	-6400	CORR1	10	10

Figure 13.2-5: Corrector A geometry and coil ampere-turns at maximum combined field

```
ERROR OF HARMONIC ANALYSIS OF Br AT RADIUS     25.40 mm
SUM (Br(p) - SUM (An cos(np) + Bn sin(np)))  0.2296E-04

MAXIMUM ABSOLUTE FIELD ERROR (T)
MAX (BrN - SUM (An cos(np) + Bn sin(np)))    0.8355E+00

MAIN FIELD:    -0.59781 NORMAL REL. MULTIPOLES (1.D-4):
b 1:  10000.00000  b 2:     -0.02913  b 3:      0.00099
b 4:      0.00000  b 5:     -2.32043  b 6:      0.00221
b 7:     -0.55706  b 8:      0.00000  b 9:     -0.00070
b10:      0.00021  b11:      5.45721  b12:      0.00000
b13:      0.97713  b14:     -0.00001  b15:      0.00000
b16:      0.00000  b17:      0.00016  b18:      0.00000
b19:      0.00013  b20:      0.00000  b

                              SKEW  REL. MULTIPOLES (1.D-4):
a 1: -10000.04258  a 2:  -3992.24722  a 3:      0.02127
a 4:      0.00000  a 5:      2.32912  a 6:     -0.00572
a 7:     -0.55691  a 8:      0.00000  a 9:      0.00071
a10:     10.88396  a11:      5.45699  a12:      0.00000
a13:     -0.97717  a14:     -0.31966  a15:      0.00000
a16:      0.00000  a17:     -0.00017  a18:      0.00000
a19:      0.00013  a20:      0.00000  a

NI/B :   -0.161E+06
```

Figure 13.2-6: Corrector A field harmonics (DQS1rot.data)

The electrical connections are very simple for this type of magnet. Each coil is powered individualy by an 80A bipolar power supply. The coil current is the sum of all components, which produce the dipole and quadrupole fields. The coil currents for the Figure 13.2-7 diagram are:

$I_1 = I_{v1}$ $\quad$ $I_7 = -I_1$

$I_2 = I_{v2} + I_{h3} + I_{sq}$ $\quad$ $I_8 = -I_{v2} - I_{h3} + I_{sq}$

$I_3 = I_{v3} + I_{h2} + I_{sq}$ $\quad$ $I_9 = -I_{v3} - I_{h2} + I_{sq}$

$I_4 = I_{h1}$ $\quad$ $I_{10} = -I_4$

$I_5 = -I_{v3} + I_{h2} - I_{sq}$ $\quad$ $I_{11} = I_{v3} - I_{h2} - I_{sq}$

$I_6 = -I_{v2} + I_{h3} - I_{sq}$ $\quad$ $I_{12} = I_{v2} - I_{h3} - I_{sq}$

The current directions for the different field components are shown in Figure 13.2-7 Skew fields can be obtained by an angular rotation of the corresponding multipole ring diagram.

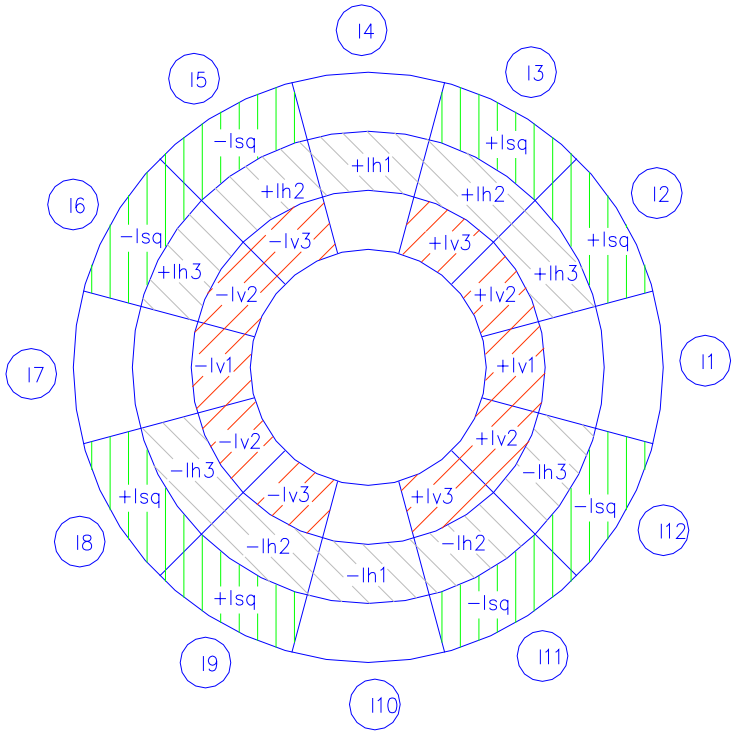

Figure 13.2-7: Current distribution in corrector type A, where

I_{v1}, I_{v2}, I_{v3} – vertical dipole currents

I_{h1}, I_{h2}, I_{h3} – horizontal dipole currents

I_{sq} –skew quadrupole current

13.2.3 Corrector Type B

This corrector generates horizontal or vertical 0.48 T*m dipole fields with a 7.5 T skew quadrupole. All corrector parameters can be obtained from corrector A design with only one dipole field component. The corrector parameters are shown in Table 13.2-3 and in Figure 13.2-8.

Table 13.2-3: Corrector type B parameters

Dipole field, T	0.6
Effective length, m	0.8
Dipole component ampere-turns, A	Iw_{d1} = 15200, Iw_{d2} = 13300, Iw_{d3} = 7600
Skew quadrupole gradient, T/m	9.375
Skew quadrupole component ampere-turns,A	Iw_q= 12100
Total coil ampere-turns at max field, A	25400
Maximum flux density in the yoke at max field, T	2.3

The coil currents for the corrector with vertical dipole are:

$$\mathbf{I_1 = I_{v1}} \qquad \mathbf{I_7 = -I_1}$$

$$\mathbf{I_2 = I_{v2} + I_{sq}} \qquad \mathbf{I_8 = -I_{v2} + I_{sq}}$$

$$\mathbf{I_3 = I_{v3} + I_{sq}} \qquad \mathbf{I_9 = -I_{v3} + I_{sq}}$$

$$\mathbf{I_4 = 0} \qquad \mathbf{I_{10} = 0}$$

$$\mathbf{I_5 = -I_3} \qquad \mathbf{I_{11} = -I_9}$$

$$\mathbf{I_6 = -I_2} \qquad \mathbf{I_{12} = -I_8}$$

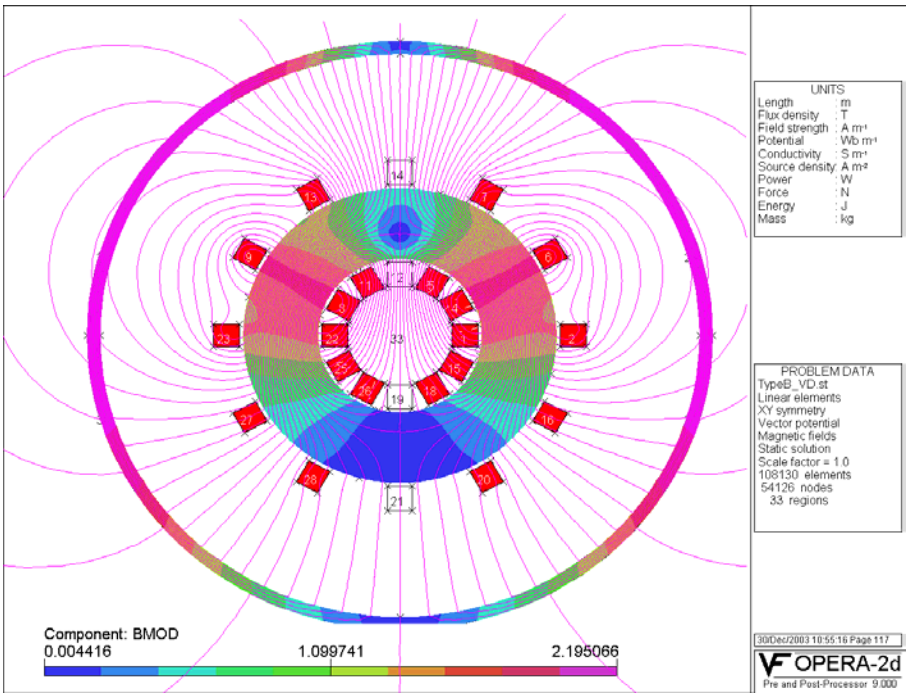

Figure 13.2-8: Flux density in corrector with the vertical dipole and skew quadrupole

The coil currents for the corrector with horizontal dipole are shown below. This type of corrector is powered by 5 independent power supplies.

$$I_1 = 0 \qquad I_7 = 0$$
$$I_2 = I_{h3} + I_{sq} \qquad I_8 = -I_6$$
$$I_3 = I_{h2} + I_{sq} \qquad I_9 = -I_5$$
$$I_4 = I_{h1} \qquad I_{10} = -I_4$$
$$I_5 = I_{h2} - I_s \qquad I_{11} = -I_3$$
$$I_6 = I_{h3} - I_{sq} \qquad I_{12} = -I_2$$

13.2.4 Corrector Type C

This corrector generates horizontal or vertical 0.48 T*m dipole fields with 25 T quadrupole and 450 T/m sextupole fields. The corrector parameters are shown in Table 13.2-4 and in Figure 13.2-9. The cold mass assembly is rotated by 15º as shown in Figure 13.2-9. The magnet design is the same as for the A and B correctors. The magnetic field, currents and forces are symmetric with respect to the median plane, resulting in only 5 independent power supplies needed.

Table 13.2-4: Corrector type C parameters

Dipole field, T	0.4
Effective length, m	1.2
Dipole component ampere-turns, A	$Iw_{d1} = 9856.2$, $Iw_{d2} = 7189$, $Iw_{d3} = 2650.9$
Quadrupole gradient, T/m	20.833
Quadrupole component ampere-turns, A	$Iw_q = 26828$
Sextupole strength, T/m^2	375
Sextupole component ampere-turns, A	21728.5
Total conductor current at all component max field, A	50-80
Maximum flux density in the yoke at max field, T	2.0

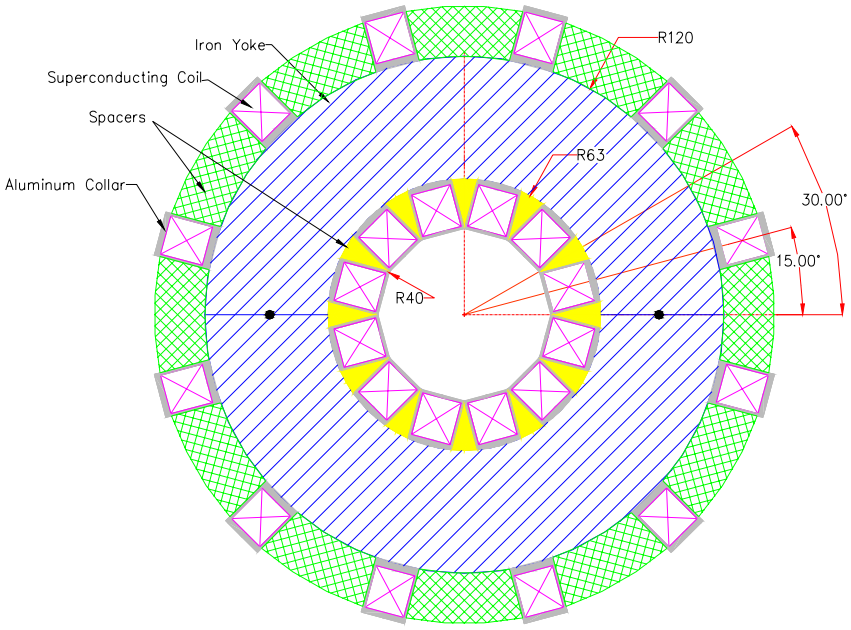

Figure 13.2-9: Cross section of Corrector C

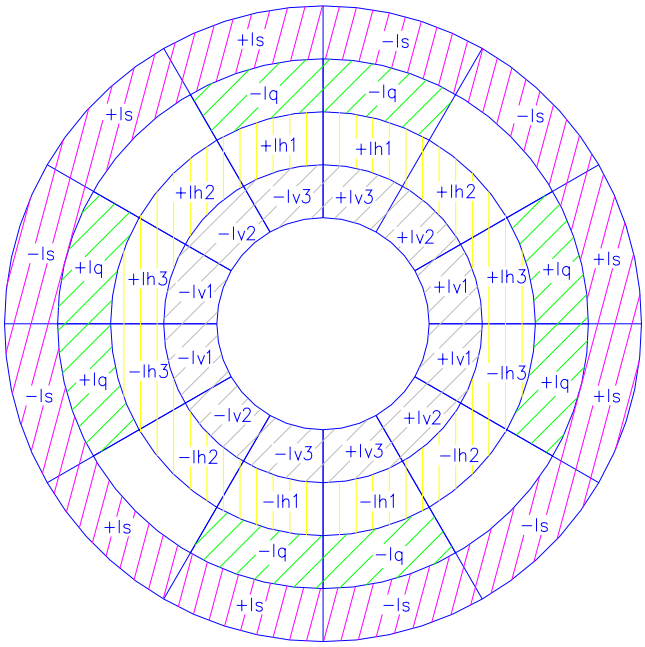

Figure 13.2-10: Azimuthal currents distribution in C corrector, where

I_{v1},I_{v2},I_{v3} - vertical dipole currents,

I_{h1},I_{h2},I_{h3} - horizontal dipole currents,

I_q - quadrupole current,

I_s - sextupole current.

The coil currents for this corrector with vertical dipole are:

$$
\begin{aligned}
I_1 &= I_{d1} + I_q + I_s \\
I_2 &= I_{d2} - I_s \\
I_3 &= I_{d3} - I_q - I_s \\
I_4 &= -I_{d3} - I_q + I_s \\
I_5 &= -I_2 \\
I_6 &= -I_{d1} + I_q - I_s \\
I_7 &= -I_6 \\
I_8 &= -I_5 \\
I_9 &= -I_4 \\
I_{10} &= -I_3 \\
I_{11} &= -I_2 \\
I_{12} &= -I_1
\end{aligned}
$$

13.2.5 Mechanical Design Concepts

There are at least two options of cold mass fabrication and assembly. The first one is to wind all racetrack coils separately on the aluminum or stainless steel bobbins, then assemble two sub assemblies with 6 coils each. In this case the iron core should be split in the median plane. After that the cold mass is vacuum impregnated with epoxy. The second option is to split the iron core into 4 or 12 sectors and use these parts as mandrels for coil winding, impregnation and support. In this case, each iron block with one coil can be tested separately. Since in all field configurations the iron blocks are attracted to each other, only positioning pins are needed to provide proper block positioning. Special attention is needed to provide a tight coil bobbin connection to the yoke because under some current combinations the Lorentz forces will be oriented inside the magnet aperture. There are also some cold mass de-centering forces. The de-centering forces for correctors A and B are rather low (160 kg) but are quite a bit higher for corrector C higher (1900 kg). The cold mass support structure should be capable of carrying this load plus the magnet weight (~500kg).

13.2.6 Electrical Circuits, Currents and Power Supplies

As mentioned previously, the electrical connections are very simple for this type of magnet. External current leads are provided for each coil and connected to separate 80 A bipolar power supplies. It is possible to reduce the number of currents and power supplies to 5 in the case of normal dipole, quadrupole and sextupole fields (see Table 13.2-5).

The coil current is the sum of all components which produce the dipole, quadrupole and sextupole fields. The current directions for different normal field components were shown in Figures 3.2-7 and 3.2-10 above. Skew fields can be obtained by the angular rotation of corresponding multipole ring diagram.

Table 13.2-5: Corrector currents, coils, and power supplies

Corrector Type	Number of PS/corrector	Max coil ampere-turns	Max coil current at 760 turns/coil
A (HD+VD+SQ)	10	33000	43.4
B (VD+SQ)	5	25400	33.4
B (HD+SQ)	5	25400	33.4
C (VD+Q+S)	5	58413	76.8
C (HD+Q+S)	10	58413	76.8

The coil current can be reduced if the superconducting wire diameter is decreased and the number of turns is increased proportionally. The conductor diameter, number of turns and

maximum current should be simultaneously optimized with a reasonable quench current margin and mechanical stability. There is about two times difference in maximum currents for A,B and C magnets. It is possible to reduce the volume of superconductor for A and B correctors by proportionally increasing the current.

It should be noted that at the magnet ends the fields are typically larger and have correspondingly lower current margins. This effect can be reduced by proper profiling of the coils and yoke at the ends.

13.3 Preliminary Test Plan for H Spool with HTS Current Leads

I. 300K tests:

- Leak check the vacuum lines
- Leak check the nitrogen lines – make sure to open EVLA and EVLB valves
- Electrical checkout of the lead and Stand 2 – follow Electrical checkout procedure (TD note # xxxx *[note to be written]*)
- Hi-pot the leads to 2kV relative to ground

II. Cool down to 4.6K.

Follow Spool cool down procedure (Operating Procedure Number: HTS-000228-1).

Monitor lead voltages by applying +-5 Amps on the leads.

Change polarity every 5 minutes. Set logging frequency of the slow scan to 10 seconds.

III. A 2-phase calibration should be done first. It should be done in "low pressure" ("Tevatron") mode. This involves:

- drop "single-phase" pressure to the 2-phase pressure by opening the stand JT valve (PV-548) wide,
- reduce feedbox power lead flow to 30 SCFH each to ensure that there is no subcooling at the "single-phase" inlet to the magnet,
- set spool piece corrector lead flows to 10 SCFH each
- reduce main storage dewar pressure to about 5 psig and/or throttle a test stand inlet valve to reduce flow to between 10" and 20",
- hold these conditions steady for 4 hours.

We want 2-phase flow throughout the "single-phase" channels. Then we compare temperature sensor readings. All single-phase readings should agree within 10 mK, and they should also agree with 2-phase readings.

IV. Do all tests (except the 2-phase calibration) in high-pressure mode ("SSC mode"). Hold 32 psia single-phase pressure during tests on stand 2.

Current tests at 4.6K:

1. Quench detection circuit checkout
2. DC tests:

Test 1.

Current (A)	He flow (g/sec)	LN2 flow (g/s)	Ramp Rate (A/s)	Duration (min)
3000	0.03	find min. flow	20	30
5000	0.03	find min flow	20	30
6000	0.03	1.2	20	30
6500	0.03	find min flow	20	30
7000	0.03	find min flow	20	30
7500	0.03	find min flow	20	30
8000	0.03	find min flow	20	30
8500	0.03	find min flow	20	30
9000	0.03	find min flow	20	30
9500	0.03	find min flow	20	180

3. Coolant loss test:

Test 2.

Current (A)	He flow (g/sec)	LN2 flow (g/s)	Ramp Rate (A/s)	Duration (min)
9500	0.03	Min.flow/0	20	Until it quenches
9500	0.03	Min.flow	20	180

3. DC tests with external B-field applied

   Under external B-field increase the current gradually. If no quench occurs at 9500A increase the LN2 pressure up to 40 PSIG.